Project: “Monitoring Sea-water intrusion in coastal aquifers and Testing pilot projects for its mitigation” Interreg CBC Italy-Croatia 2014.-2020.

Priority Axis: Safety and resilience

Specific objective: Improve the climate change monitoring and planning of adaptation measures tackling specific effects, in the cooperation area

(D_4.1.3) Proposed actions and/or pilot solutions for salt water intrusion mitigation tested in laboratory and/or numerical model: report on procedures, analysed combinations, parameters and results

Work Package 4: Testing

Activity 1: Neretva coastal plain

Partner in charge: PP4 (UNIST-FGAG)

Partners involved: PP4 (UNIST-FGAG), PP5 (CROATIAN WATERS), PP6 (DUNEA)

Final version

Public report

September, 2022

Contents

Results of climate change modelling – numerical modelling

Model response due to sea level rise

Next figures show changes in salinity field for the layer of sand and the layer of gravel due to sea level rise. Simulations were set on flow and transport steady state simulation obtained for existing state. Simulations were set for 160 years and in that period steady state for head and for concentration is achieved for all locations.

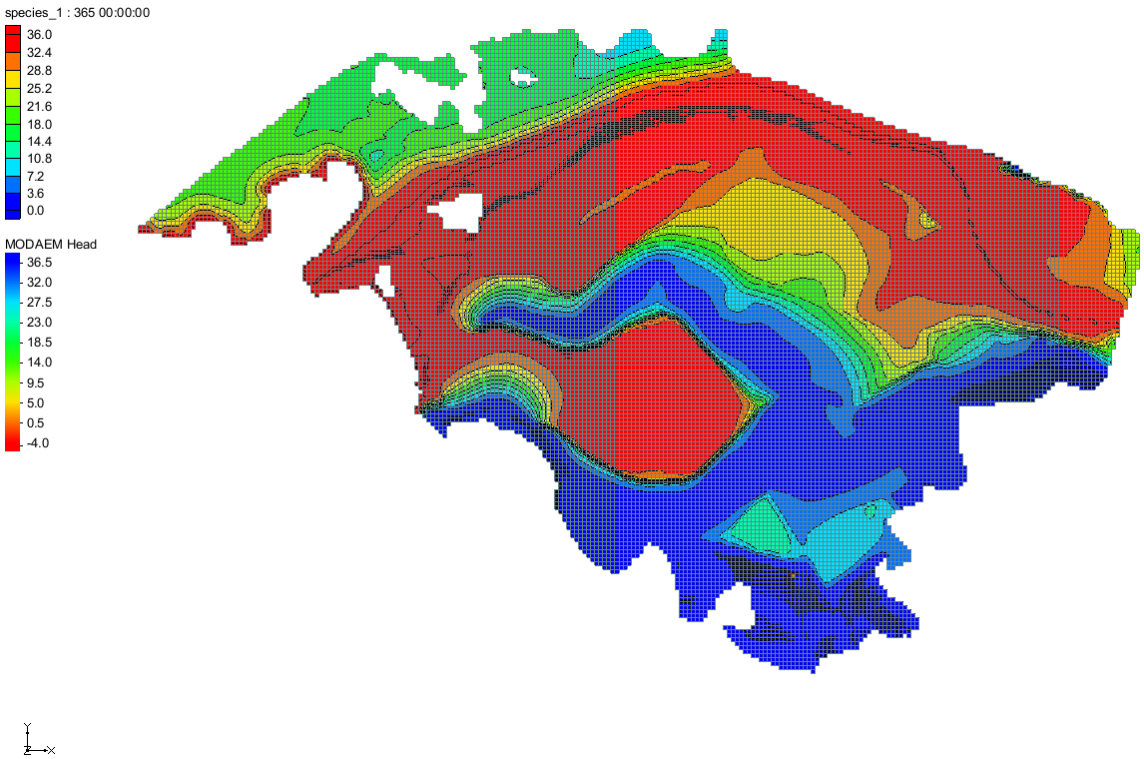

Figure 1 Salinity field for the layer of sand before climate changes

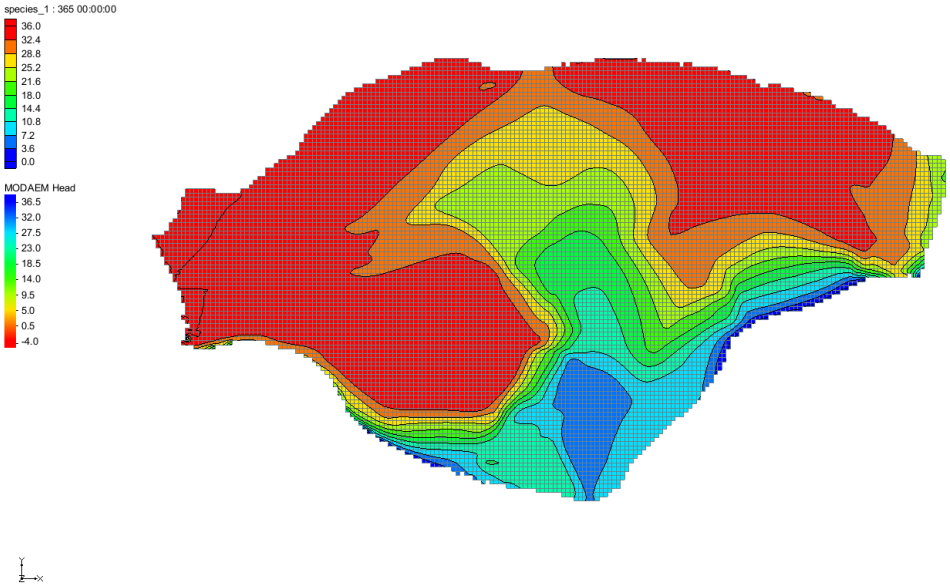

Figure 2 Salinity field for the layer of gravel before climate changes

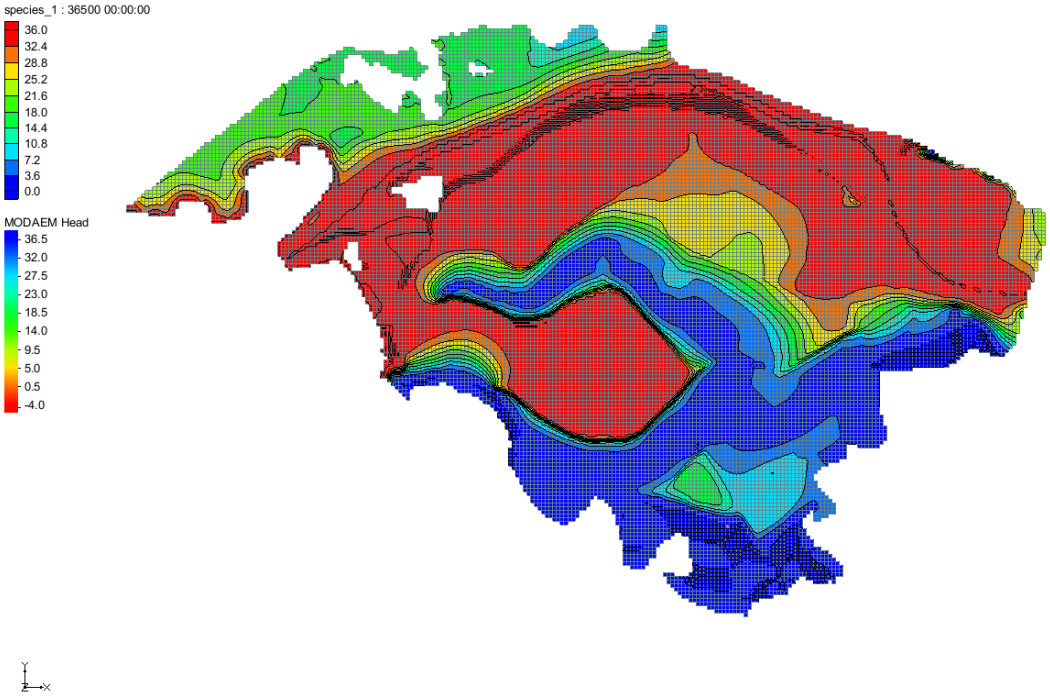

Figure 3 Salinity field for the layer of sand after 160 years of SLR for 43 cm

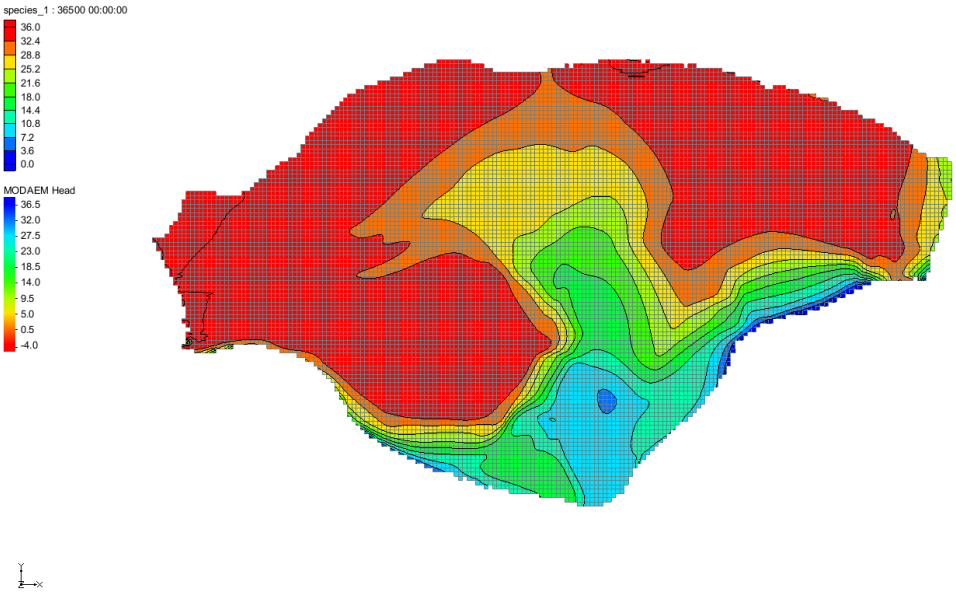

Figure 4 Salinity field for the layer of gravel after 160 years of SLR for 43 cm

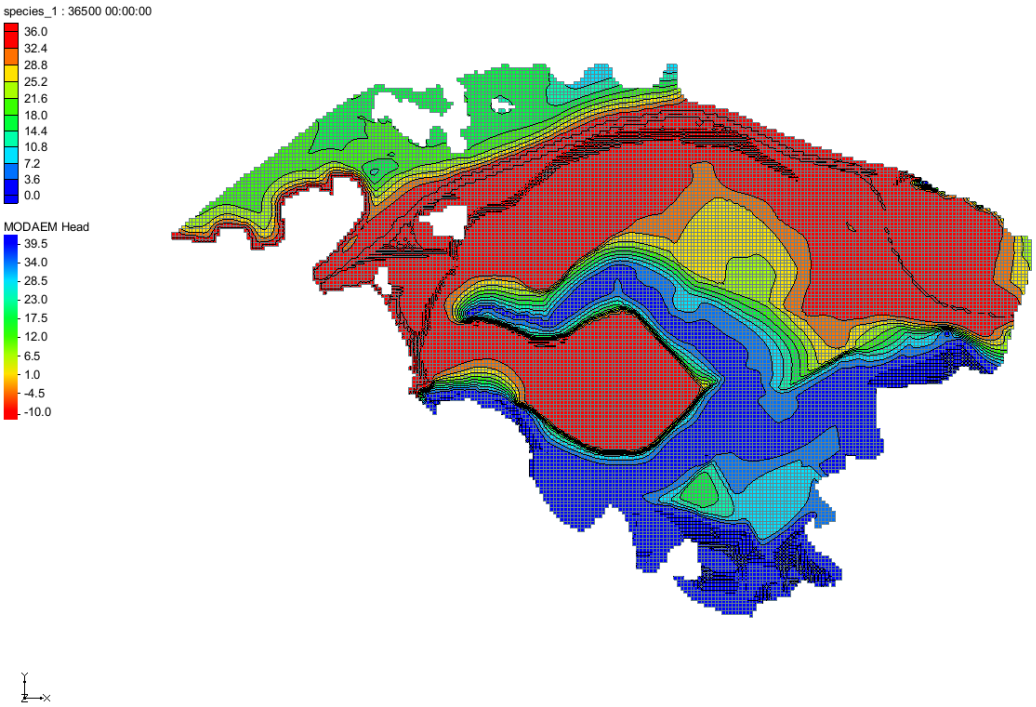

Figure 5 Salinity field for the layer of sand after 160 years of SLR for 84 cm

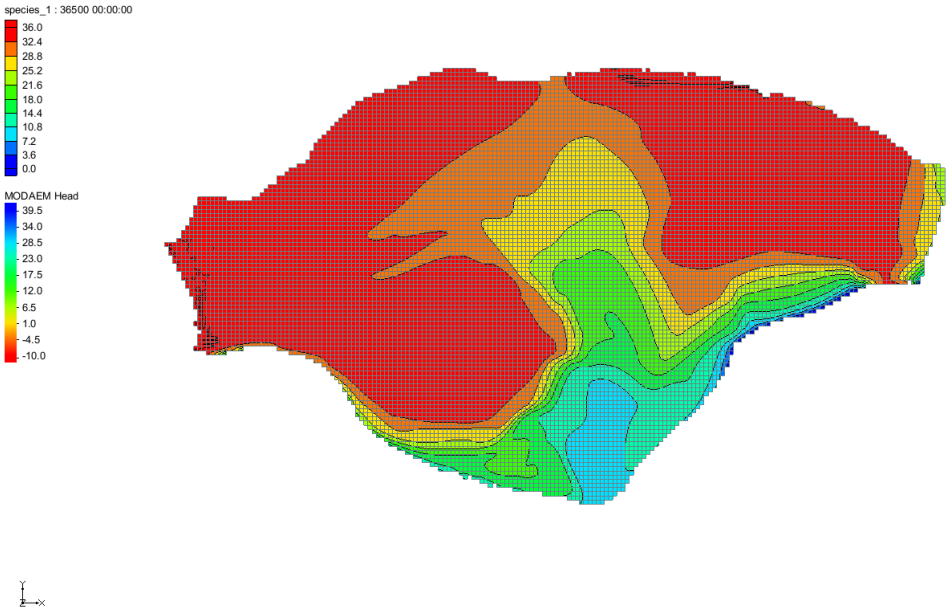

Figure 6 Salinity field for the layer of gravel after 160 years of SLR for 84 cm

Next figures show the change of head and concentration for three shallow piezometers (P1, P2 and P4) and for four deep piezometers (D1, D2, D3 and D4) due to sea level rise.

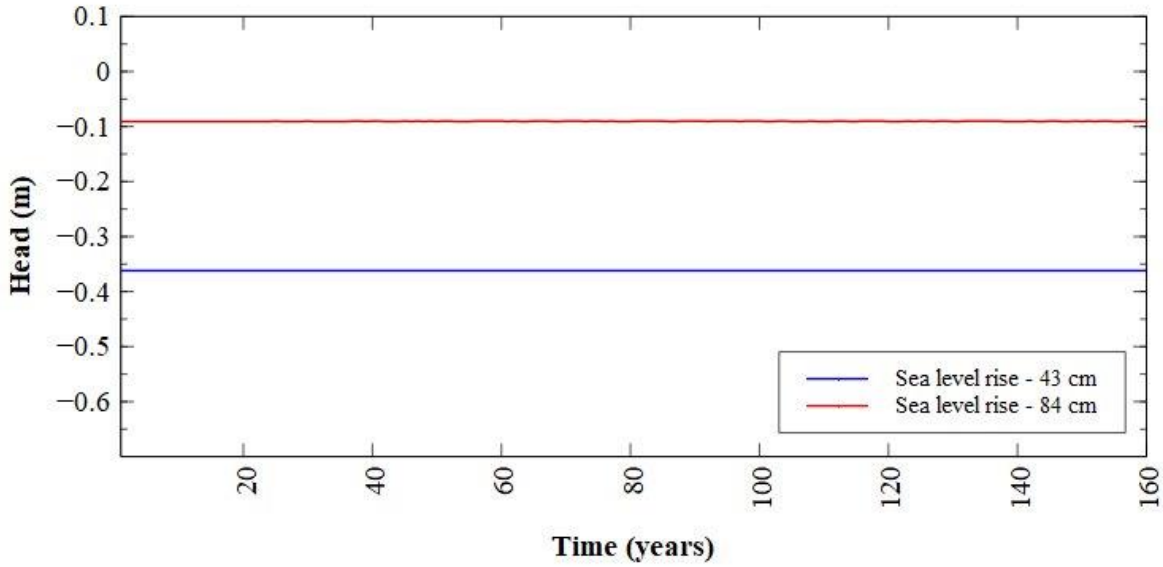

Figure 7 Change of head for piezometer P1 for sea level rise for 43 and 84 cm

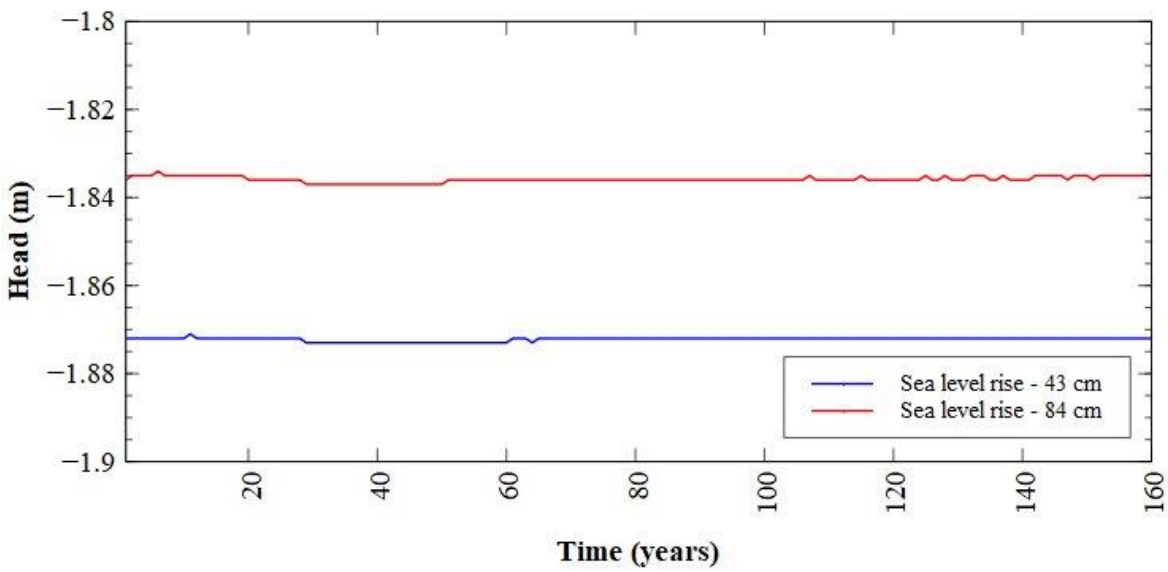

Figure 8 Change of head for piezometer P2 for sea level rise for 43 and 84 cm

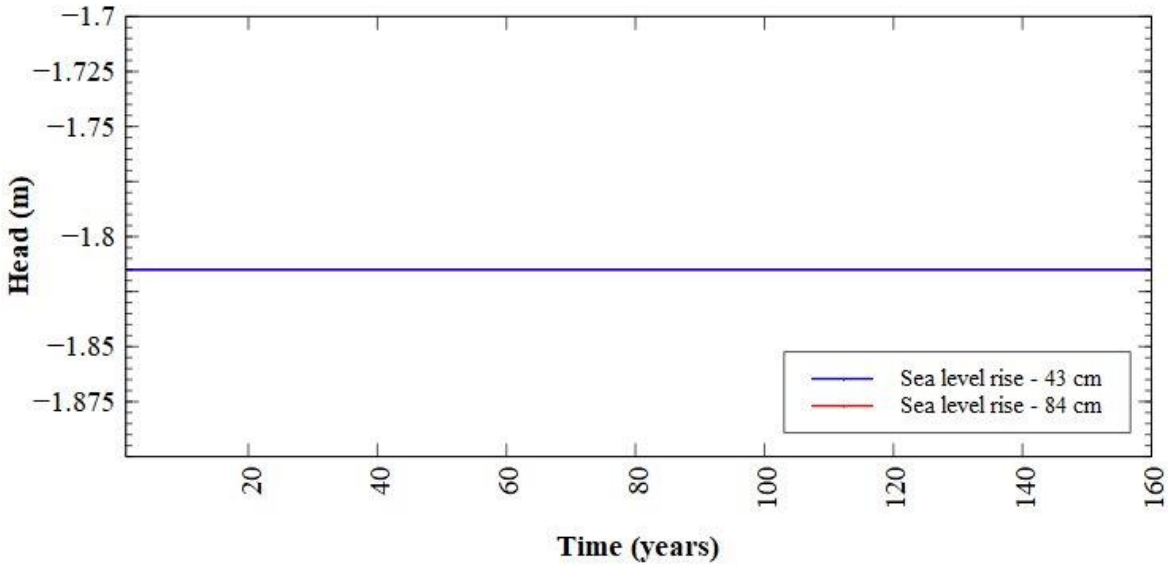

Figure 9 Change of head for piezometer P4 for sea level rise for 43 and 84 cm

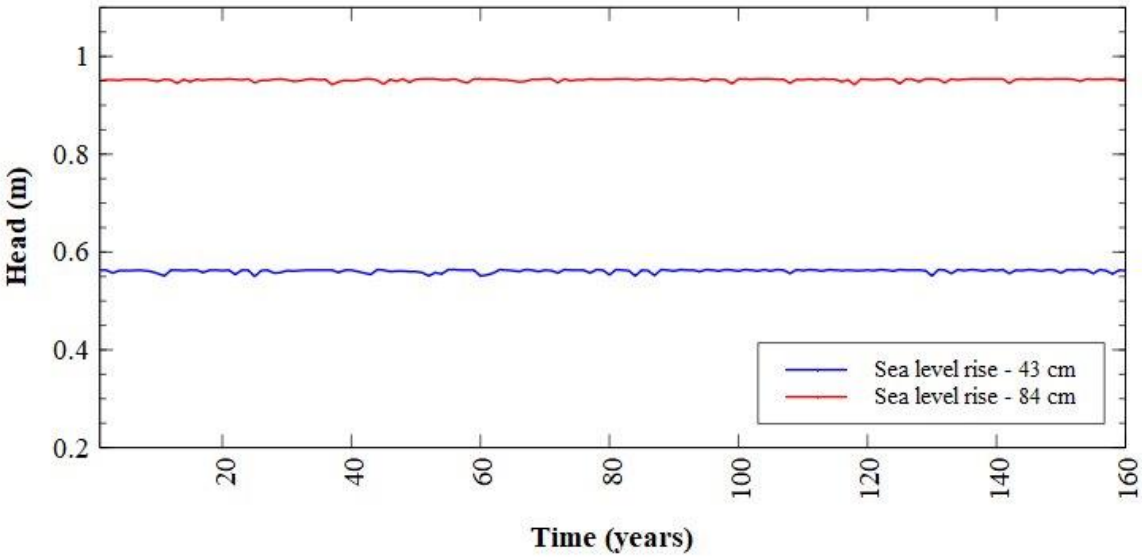

Figure 10 Change of head for piezometer D1 for sea level rise for 43 and 84 cm

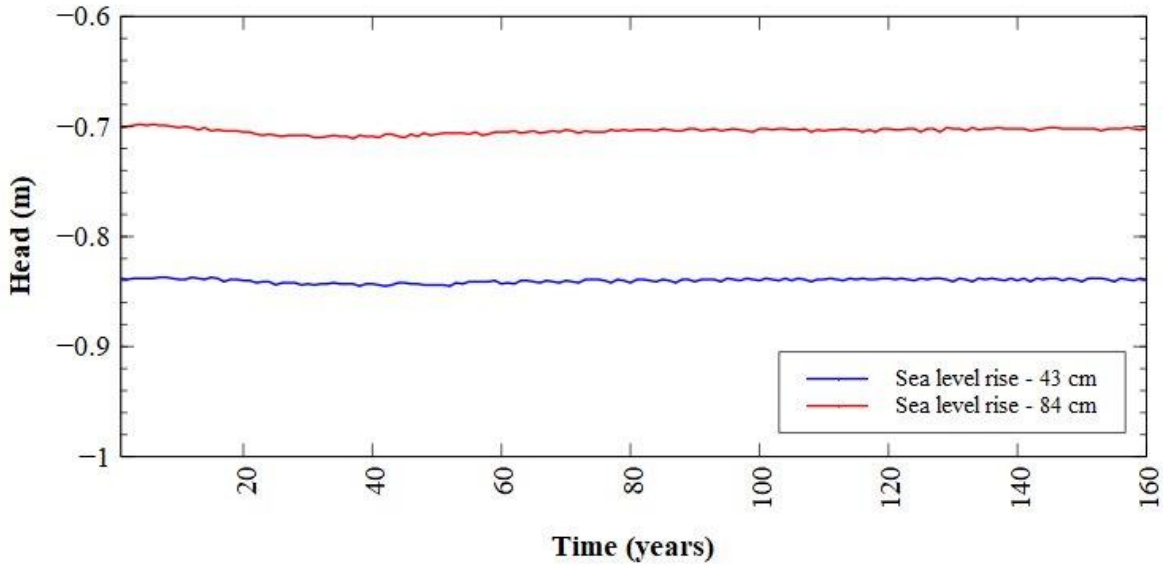

Figure 11 Change of head for piezometer D2 for sea level rise for 43 and 84 cm

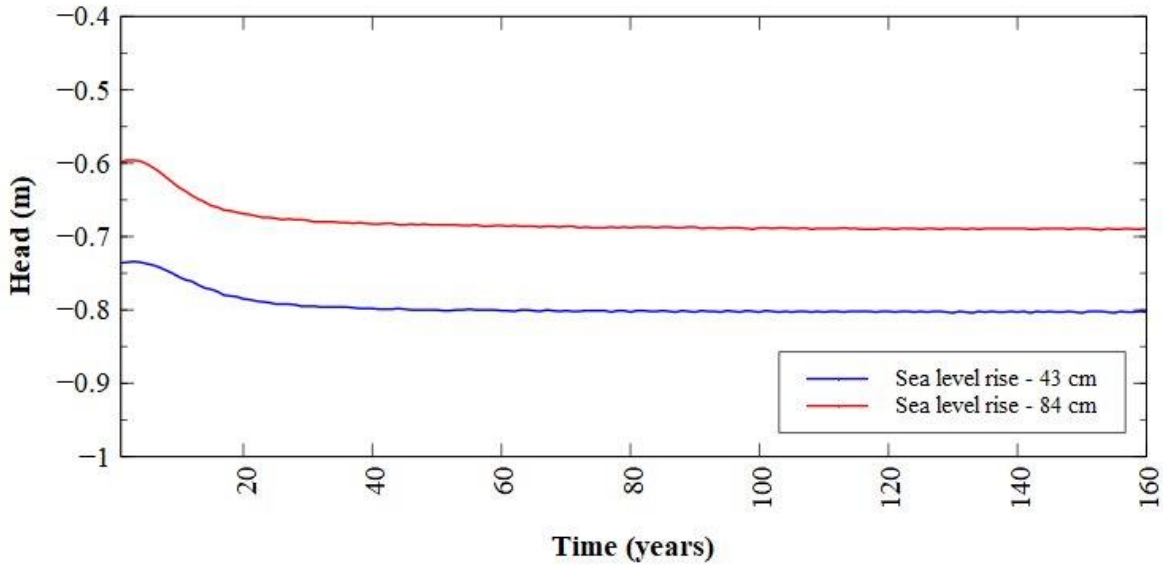

Figure 12 Change of head for piezometer D3 for sea level rise for 43 and 84 cm

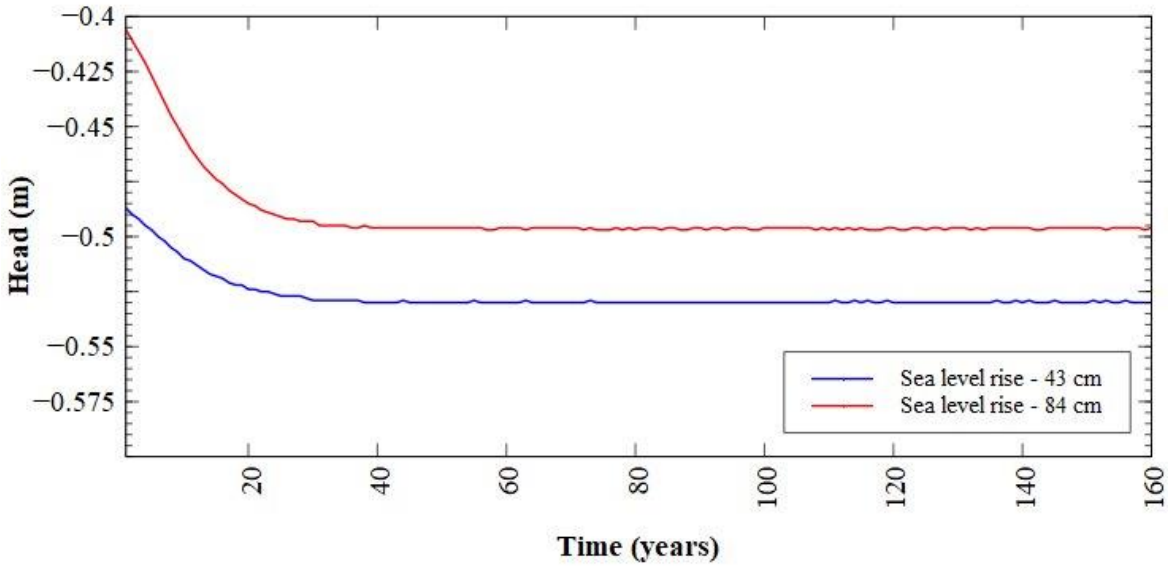

Figure 13 Change of head for piezometer D4 for sea level rise for 43 and 84 cm

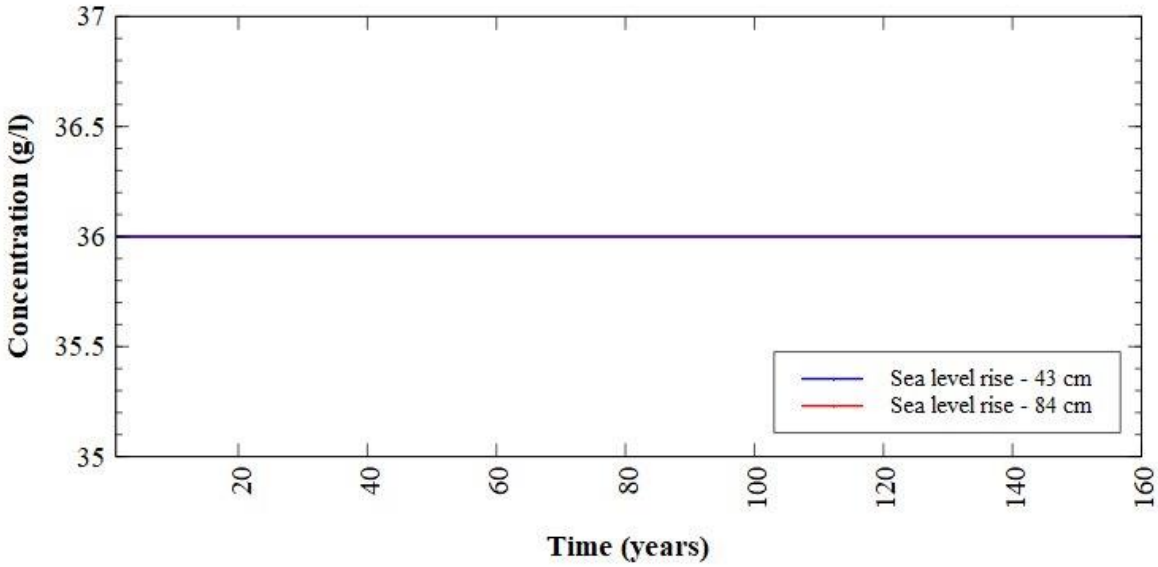

Figure 14 Change of concentration for piezometer P1 for sea level rise for 43 and 84 cm

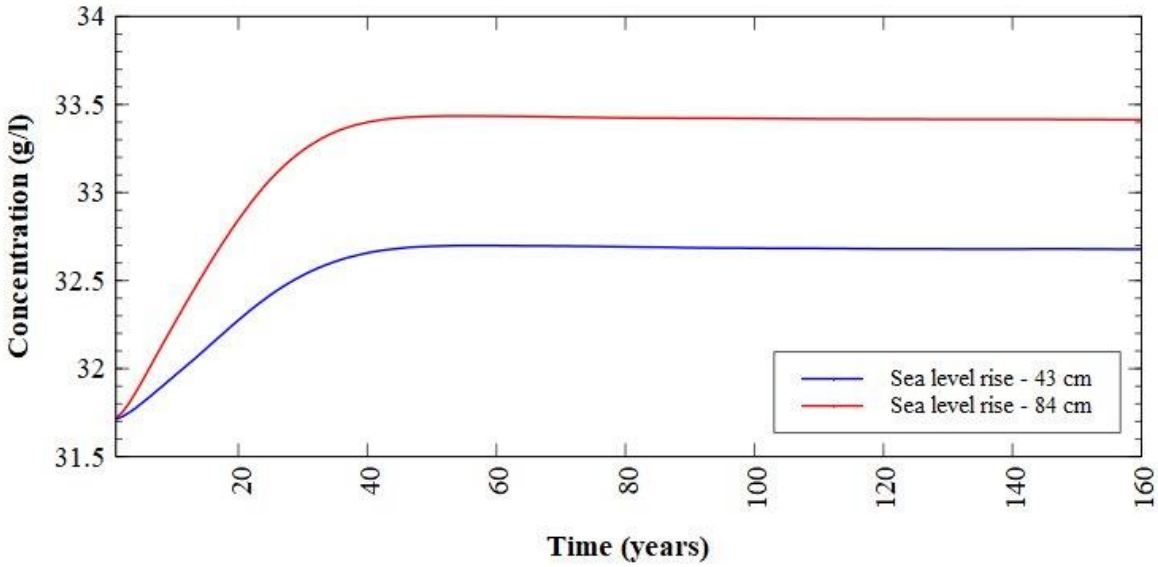

Figure 15 Change of concentration for piezometer P2 for sea level rise for 43 and 84 cm

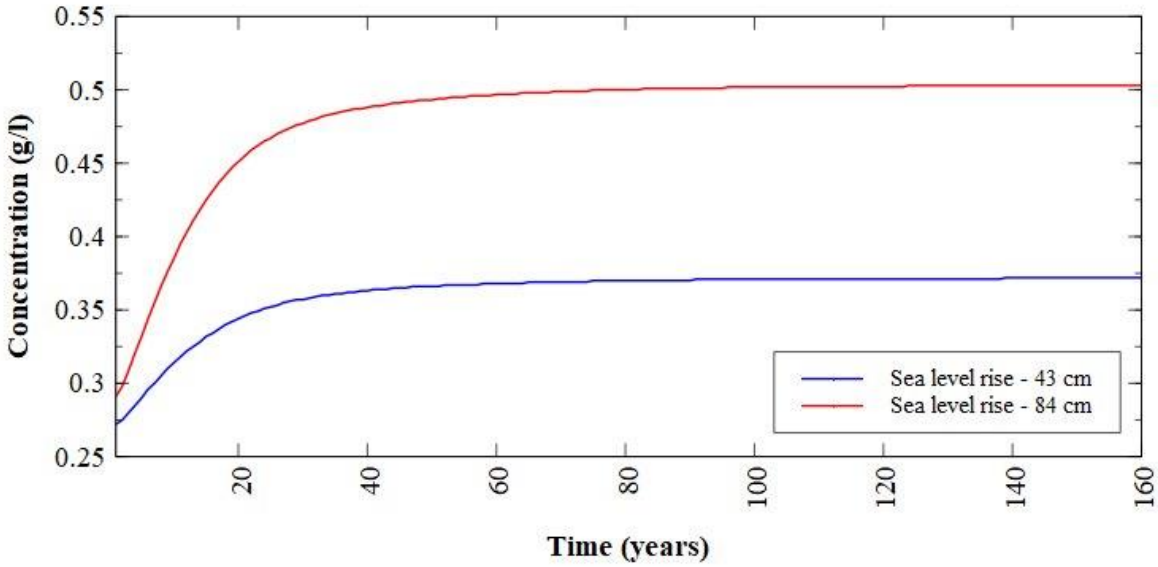

Figure 16 Change of concentration for piezometer P4 for sea level rise for 43 and 84 cm

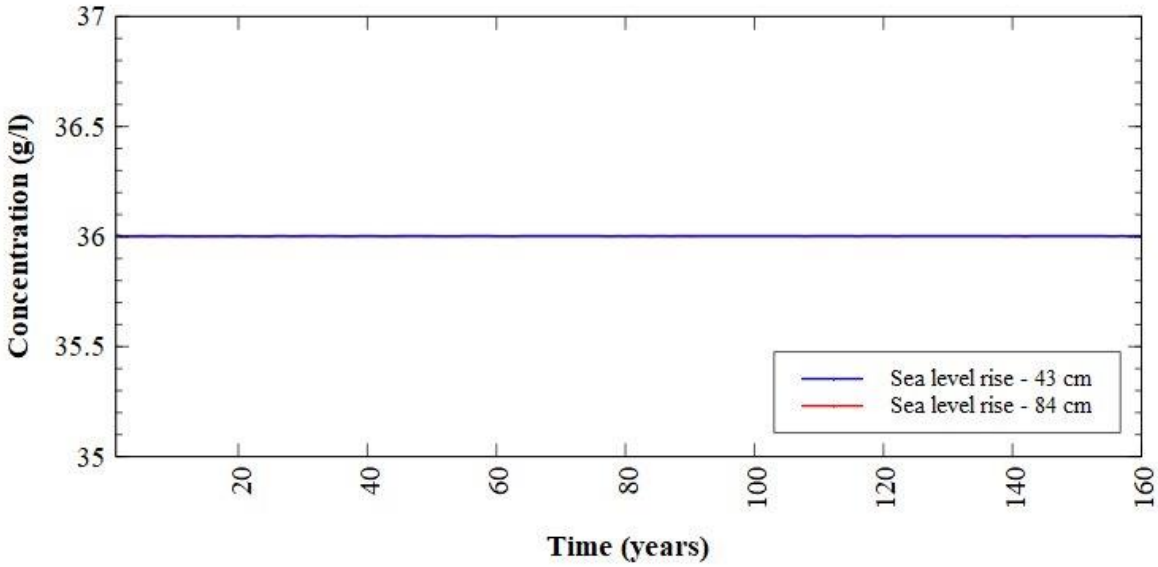

Figure 17 Change of concentration for piezometer D1 for sea level rise for 43 and 84 cm

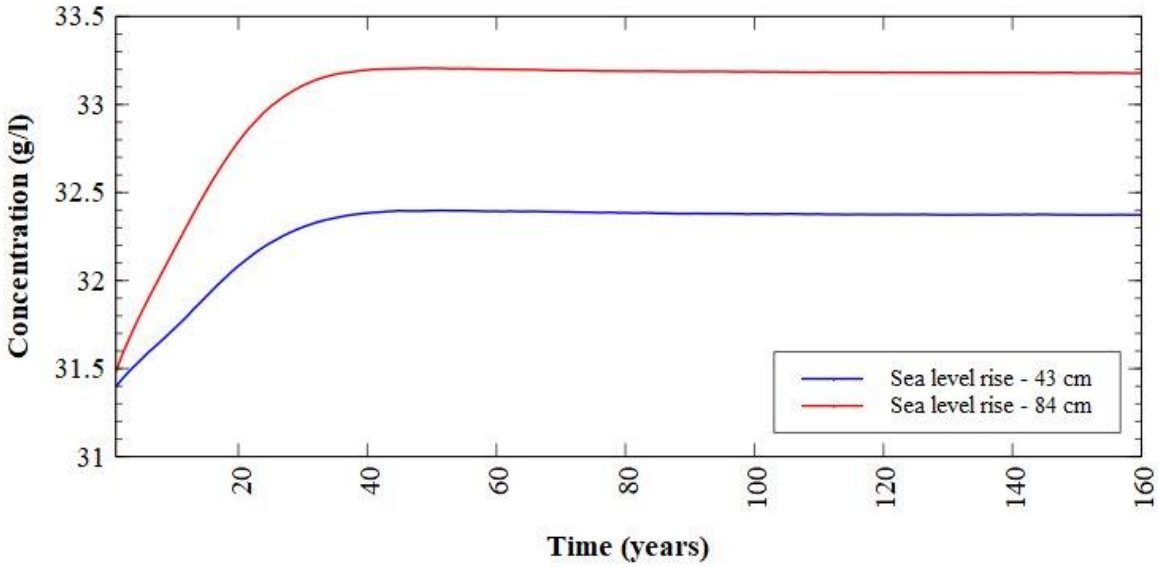

Figure 18 Change of concentration for piezometer D2 for sea level rise for 43 and 84 cm

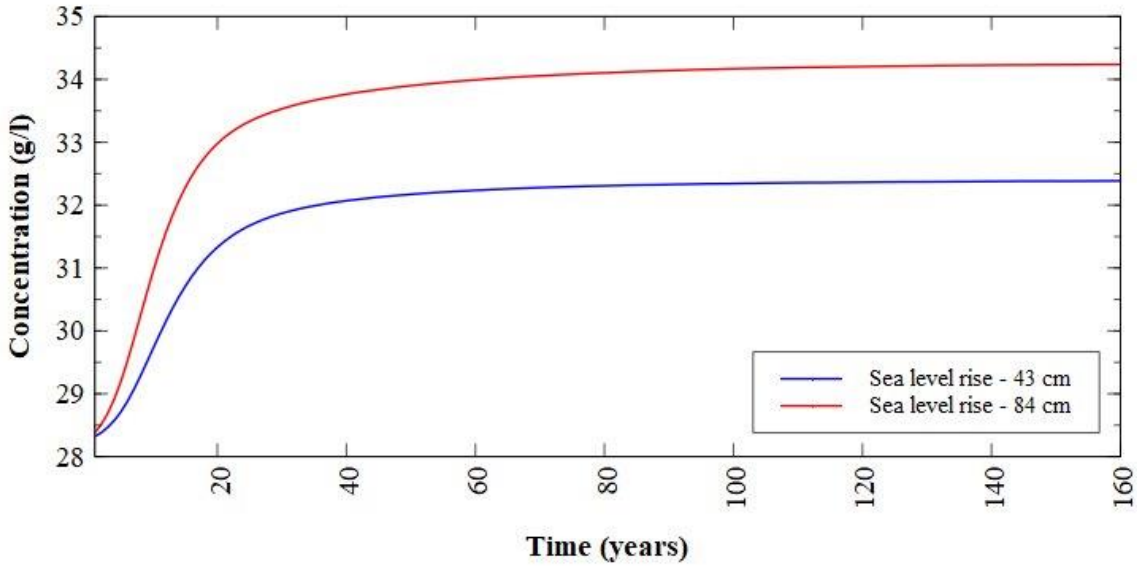

Figure 19 Change of concentration for piezometer D3 for sea level rise for 43 and 84 cm

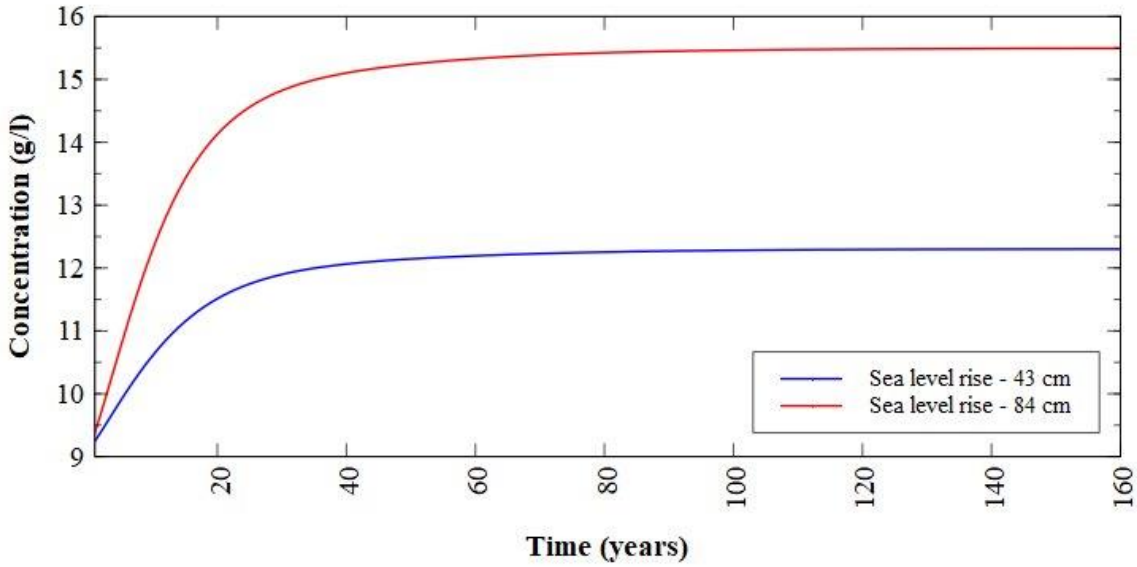

Figure 20 Change of concentration for piezometer D4 for sea level rise for 43 and 84 cm

Table 1 Change of head and concentration for all 7 locations due to sea level rise

LOCATION	Change of head for 0.43 m SLR (m)	Change of head for 0.84 m SLR (m)	Change of concentration for 0.43 m SLR (g/l)	Change of concentration for 0.84 m SLR (g/l)
P1	+0.28	+0.55	0.0	0.0
P2	+0.04	+0.07	+0.99	+1.72
P4	+0.005	+0.005	+0.1	+0.21
D1	+0.39	+0.78	0.0	0.0
D2	+0.13	+0.27	+1.0	+1.73
D3	+0.08	+0.19	+4.07	+5.86
D4	+0.04	+0.08	+3.06	+6.12

Model response due to precipitation decline

Next figures show changes in salinity field for the layer of sand and the layer of gravel due to precipitation decline. Simulations were set on flow and transport steady state simulation obtained for existing state. Simulations were set for 100 years and in that period steady state for head and for concentration is achieved for all locations.

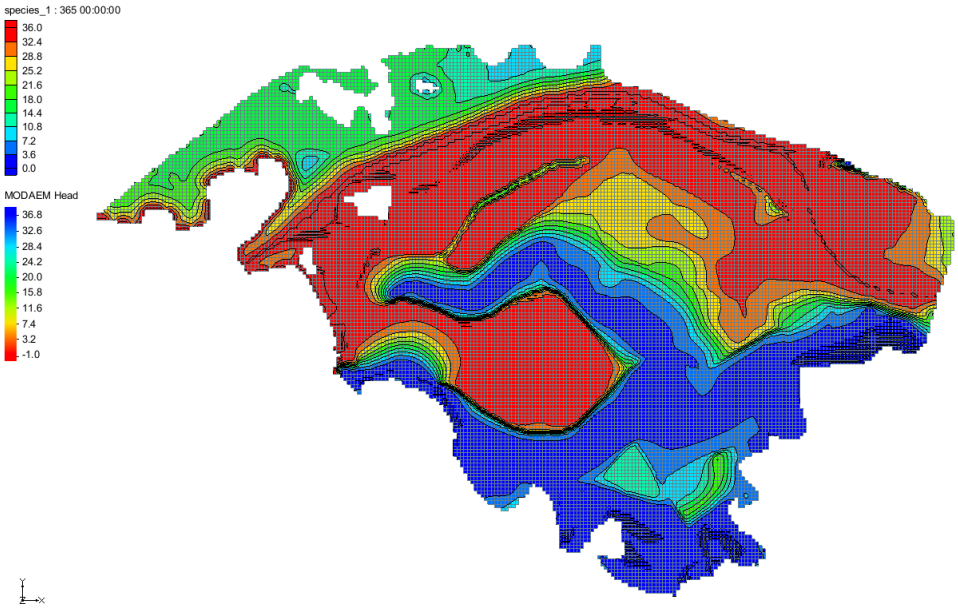

Figure 21 Salinity field for the layer of sand before climate changes

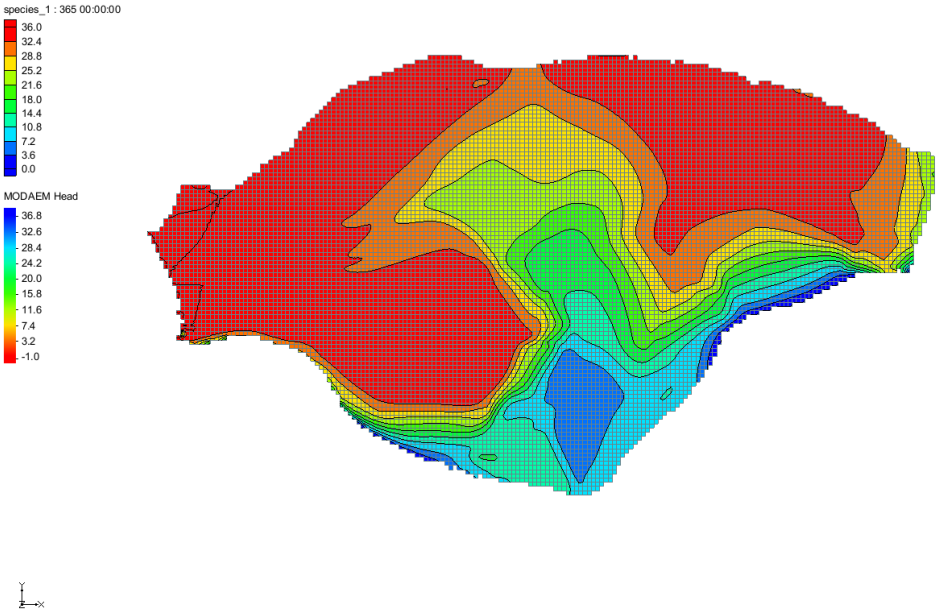

Figure 22 Salinity field for the layer of gravel before climate changes

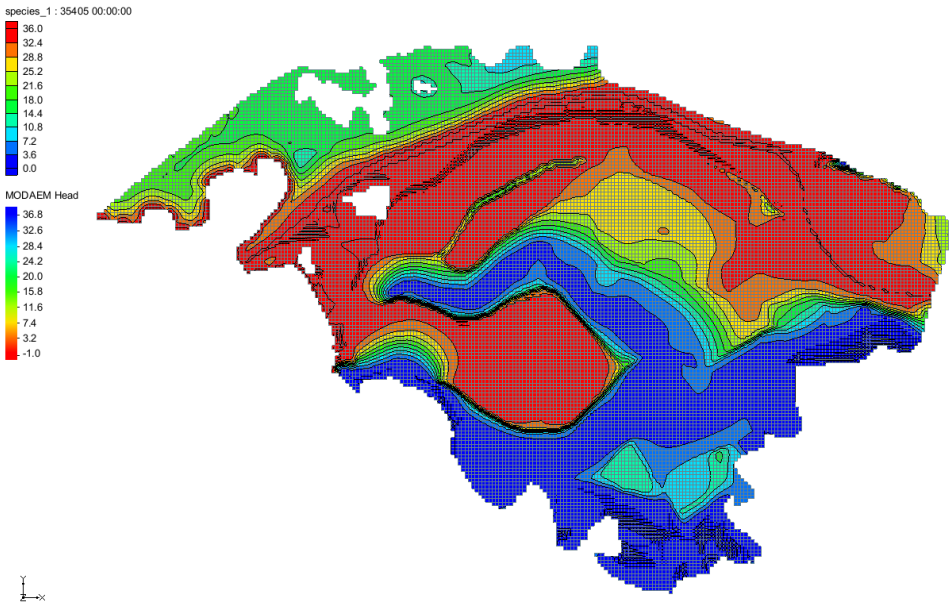

Figure 23 Salinity field for the layer of sand after 100 years of precipitation decline for 10%

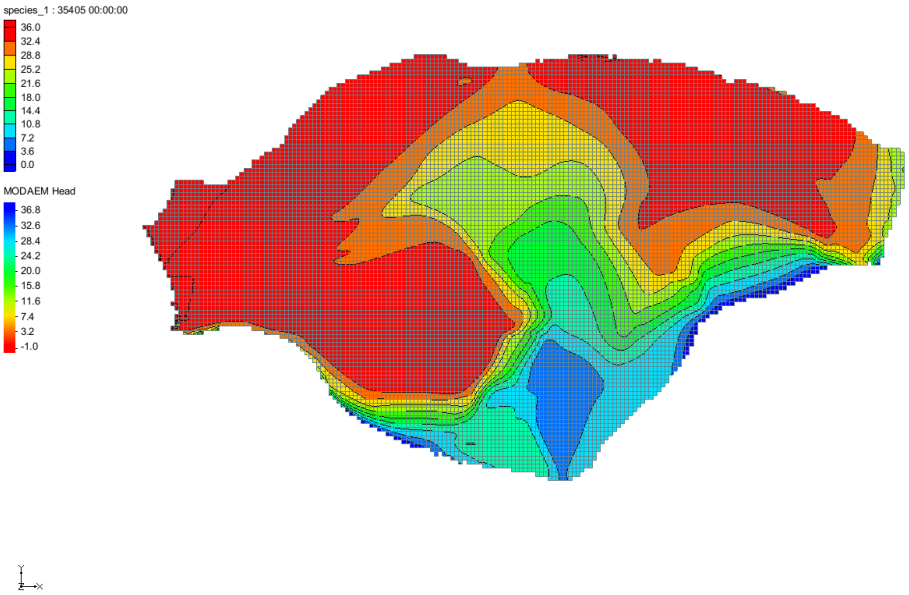

Figure 24 Salinity field for the layer of gravel after 100 years of precipitation decline for 10%

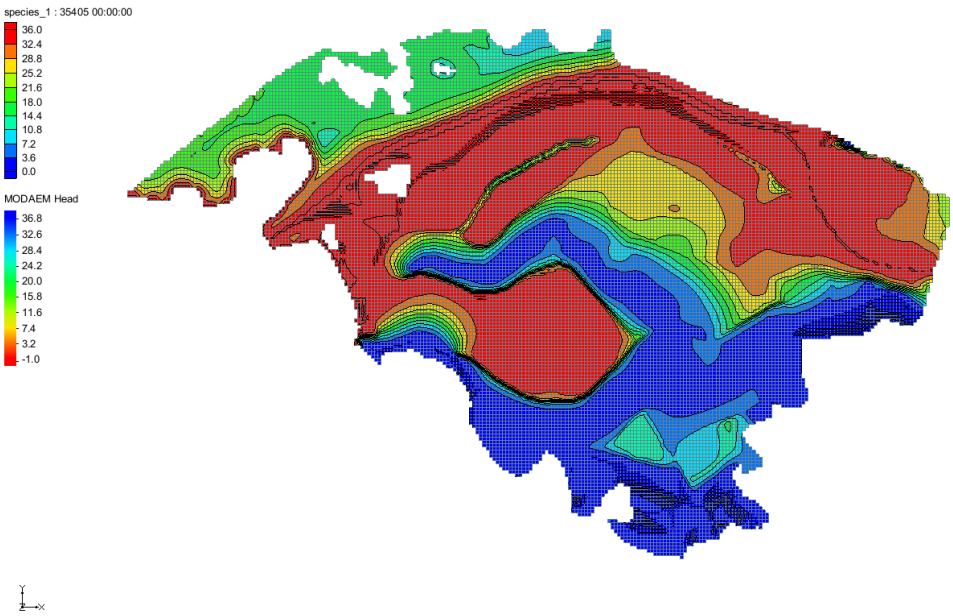

Figure 25 Salinity field for the layer of sand after 100 years of precipitation decline for 20%

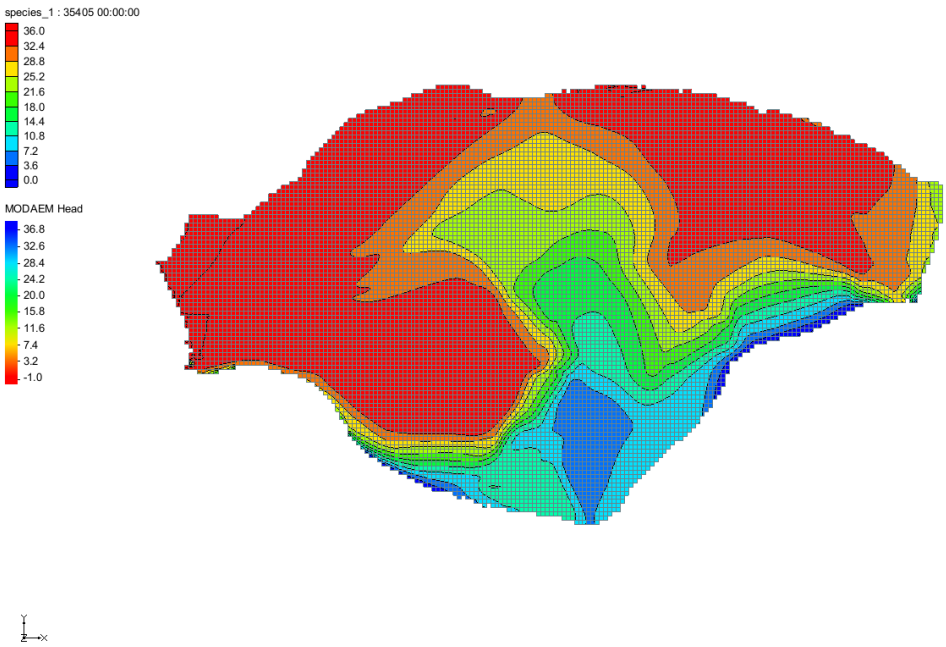

Figure 26 Salinity field for the layer of gravel after 100 years of precipitation decline for 20%

Next figures show the change of head and concentration for three shallow piezometers (P1, P2 and P4) and for four deep piezometers (D1, D2, D3 and D4) due to change in precipitation values. Simulations were set for 100 years and in that period steady state for head and for concentration is achieved for all locations.

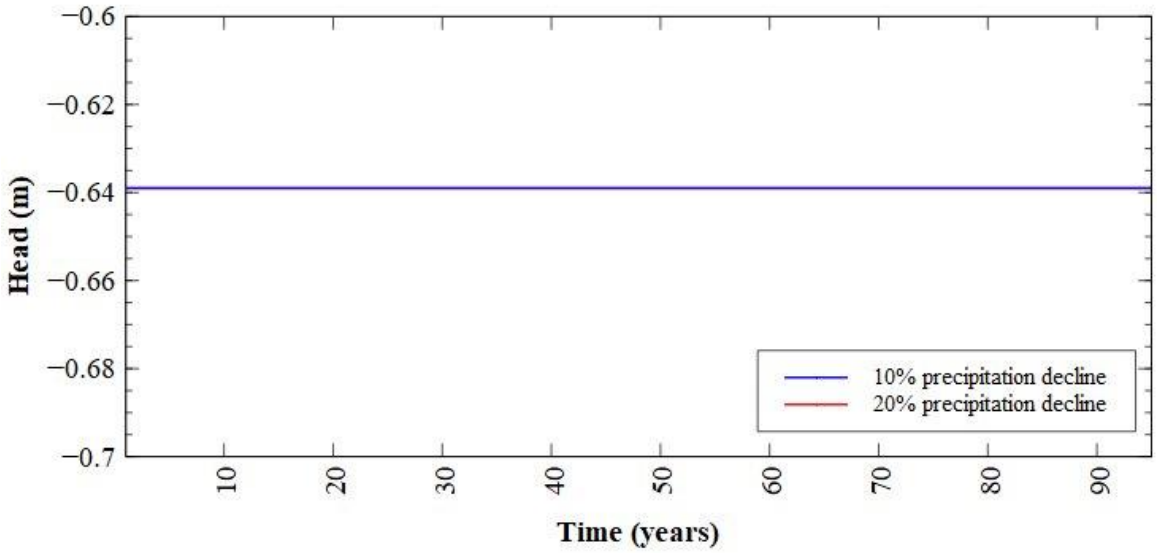

Figure 27 Change of head for piezometer P1 for precipitation decline for 10 and 20%

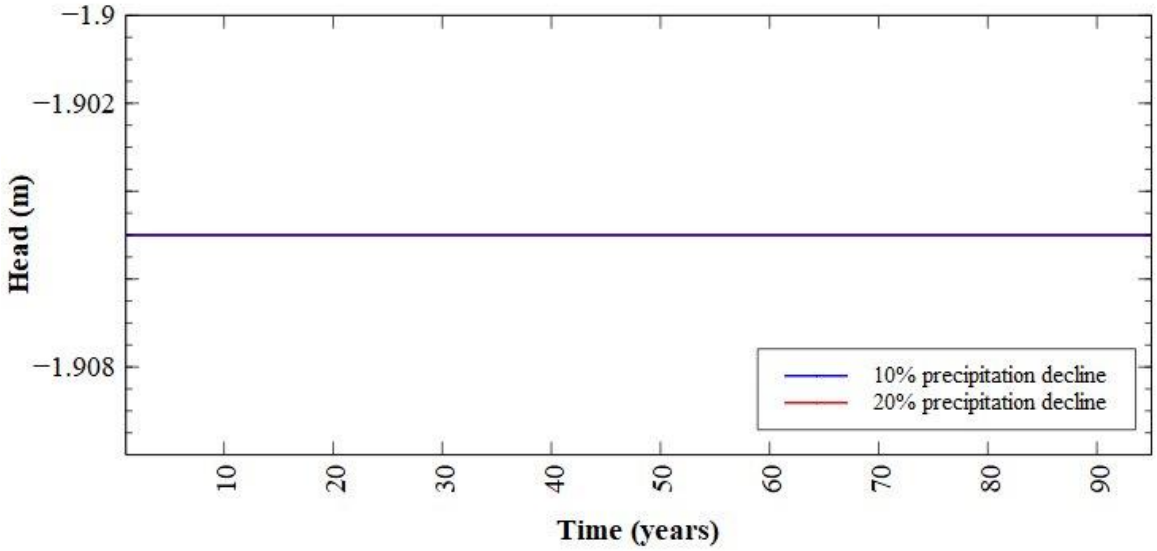

Figure 28 Change of head for piezometer P2 for precipitation decline for 10 and 20%

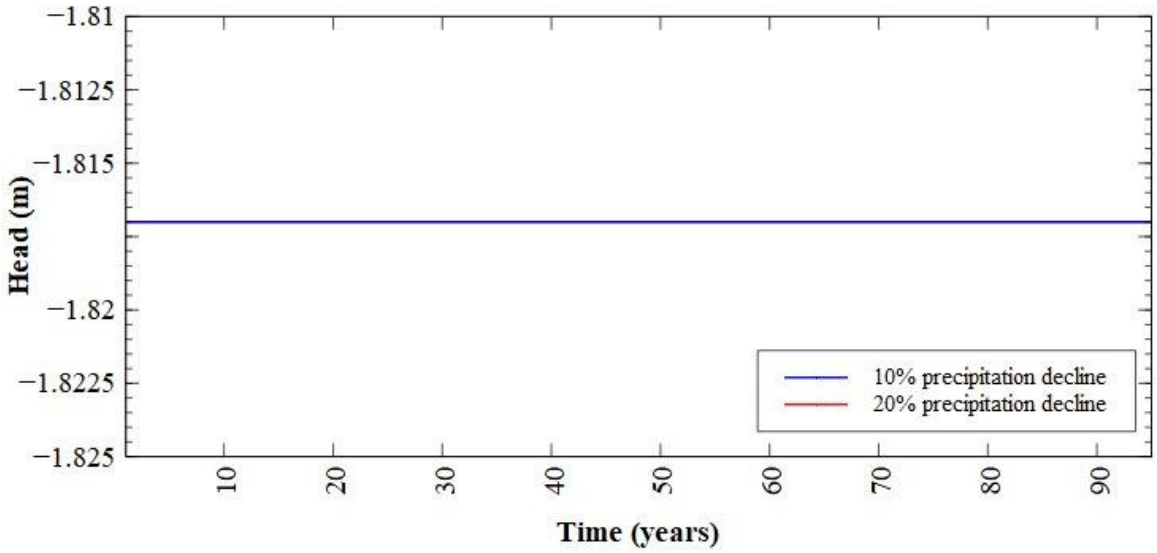

Figure 29 Change of head for piezometer P4 for precipitation decline for 10 and 20%

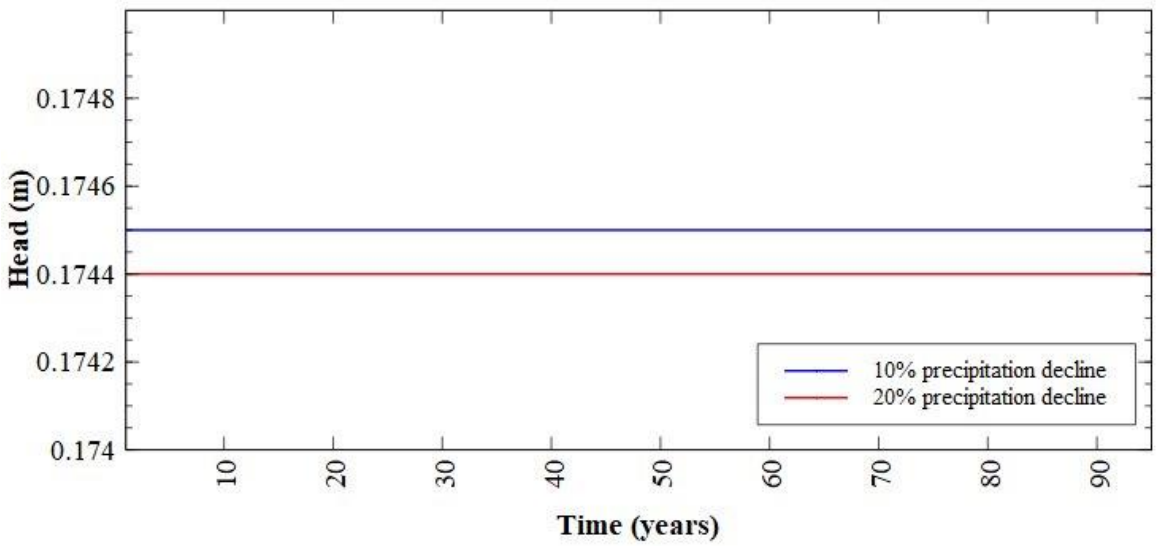

Figure 30 Change of head for piezometer D1 for precipitation decline for 10 and 20%

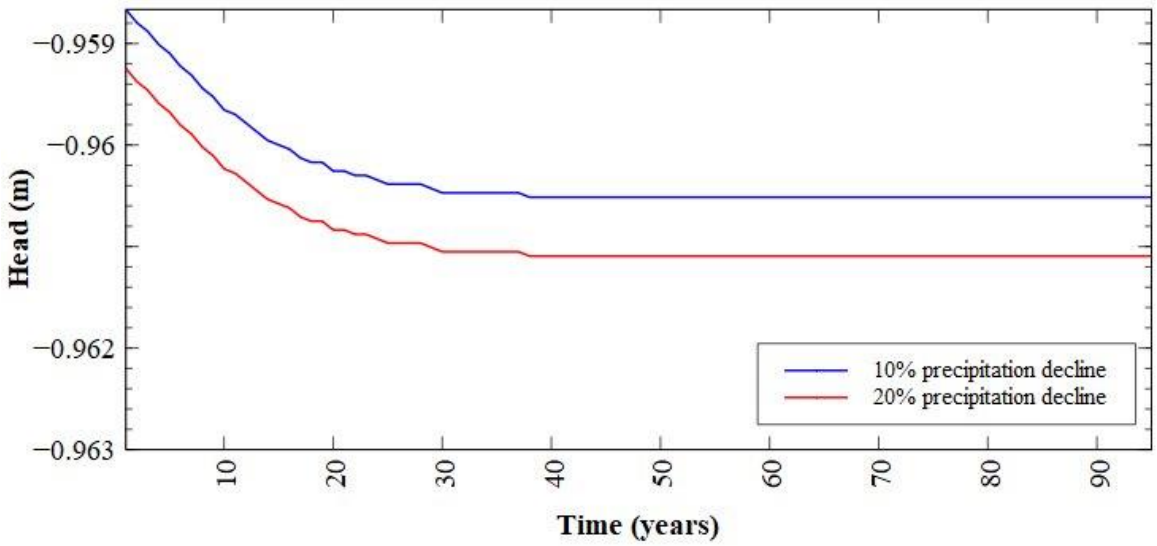

Figure 31 Change of head for piezometer D2 for precipitation decline for 10 and 20%

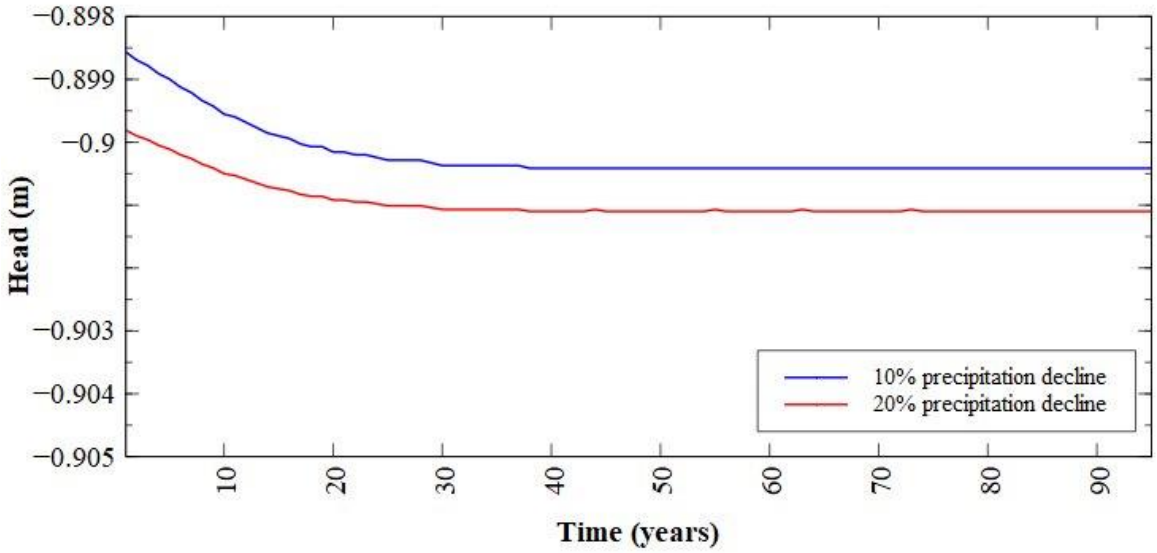

Figure 32 Change of head for piezometer D3 for precipitation decline for 10 and 20%

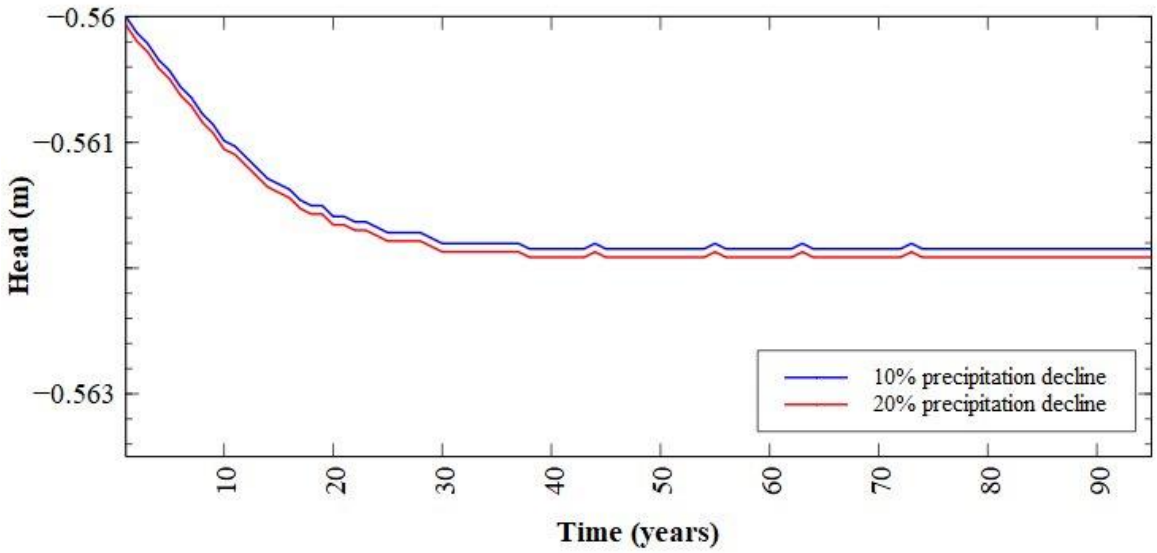

Figure 33 Change of head for piezometer D4 for precipitation decline for 10 and 20%

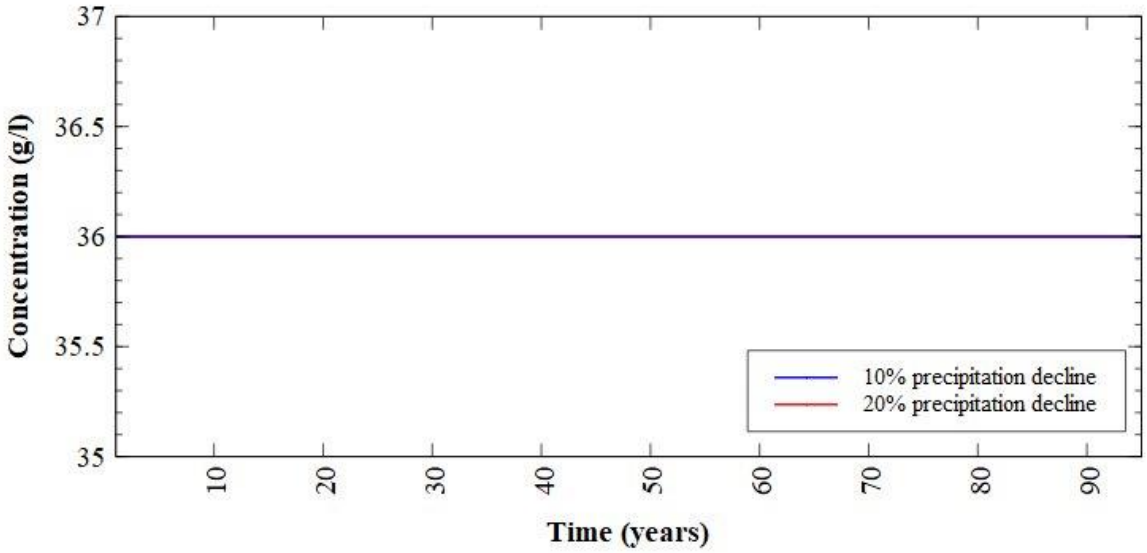

Figure 34 Change of concentration for piezometer P1 for precipitation decline for 10 and 20%

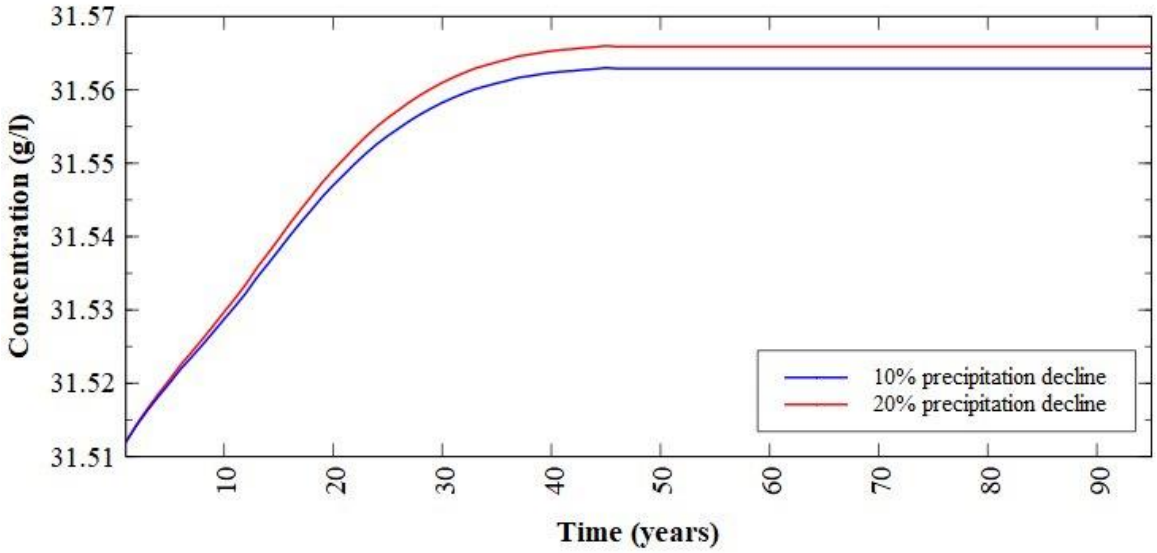

Figure 35 Change of concentration for piezometer P2 for precipitation decline for 10 and 20%

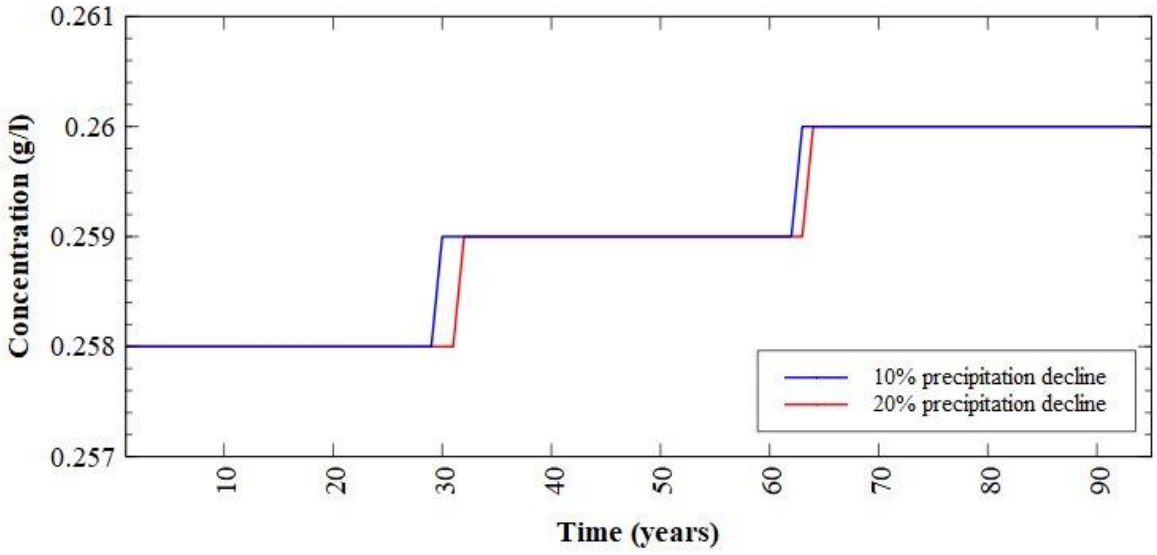

Figure 36 Change of concentration for piezometer P4 for precipitation decline for 10 and 20%

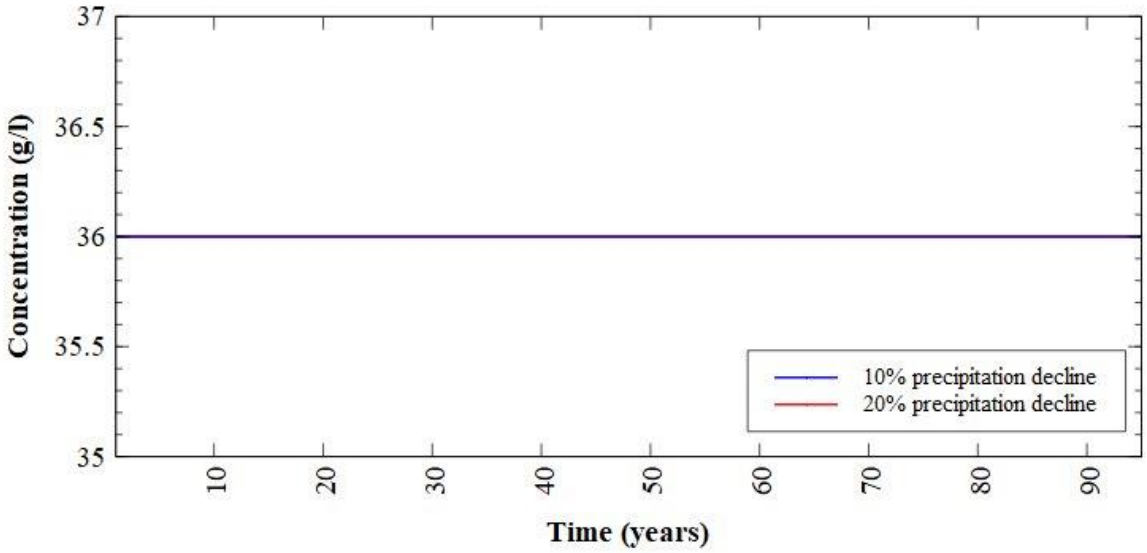

Figure 37 Change of concentration for piezometer D1 for precipitation decline for 10 and 20%

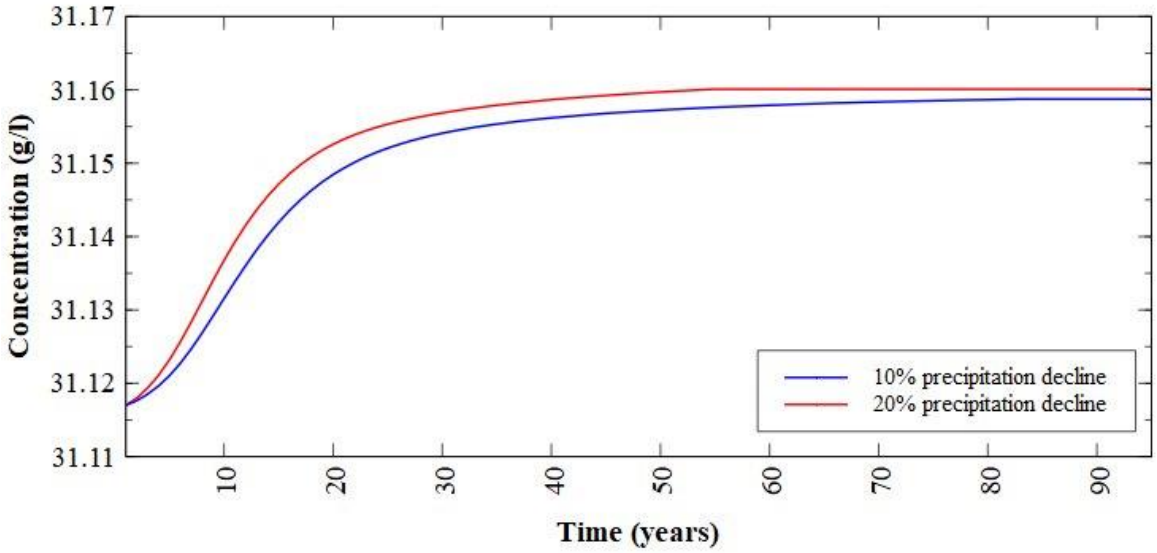

Figure 38 Change of concentration for piezometer D2 for precipitation decline for 10 and 20%

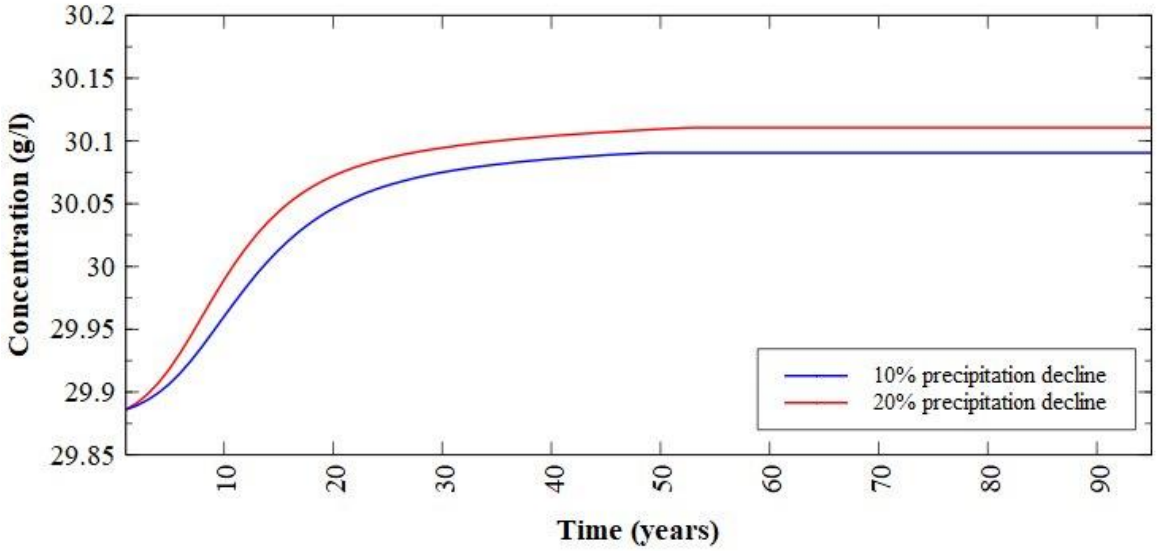

Figure 39 Change of concentration for piezometer D3 for precipitation decline for 10 and 20%

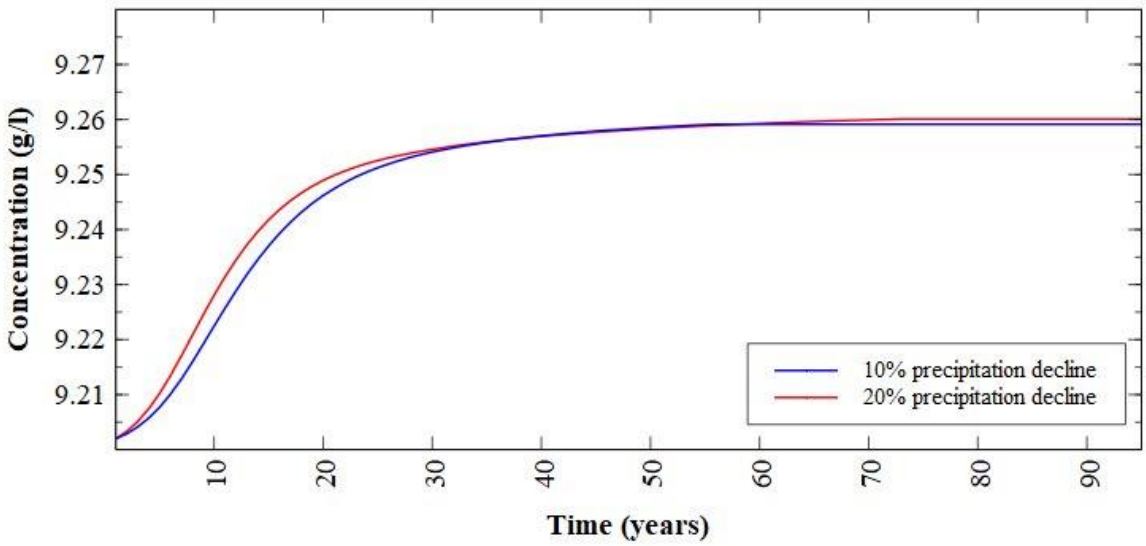

Figure 40 Change of concentration for piezometer D4 for precipitation decline for 10 and 20%

Table 2 Change of head and concentration for all 7 locations due to precipitation decline

LOCATION	Change of head for 10% precipitation decline (m)	Change of head for 20% precipitation decline (m)	Change of concentration for 10% precipitation decline (g/l)	Change of concentration for 20% precipitation decline (g/l)
P1	0.0	0.0	0.0	0.0
P2	-0.001	-0.001	+0.0051	+0.0054
P4	0.0	0.0	+0.002	+0.002
D1	0.0	-0.002	0.0	0.0
D2	-0.005	-0.004	+0.0013	+0.0013
D3	-0.003	-0.003	+0.002	+0.002
D4	-0.002	-0.002	+0.001	+0.001

Mitigation measures numerical modelling

Three mitigation measures scenarios suitable for River Neretva Valley were proposed and tested in the model. Those scenarios are:

- Impermeable underground barrier below Diga embankment
- Barrier on River Neretva near Komin
- Barrier on River Neretva near Komin with channel parallel with River Neretva

Figure 41 shows location of underground barrier below Diga, barrier on River Neretva and existing channel parallel with River Neretva used as source of fresh water in combination with barrier on River Neretva.

Figure 41 Location of elements for mitigation measures

Impermeable underground barrier below Diga embankment (M1)

Impermeable underground barrier below Diga embankment is the first mitigation measure tested in the model. Main idea behind this mitigation measure is that impermeable underground barrier should prevent salt water intrusion below Diga embankment. Impermeable underground barrier was located from the River Neretva on northwest up to pumping station Modrič on southeast, below Diga embankment.

Since Diga embankment is artificially made embankment constructed in 1960s it is made out of different kind of material than the rest of the valley. The model of existing state adopted higher values for hydraulic conductivity for the area of Diga embankment and defined it as more permeable area.

Mitigation measure scenario M1 was tested as steady state (transient constant) simulation set for the period of 160 years.

Flow boundary conditions for mitigation measure M1 simulation were mean values of boundary condition determined for existing state simulations. Flow initial condition for mitigation measure M1 simulation were head results of flow steady state simulation.

Transport boundary conditions for mitigation measure M1 simulation were concentration value of 36 g/l along the sea line and in River Neretva. Boundary conditions for Opuzen, Mala Neretva and channels were defined as $dC/cX \neq 0$, $dC/dZ \neq 0$. Transport initial condition for mitigation measure M1 simulation were the values of concentration obtained in flow and transport steady state simulation.

For simulation of impermeable underground barrier below Diga embankment the material of clay was used. Material was set along the whole area of Diga embankment in the first five layers of the model. All geological characteristics of the clay were used with the value of horizontal hydraulic conductivity 10^{-9} m/s.

Figure 42 shows the values of horizontal hydraulic conductivity in the layer of sand set for mitigation measure M1.

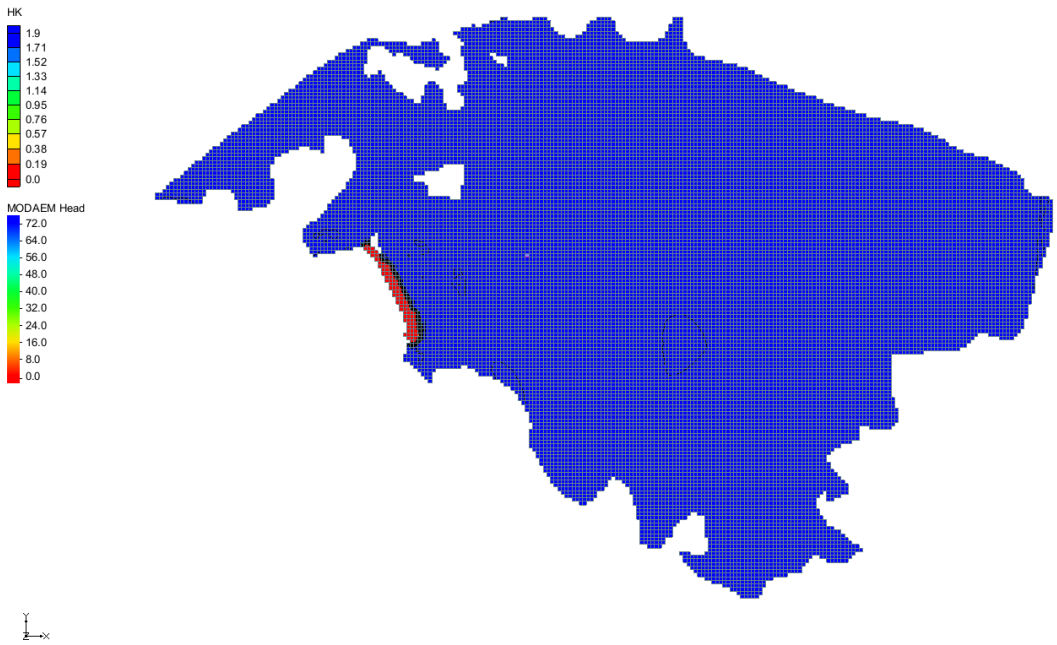

Figure 42 Values of horizontal hydraulic conductivity in the layer of sand for mitigation measure M1

Barrier on River Neretva near Komin (M2)

Barrier on River Neretva near Komin is the second mitigation measure tested in the model.

Since the salt water wedge is noticed in all samplings taken on River Neretva (near Komin and Opuzen) during summer period it was possible to conclude that River Neretva is a source of salt water during the summer period. Main idea behind this mitigation measure is that barrier on River Neretva near Komin should prevent salt water intrusion trough river Neretva during the summer period. The barrier should also increase water level in River Neretva upstream from the barrier for 30 cm. In case of implementation of the barrier, River Neretva (with its increased level of fresh water upstream from the barrier) would serve as source of fresh water available for irrigation.

Mitigation measure scenario M2 was tested as steady state (transient constant) simulation set for the period of 160 years.

Flow boundary conditions for mitigation measure M2 simulation were mean values of all boundary condition determined for existing state simulations. The only exception was boundary condition for River Neretva upstream from barrier near Komin. Head values in the River Neretva upstream from the barrier were elevated for 30 cm based on estimated level of increase. Flow initial condition for mitigation measure M2 simulation were head results of flow steady state simulation.

Transport boundary conditions for mitigation measure M2 simulation were concentration value of 36 g/l along the sea line. Boundary conditions for Opuzen, Mala Neretva and channels were defined as $dC/cX \neq 0$, $dC/dZ \neq 0$. Transport initial condition for mitigation measure M2 simulation were the values of concentration obtained in flow and transport steady state simulation.

Transport boundary conditions for River Neretva was set as concentration value of 36 g/l up to barrier near Komin and as concentration value of 0 g/l upstream from barrier near Komin.

Barrier on River Neretva near Komin with channel parallel with River Neretva (M3)

Barrier on River Neretva near Komin with channel parallel with River Neretva is the third mitigation measure tested in the model and it is based on second mitigation measure scenario. Main idea behind this mitigation measure is that barrier on River Neretva near Komin should increase level of fresh water upstream from the barrier witch is possible to use as a source of fresh water for channel parallel with River Neretva. With barrier on River Neretva near Komin and channel parallel with River Neretva the greater part of the valley has access to fresh water during the whole year.

Mitigation measure scenario M3 was tested as steady state (transient constant) simulation set for the period of 160 years.

Flow boundary conditions for mitigation measure M3 simulation were mean values of all boundary condition determined for existing state simulations. The only exception was boundary condition for River Neretva upstream from barrier near Komin. Head values in the River Neretva upstream from the barrier were elevated for 30 cm based on estimated level of increase. Flow initial condition for mitigation measure M3 simulation were head results of flow steady state simulation.

Transport boundary conditions for mitigation measure M3 simulation were concentration value of 36 g/l along the sea line. Boundary conditions for Opuzen, Mala Neretva and channels were defined as dC/cX≠0, dC/dZ≠0. Transport initial condition for mitigation measure M3 simulation were the values of concentration obtained in flow and transport steady state simulation.

Transport boundary conditions for River Neretva was set as concentration value of 36 g/l up to barrier near Komin and as concentration value of 0 g/l upstream from barrier near Komin. Transport boundary conditions for channel parallel with River Neretva and used as a source of fresh water was set with a concentration value of 0 g/l.

Figure 43 shows transport boundary conditions set for mitigation measure M3.

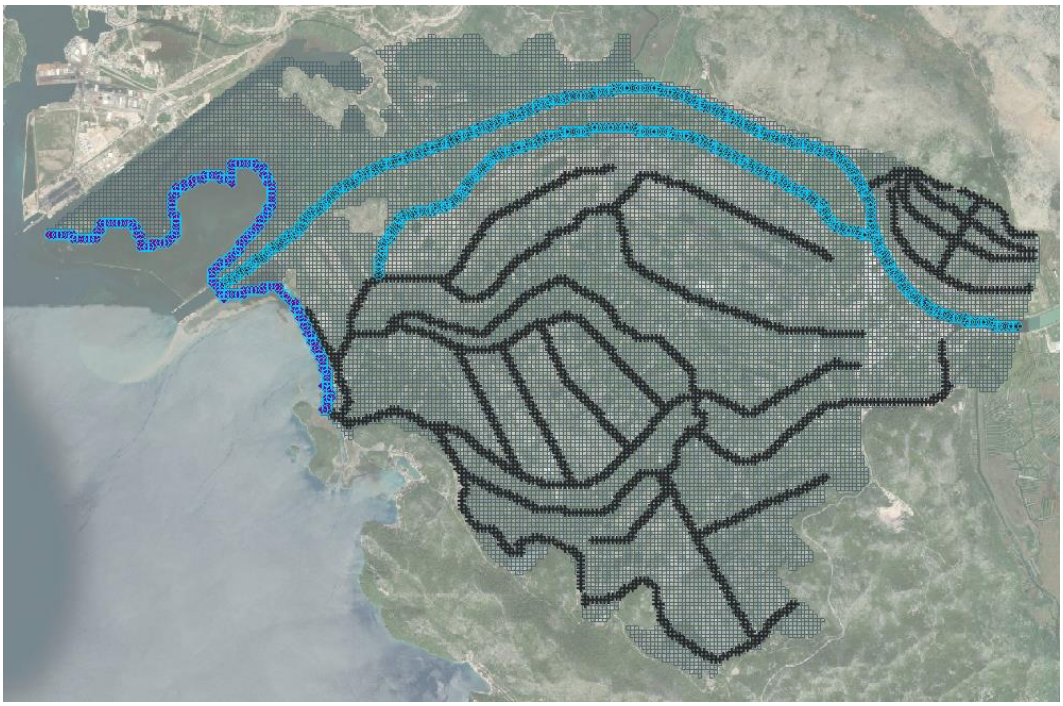

Figure 43 Transport boundary conditions for mitigation measure M3

Model application of mitigation strategies for the selected scenarios of climate changes

Results for all mitigation measures are shown on next figures. Results are shown only for surface layer since the purpose of mitigation measures is to prevent salt water intrusion and improve conditions for agriculture. Since head distribution is connected with channel regime and it is under small influence of climate changes in surface layer, only salinity distribution is shown.

Mitigation measures are marked as follows:

- Impermeable underground barrier below Diga embankment – M1
- Barrier on River Neretva near Komin – M2
- Barrier on River Neretva near Komin with channel parallel with River Neretva – M3

Figure 44 to Figure 47 present transport initial state for mitigation measure scenarios. This salinity fields are result of steady state simulations obtained for climate change scenarios.

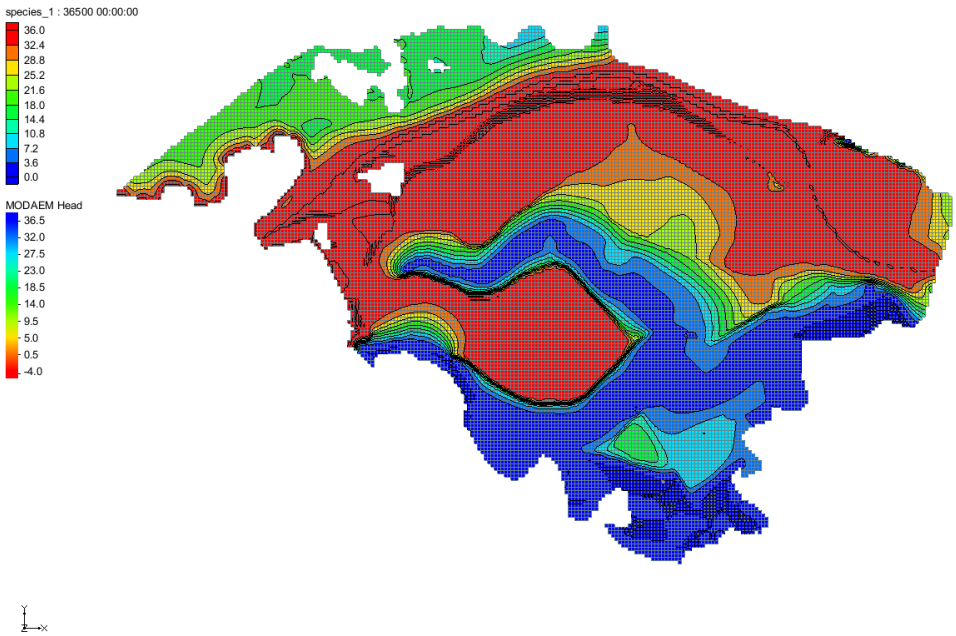

Figure 44 Salinity field in the layer of sand for SLR for 43 cm

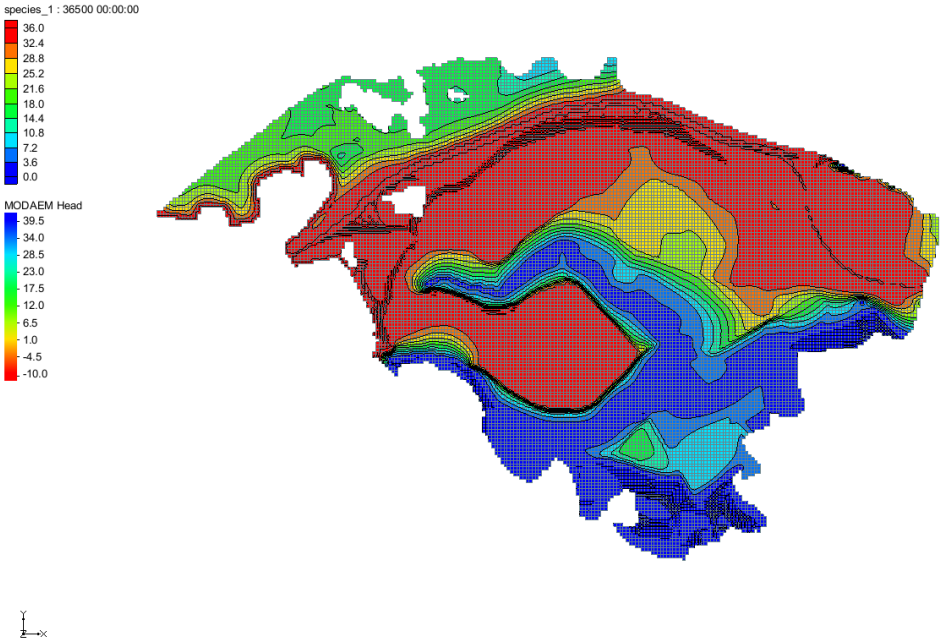

Figure 45 Salinity field in the layer of sand for SLR for 84 cm

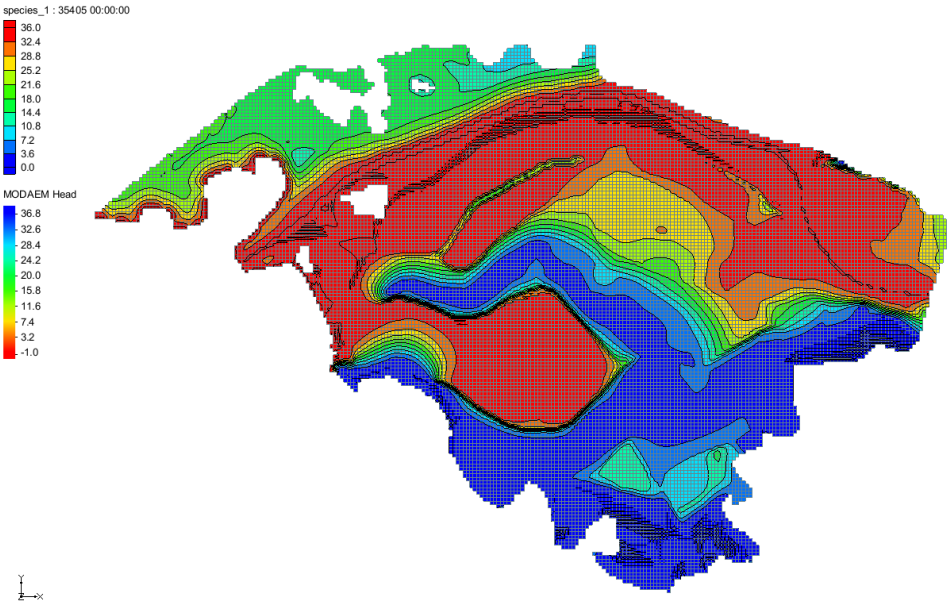

Figure 46 Salinity field in the layer of sand for precipitation decline for 10%

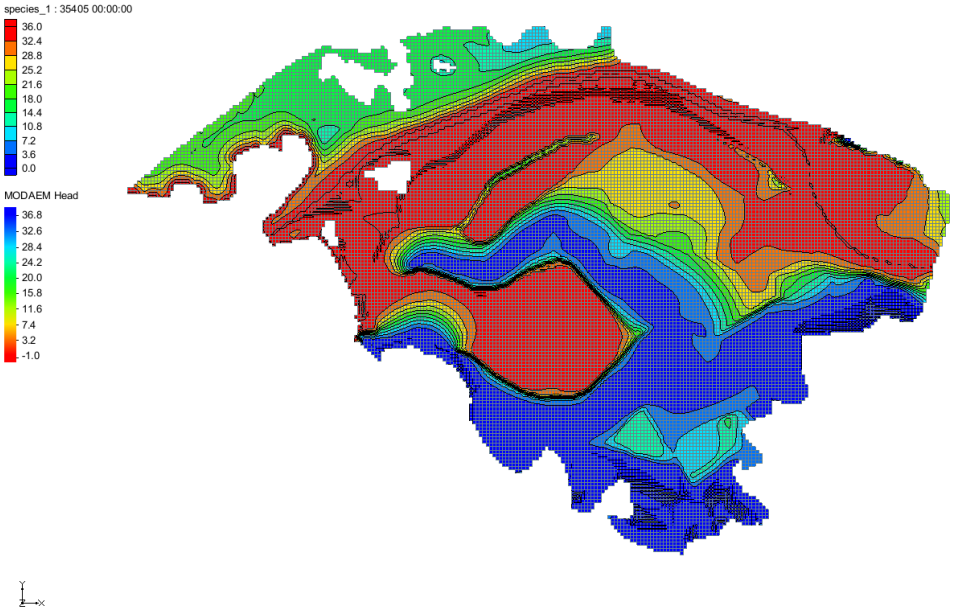

Figure 47 Salinity field in the layer of sand for precipitation decline for 20%

Changes in head and concentration for all piezometer location due to selected climate change scenarios are numerically shown in Table 1 and Table 2. Based on the figures presenting climate change final results, it is possible to conclude that changes in head and concentration for all climate change scenarios and on all locations shown on the model scale look quite similar.

Next figures present salinity fields for different mitigation measures after 1 and 160 years. Since the figures for different climate change scenarios look quite similar, only representative figures are presented.

Exact values for different climate change and locations are shown in next chapter.

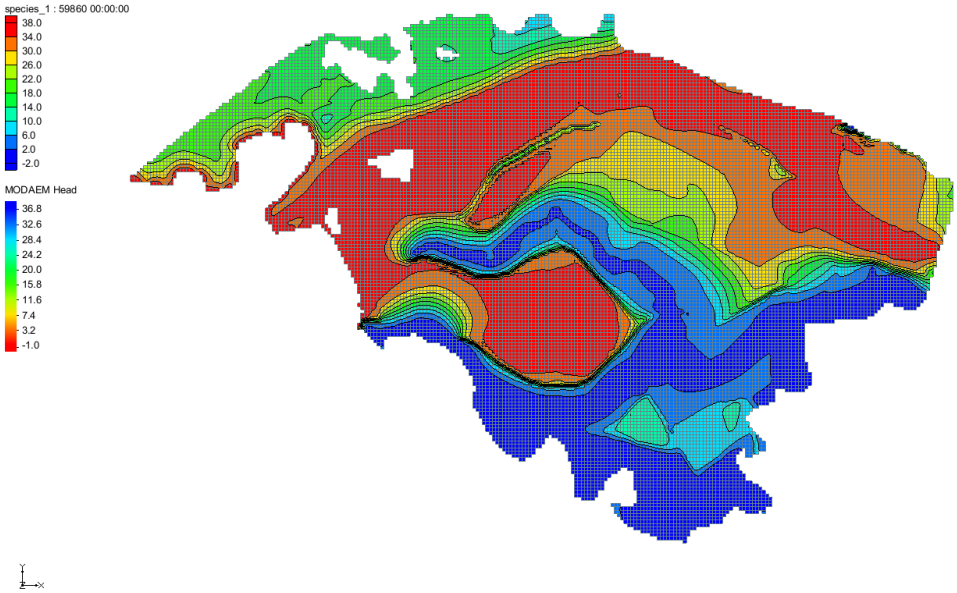

Figure 48 Salinity field for the layer of sand after 160 years due to mitigation measure M1

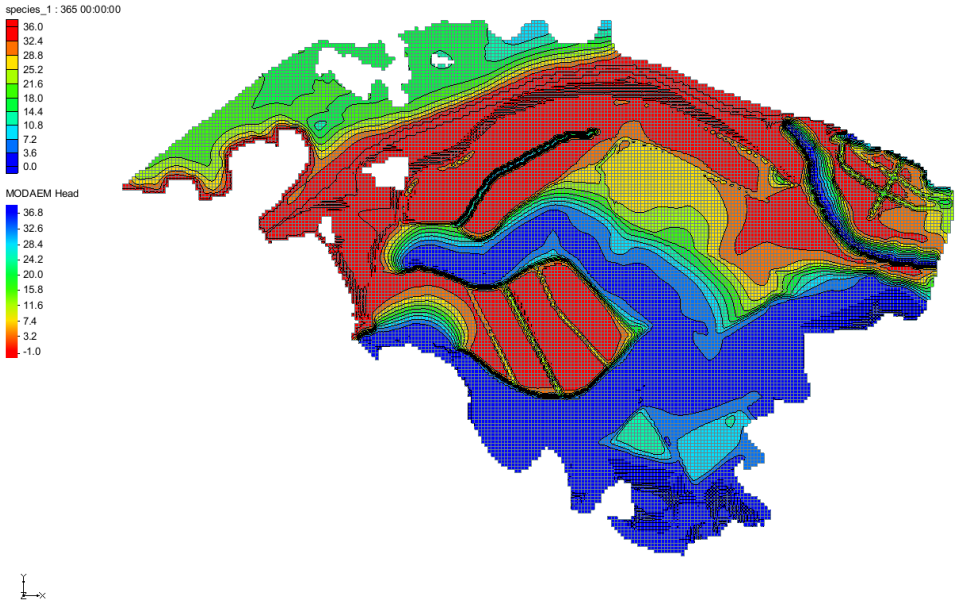

Figure 49 Salinity field for the layer of sand after 1 year due to mitigation measure M2

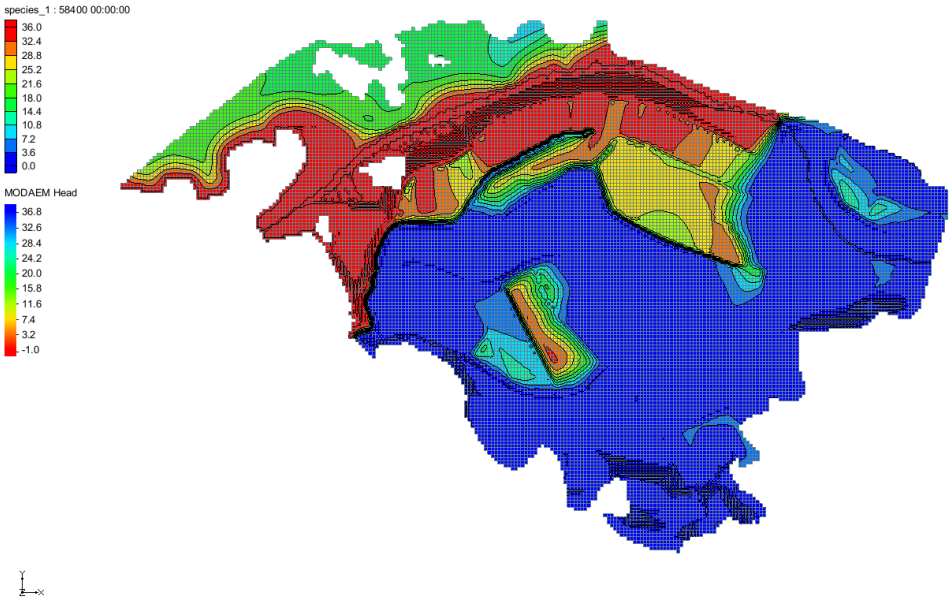

Figure 50 Salinity field for the layer of sand after 160 years due to mitigation measure M2

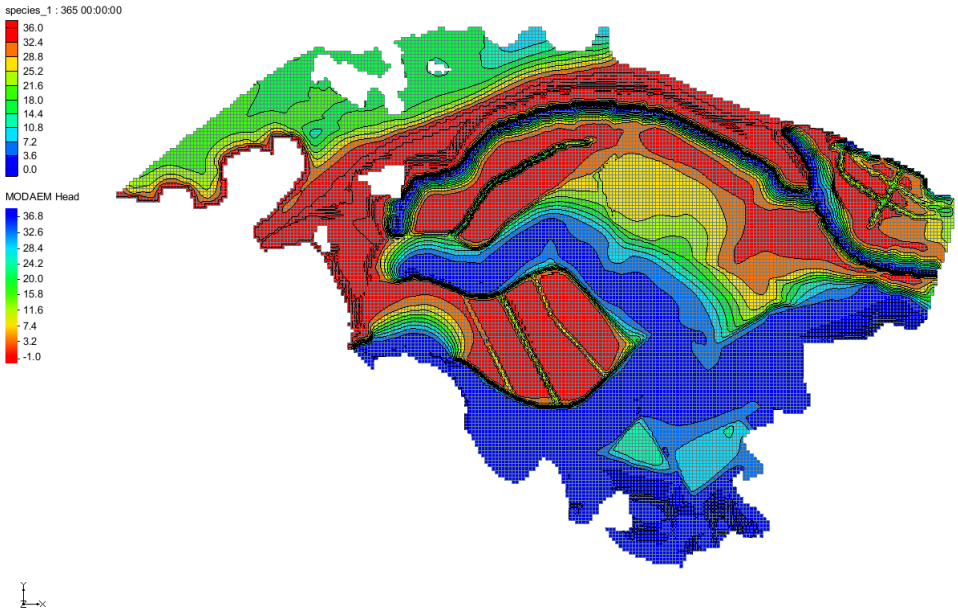

Figure 51 Salinity field for the layer of sand after 1 year due to mitigation measure M3

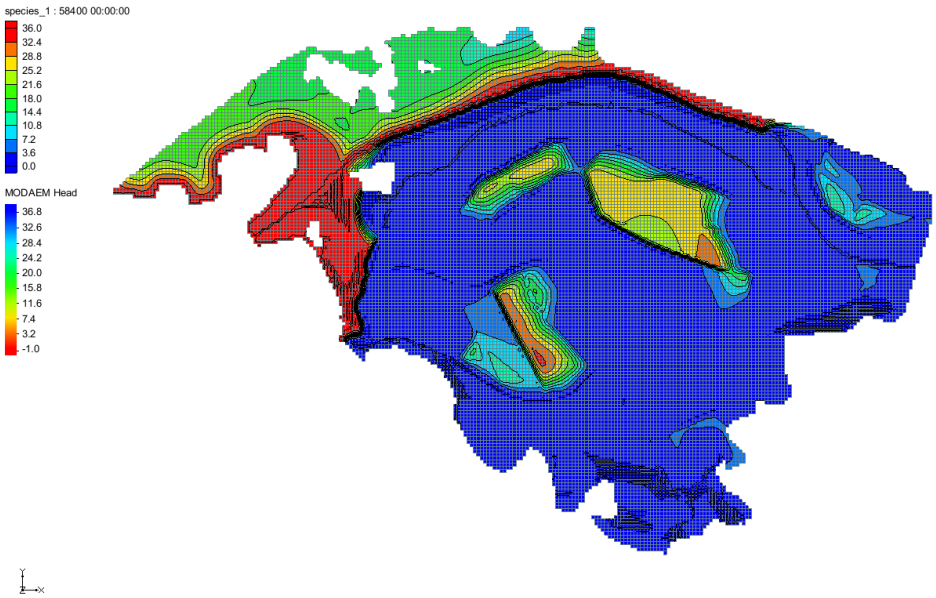

Figure 52 Salinity field for the layer of sand after 160 years due to mitigation measure M3

The efficiency of mitigation strategies for the selected scenarios of climate changes – numerical modelling

On the next figures change of concentration values is shown for three shallow piezometers due to mitigation measures for scenarios after climate changes. Period of 160 years is shown and in that period steady state is established in all locations.

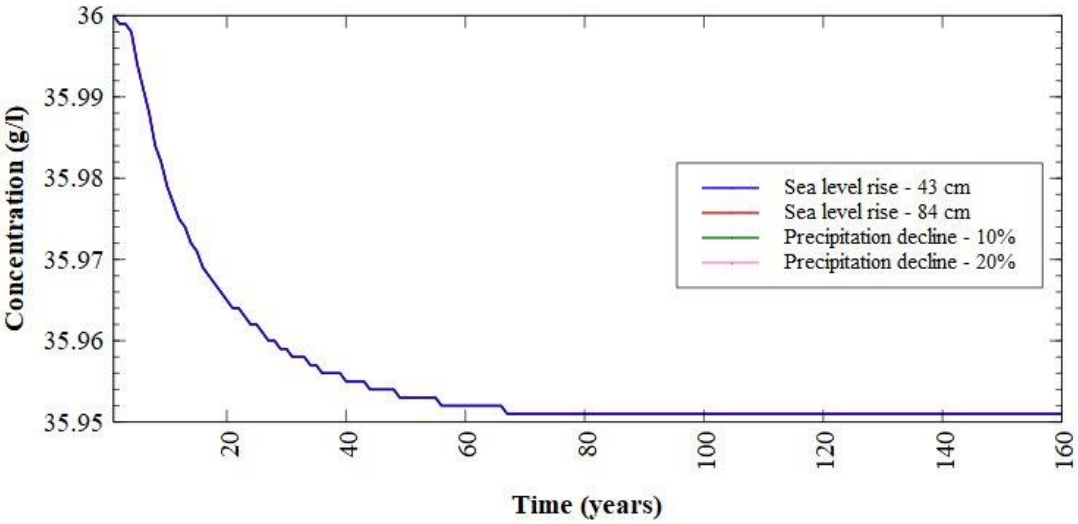

Figure 53 Change of concentration for piezometer P1 for mitigation measure M1 after climate changes

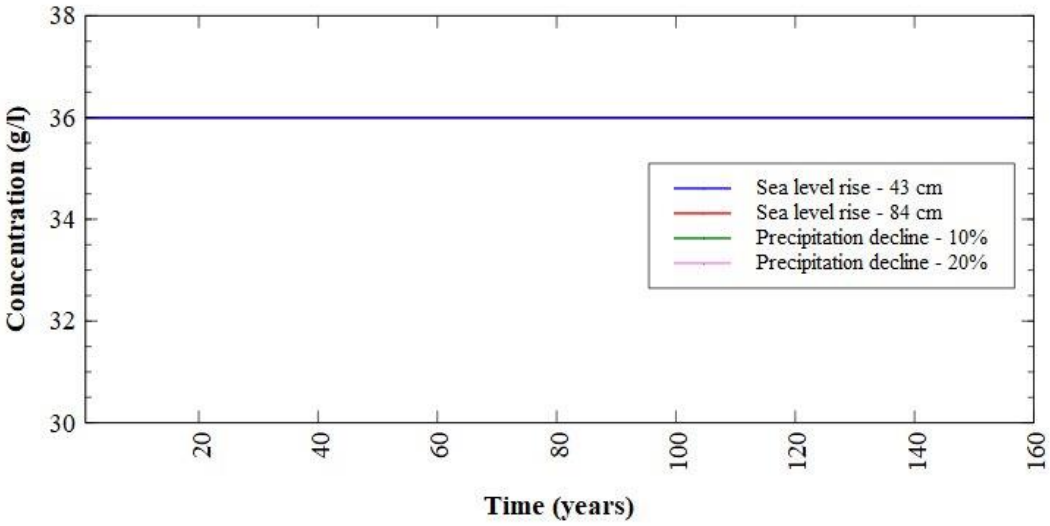

Figure 54 Change of concentration for piezometer P1 for mitigation measure M2 after climate changes

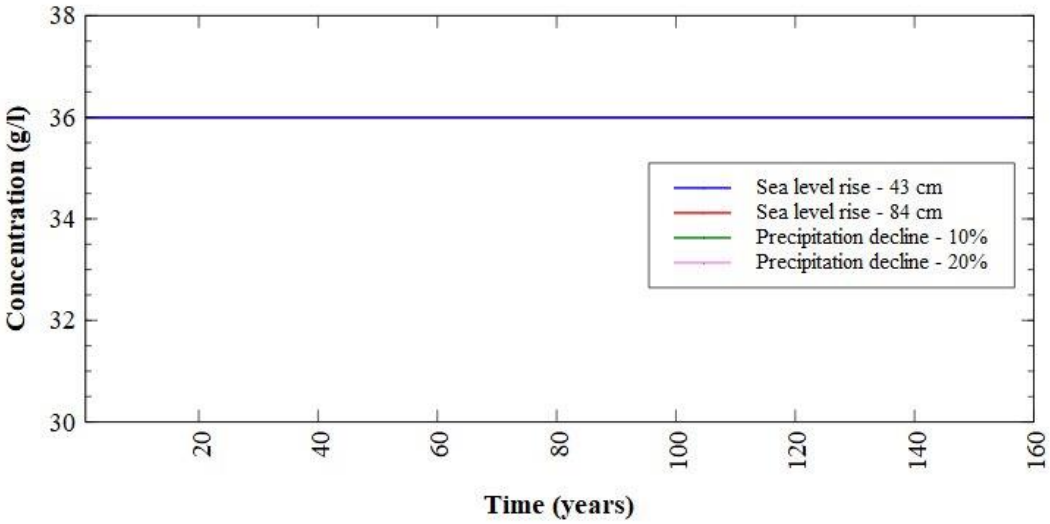

Figure 55 Change of concentration for piezometer P1 for mitigation measure M3 after climate changes

Table 3 Change of concentration and time needed to achieve steady state on location P1 for all mitigation measures after climate changes

		Mitigation measure M1	Mitigation measure M2	Mitigation measure M3
Change of concentration (g/l)	0.43 m SLR	-0.05	0	0
	0.84 m SLR	-0.05	0	0
	10% precipitation decline	-0.05	0	0
	20% precipitation decline	-0.05	0	0
Time needed to achieve steady state (years)	0.43 m SLR	67	0	0
	0.84 m SLR	67	0	0
	10% precipitation decline	67	0	0
	20% precipitation decline	67	0	0

Based on Figure 53 to Figure 55 and Table 3 it is possible to conclude that changes of concentration values on location P1 are quite small. The only mitigation measure that shows any effect at lowering concentration values is mitigation measure M1 (impenetrable underground barrier bellow Diga embankment). Mitigation measure M1 lowers concentration value for 0.05 g/l during the period of 67 years after all climate changes. The reason for low efficiency of mitigation measures on lowering concentration on location P1 is its vicinity to the sea and permeability of Diga embankment.

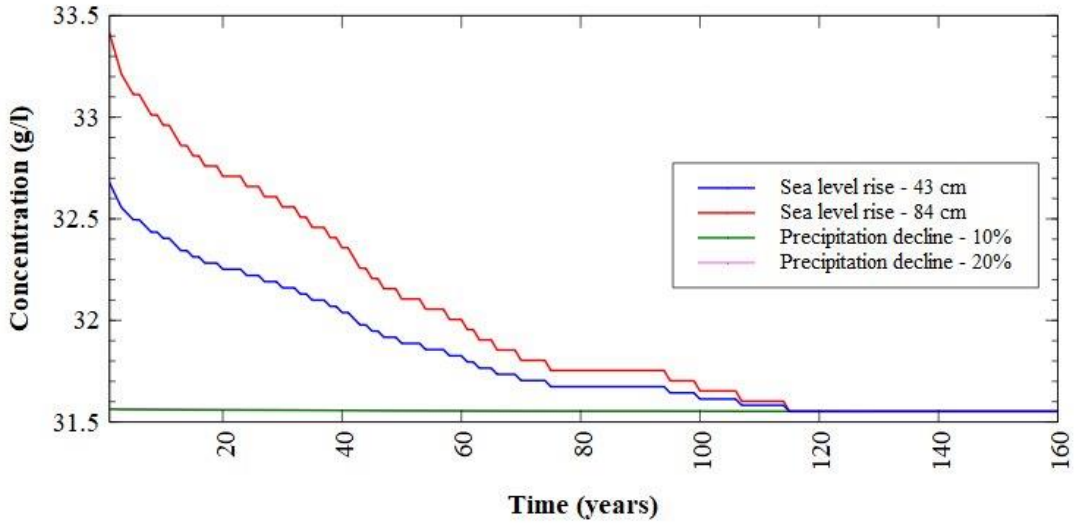

Figure 56 Change of concentration for piezometer P2 for mitigation measure M1 after climate changes

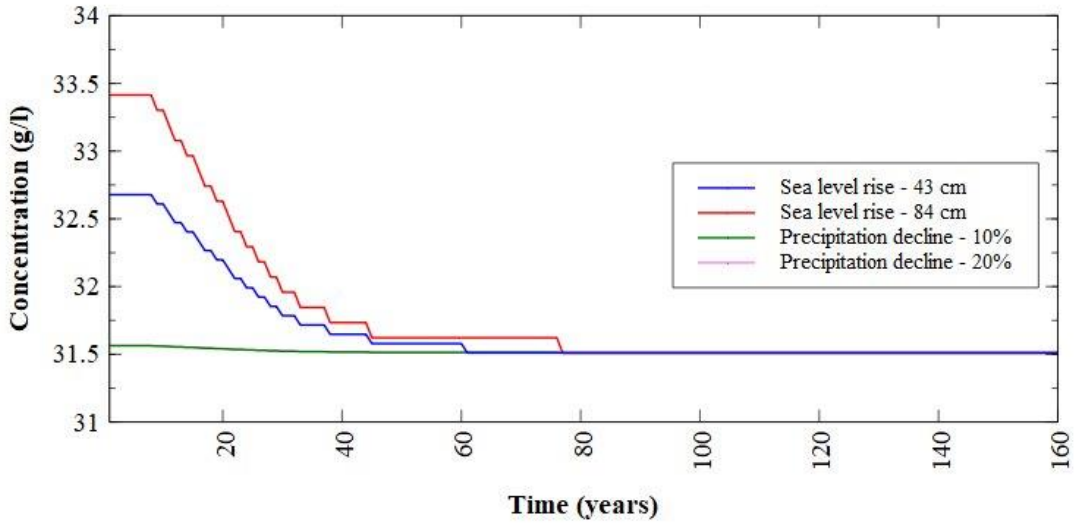

Figure 57 Change of concentration for piezometer P2 for mitigation measure M2 after climate changes

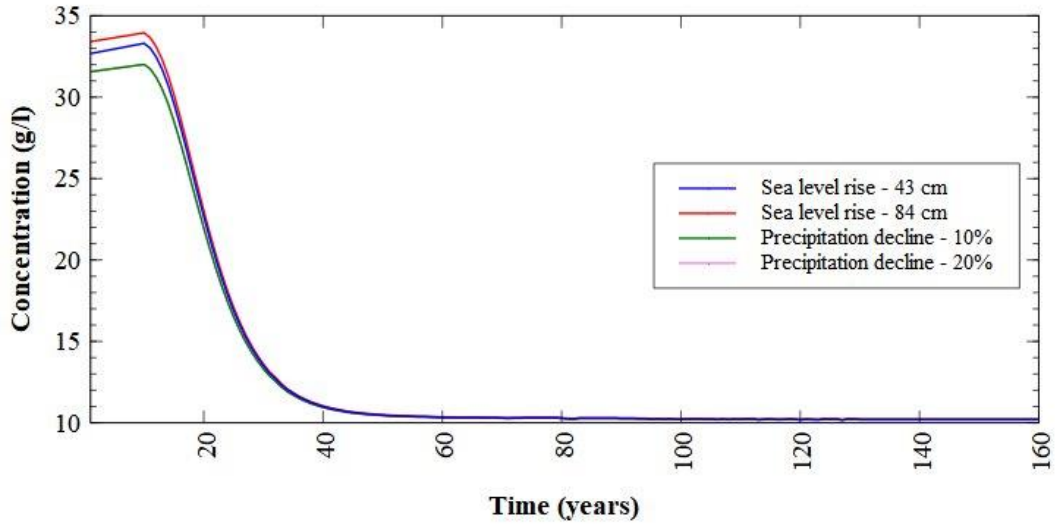

Figure 58 Change of concentration for piezometer P2 for mitigation measure M3 after climate changes

Table 4 Change of concentration and time needed to achieve steady state on location P2 for all mitigation measures after climate changes

		Mitigation measure M1	Mitigation measure M2	Mitigation measure M3
Change of concentration (g/l)	0.43 m SLR	-1.126	-1.168	-22.504
	0.84 m SLR	-1.862	-1.904	-23.227
	10% precipitation decline	-0.012	-0.053	-21.397
	20% precipitation decline	-0.015	-0.056	-21.400
Time needed to achieve steady state (years)	0.43 m SLR	115	60	130
	0.84 m SLR	120	76	132
	10% precipitation decline	38	33	50
	20% precipitation decline	40	34	51

Based on Figure 56 to Figure 58 it is possible to sea changes of concentration for location P2 for mitigation measures after climate changes. From the Table 4 it is possible to conclude that mitigation measures M1 and M2 have very limited range in lowering concentration values. In both cases concentration value is reduced up to 2 g/l during the period of 120 years.

Mitigation measure M3 (barrier on River Neretva near Komin with channel parallel with River Neretva) shows best results and lowers concentration on the value around 10.2 g/l during the period of 132 years and the biggest drop in concentration values is during the first 50 years. Concentration on location P2 is lowered due to channel parallel with River Neretva that is a new source of fresh water in that area of the valley.

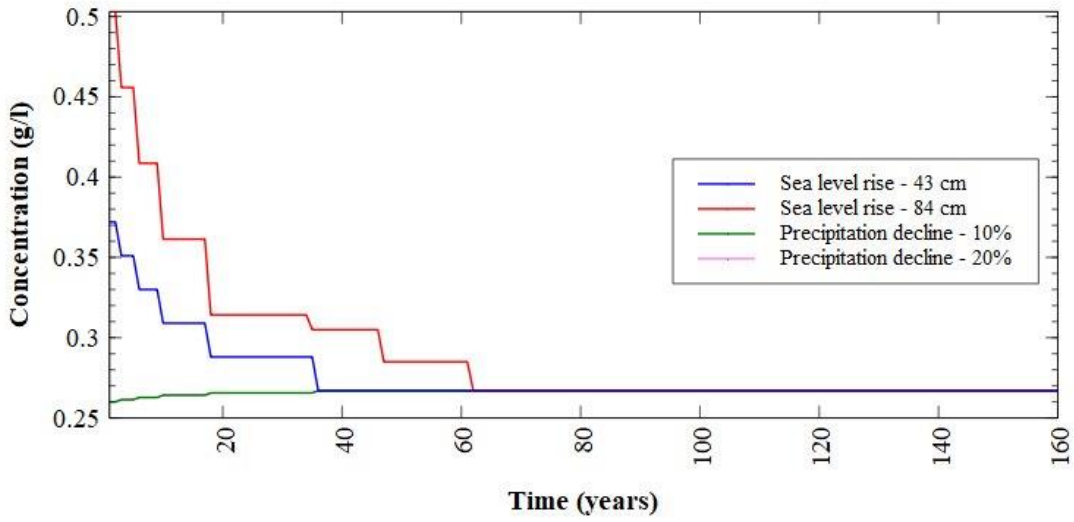

Figure 59 Change of concentration for piezometer P4 for mitigation measure M1 after climate changes

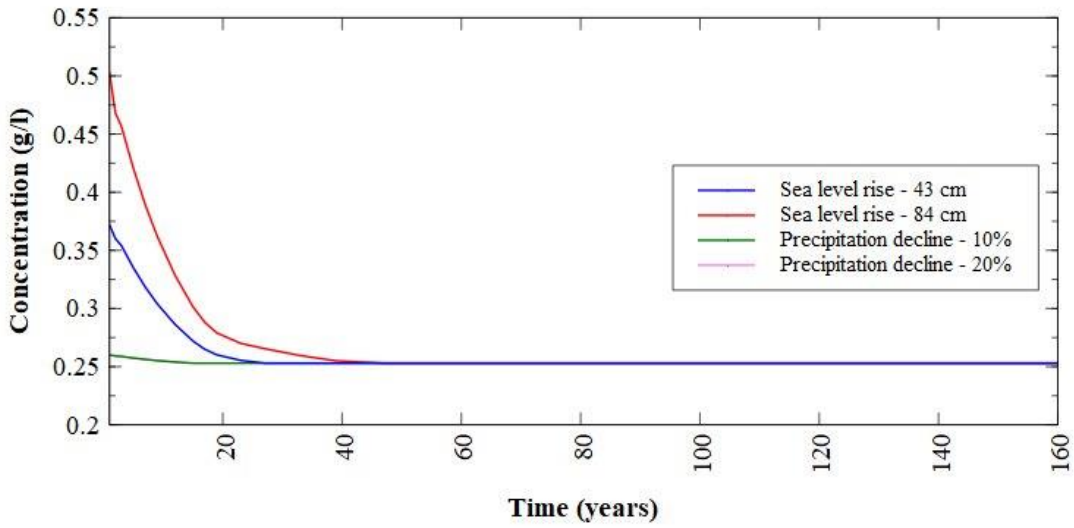

Figure 60 Change of concentration for piezometer P4 for mitigation measure M2 after climate changes

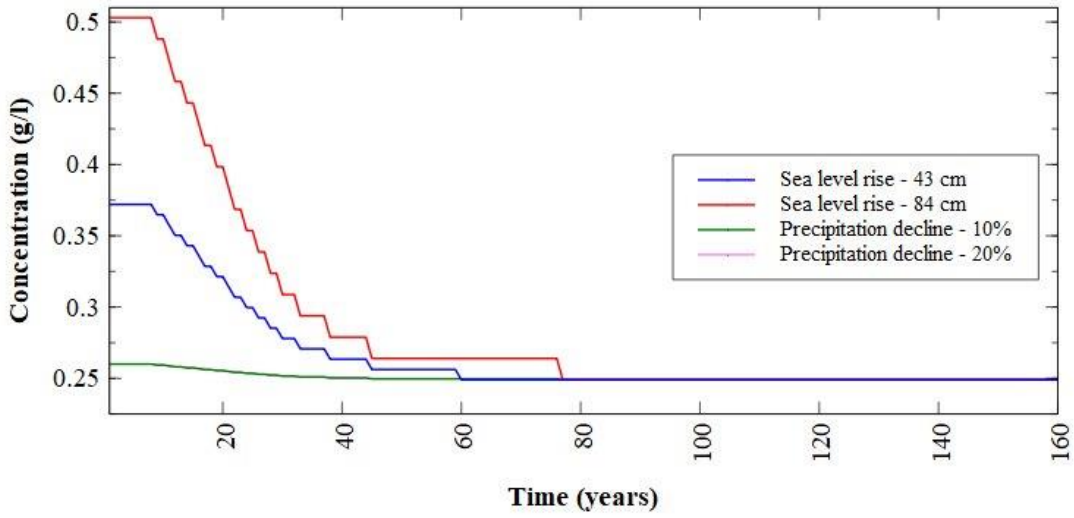

Figure 61 Change of concentration for piezometer P4 for mitigation measure M3 after climate changes

Table 5 Change of concentration and time needed to achieve steady state on location P4 for all mitigation measures after climate changes

		Mitigation measure M1	Mitigation measure M2	Mitigation measure M3
Change of concentration (g/l)	0.43 m SLR	-0.105	-0.119	-0.123
	0.84 m SLR	-0.236	-0.250	-0.254
	10% precipitation decline	-0.007	-0.007	-0.011
	20% precipitation decline	-0.007	-0.007	-0.011
Time needed to achieve steady state (years)	0.43 m SLR	36	27	60
	0.84 m SLR	62	46	77
	10% precipitation decline	36	15	45
	20% precipitation decline	36	15	45

On Figure 59 to Figure 61 and Table 5 it is possible to sea changes of concentration for location P4 for mitigation measures after climate changes. Since the location P4 is under greatest influence of River Mala Neretva, which is the source of fresh water during the whole year, local channels and pumping station Prag-Vidrice starting concentration values on location P4 are not high and all mitigation measures show similar results.

Laboratory modelling of active seawater conditions

To perform analysis of the seawater cline in active conditions along the Neretva coastal area, a number of laboratory experiments have been performed. To include climate change scenarios, seawater and inland water levels changes have been performed. In this way, climate changes of seawater elevation change, inland water change due to the precipitation and evapotranspiration changes have been performed.

For this purpose, natural conditions of the active seawater cline have been demonstrated for different gradients in Figure 62 to Figure 71 and Figure 72 to Figure 76.

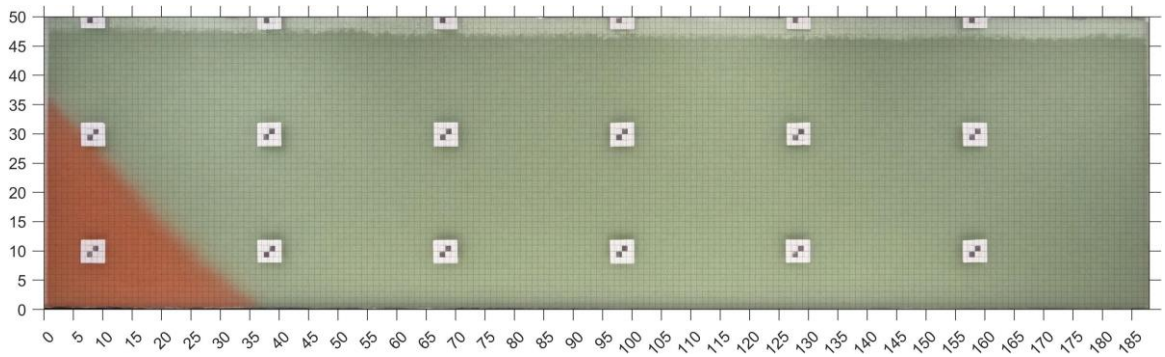

Figure 62 Sea water cline at t= 10 min for the active intrusion hSEA = 40 cm; hINLAND=39 cm

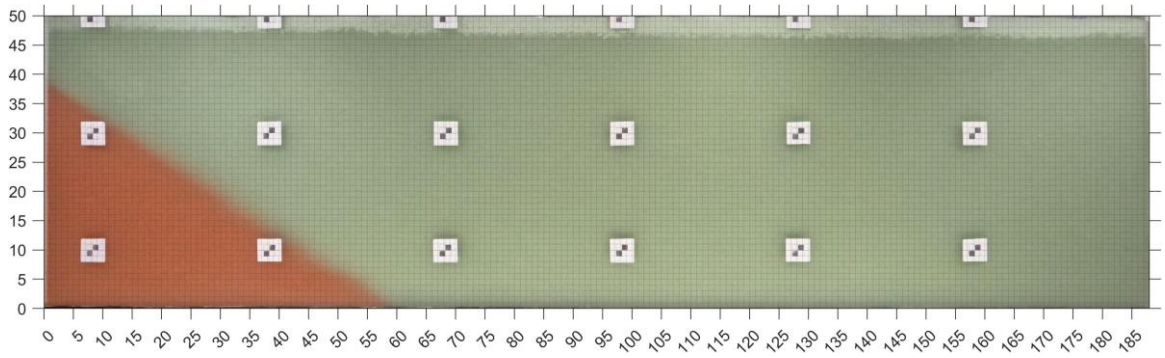

Figure 63 Sea water cline at t= 20 min for the active intrusion hSEA = 40 cm; hINLAND=39 cm

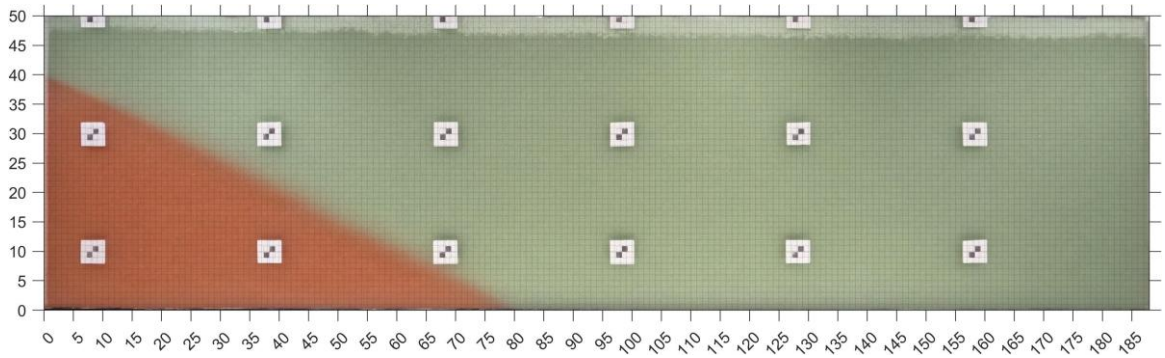

Figure 64 Sea water cline at t= 30 min for the active intrusion hSEA = 40 cm;hINLAND=39 cm

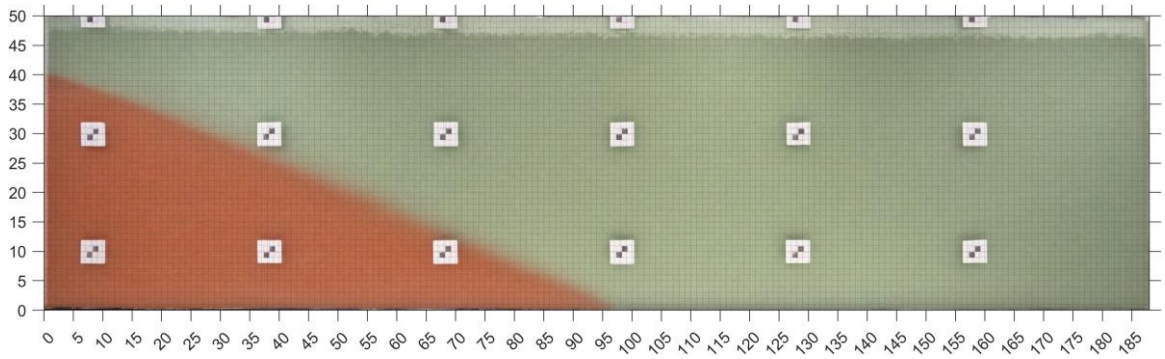

Figure 65 Sea water cline at t= 40 min for the active intrusion hSEA = 40 cm;hINLAND=39 cm

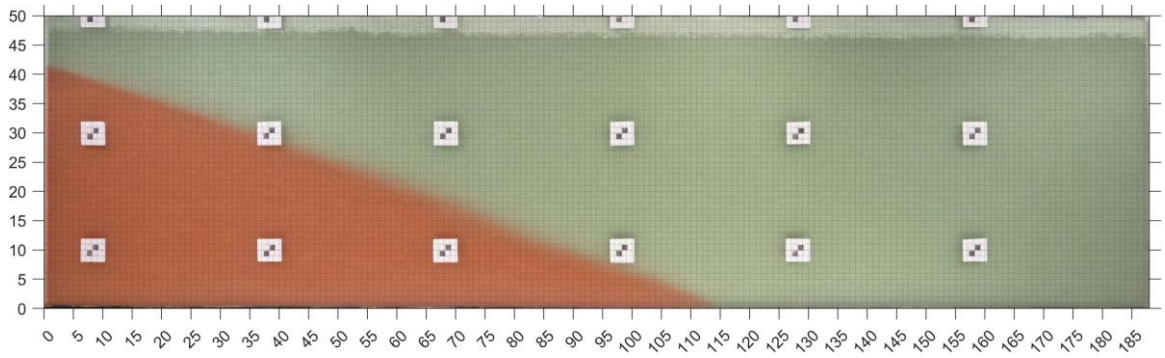

Figure 66 Sea water cline at t= 50 min for the active intrusion hSEA = 40 cm;hINLAND=39 cm

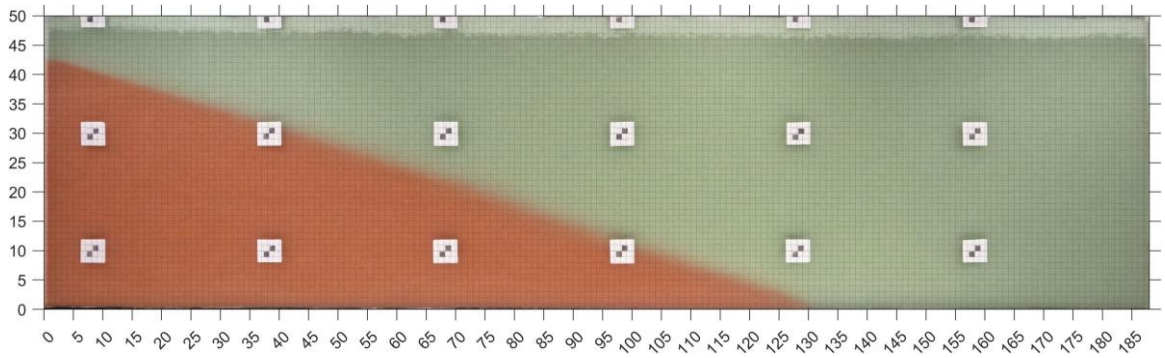

Figure 67 Sea water cline at t= 60 min for the active intrusion hSEA = 40 cm;hINLAND=39 cm

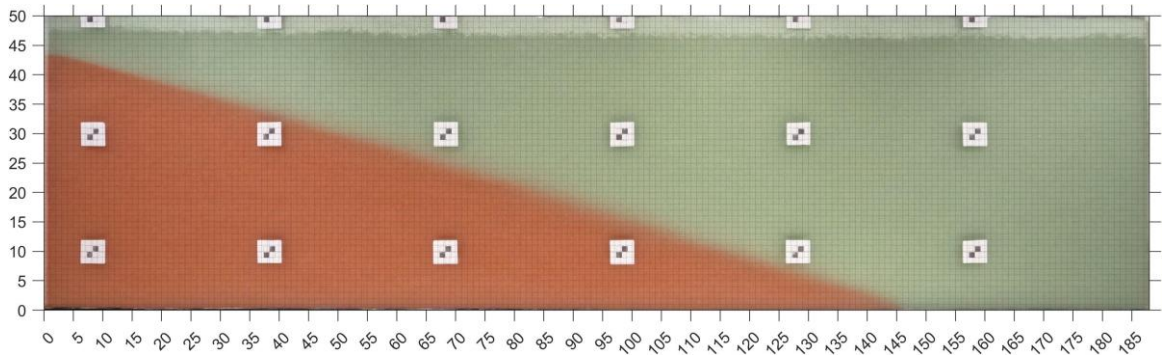

Figure 68 Sea water cline at t= 70 min for the active intrusion hSEA = 40 cm;hINLAND=39 cm

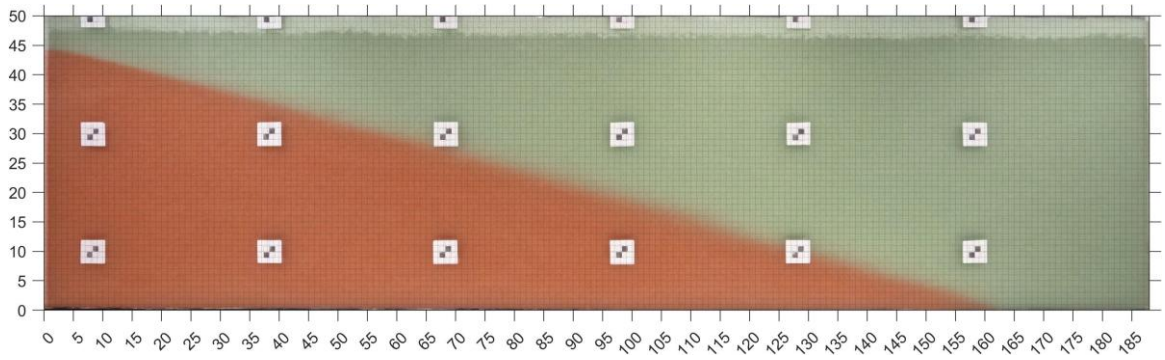

Figure 69 Sea water cline at t= 80 min for the active intrusion hSEA = 40 cm;hINLAND=39 cm

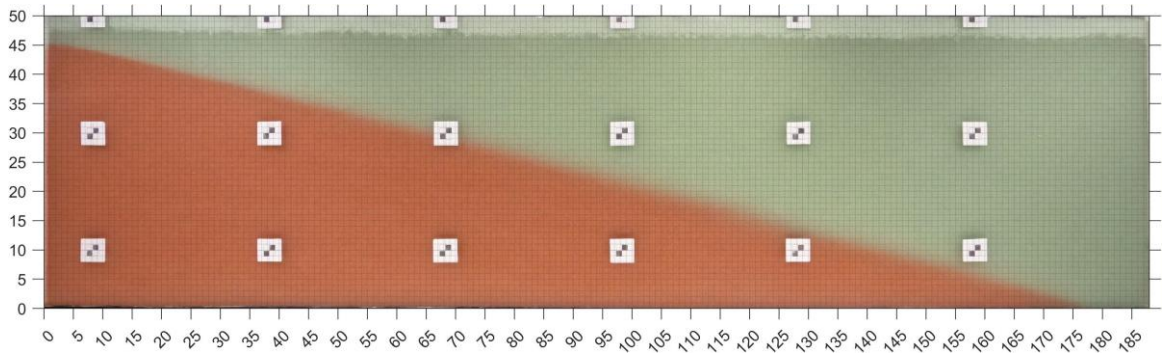

Figure 70 Sea water cline at t= 90 min for the active intrusion hSEA = 40 cm;hINLAND=39 cm

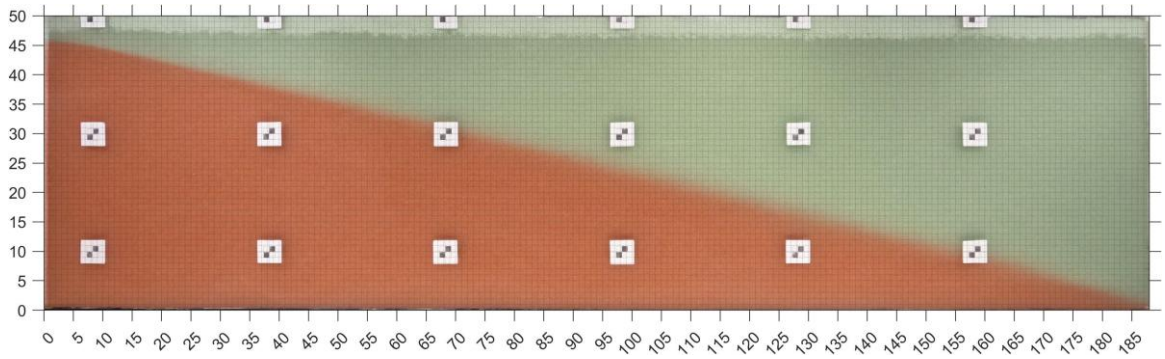

Figure 71 Sea water cline at t= 100 min for the active intrusion hSEA = 40 cm;hINLAND=39 cm

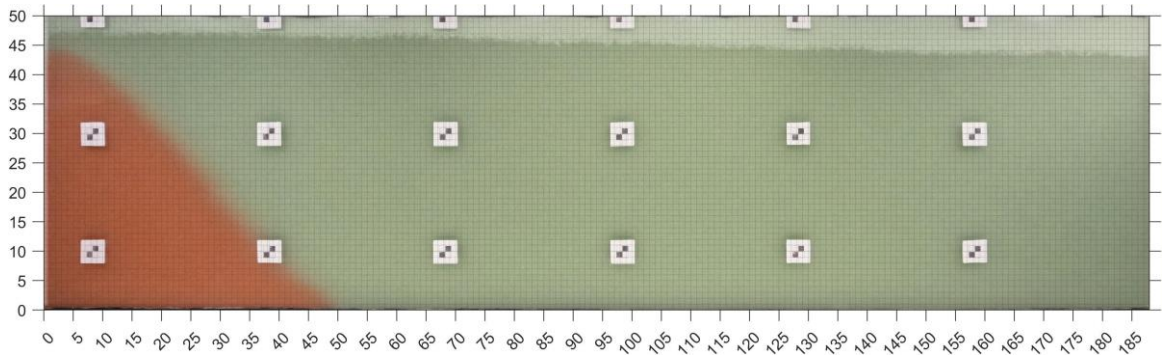

Figure 72 Sea water cline at t= 10 min for the active intrusion hSEA = 40 cm;hINLAND=36 cm

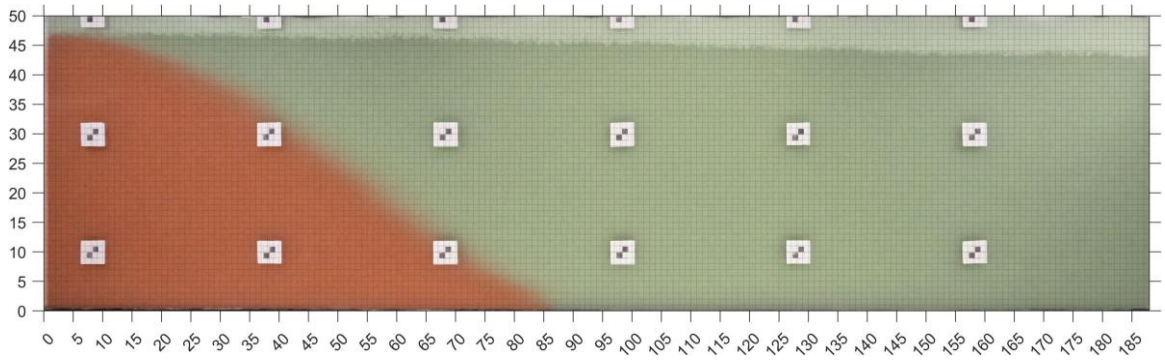

Figure 73 Sea water cline at t= 20 min for the active intrusion hSEA = 40 cm;hINLAND=36 cm

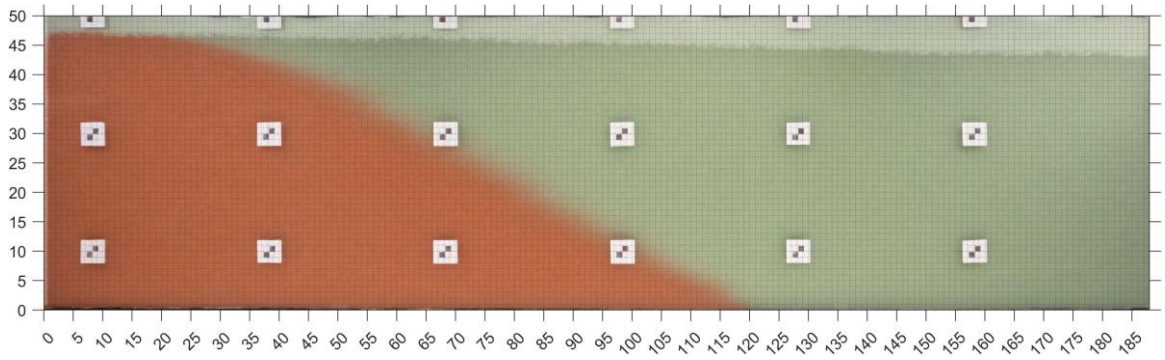

Figure 74 Sea water cline at t= 30 min for the active intrusion hSEA = 40 cm;hINLAND=36 cm

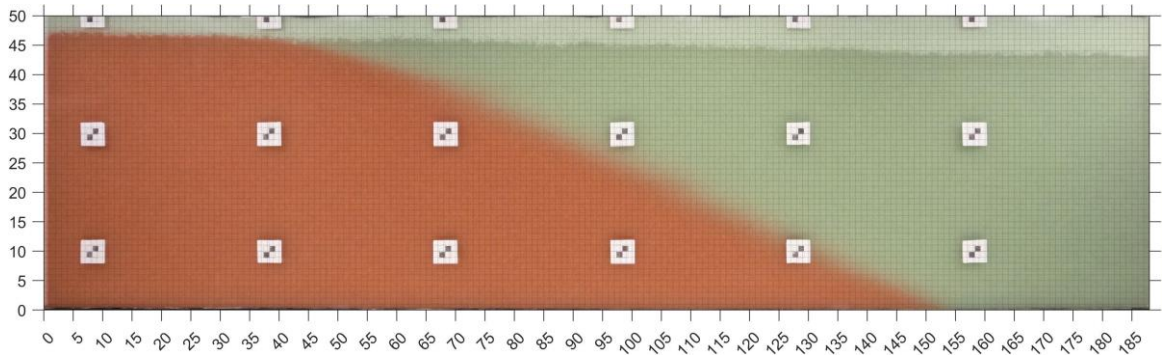

Figure 75 Sea water cline at t= 40 min for the active intrusion hSEA = 40 cm;hINLAND=36 cm

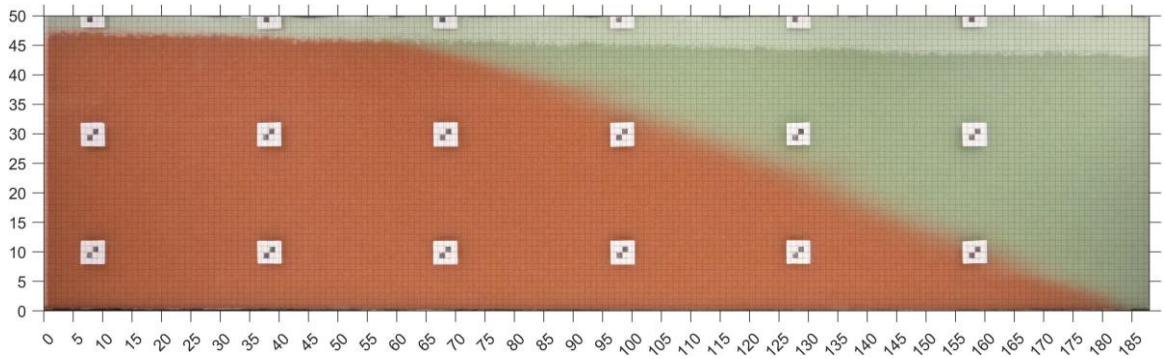

Figure 76 Sea water cline at t= 50 min for the active intrusion hSEA = 40 cm;hINLAND=36 cm

Laboratory modelling of mitigation measures- impermeable submerged barrier

Influence of the partially penetrated impermeable barrier to seawater cline features for different conditions have been analysed and presented below. For this purpose, mitigated conditions of the active seawater cline have been demonstrated for different gradients in Figure 77 to Figure 88and Figure 89 to **Error! Reference source not found.**.

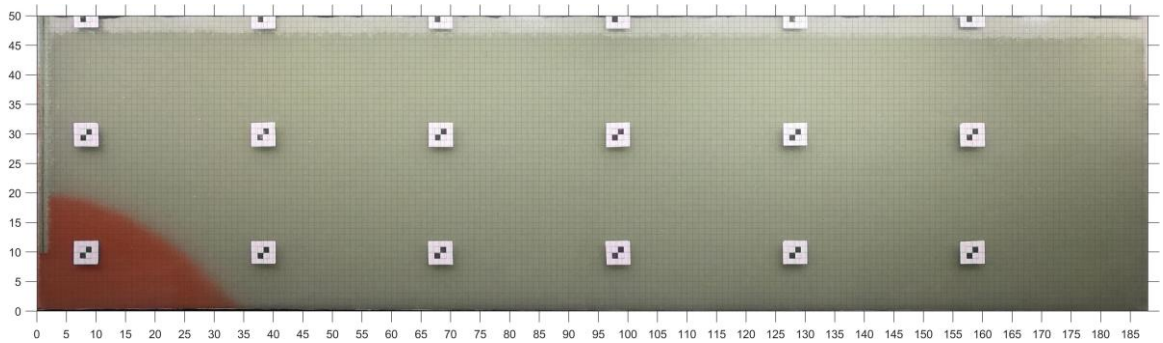

Figure 77 Sea water cline at t= 10 min for the active intrusion hSEA = 40 cm;hINLAND=39 cm and impermeable barrier depth d = 30 cm

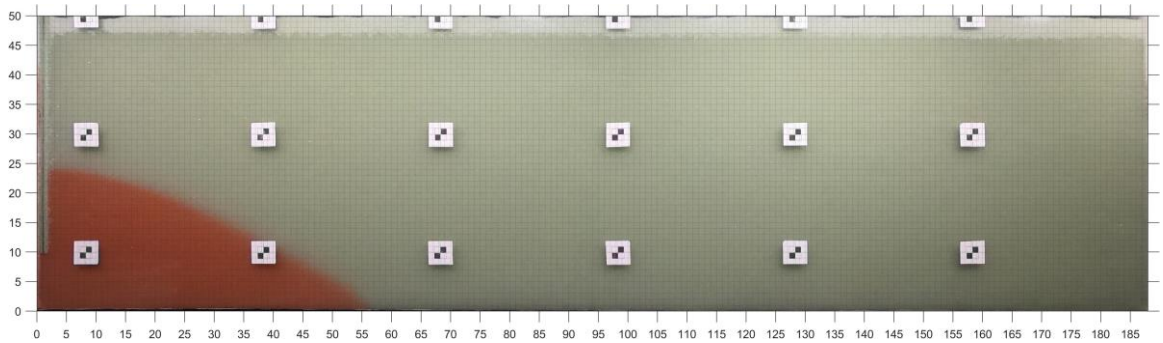

Figure 78 Sea water cline at t= 20 min for the active intrusion hSEA = 40 cm;hINLAND=39 cm and impermeable barrier depth d = 30 cm

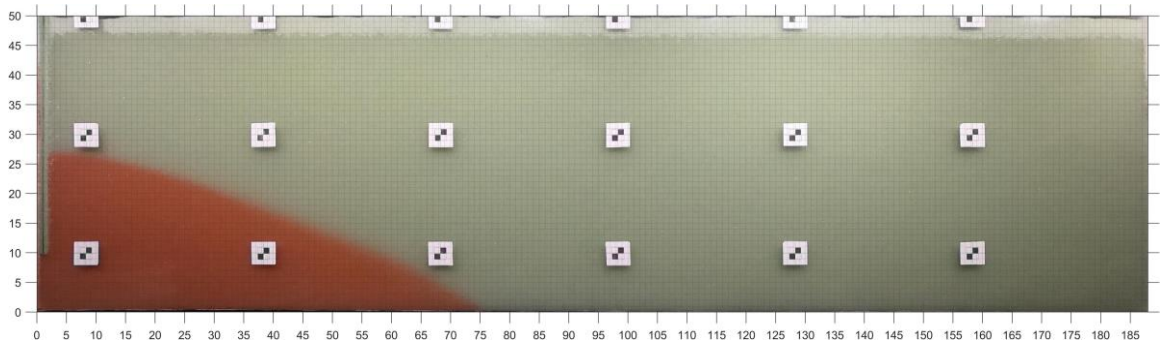

Figure 79 Sea water cline at t= 30 min for the active intrusion hSEA = 40 cm;hINLAND=39 cm and impermeable barrier depth d = 30 cm

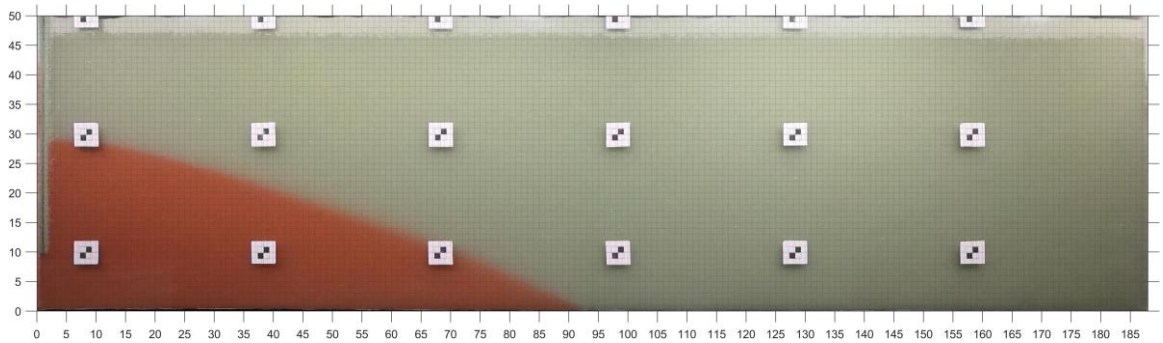

Figure 80 Sea water cline at t= 40 min for the active intrusion hSEA = 40 cm;hINLAND=39 cm and impermeable barrier depth d = 30 cm

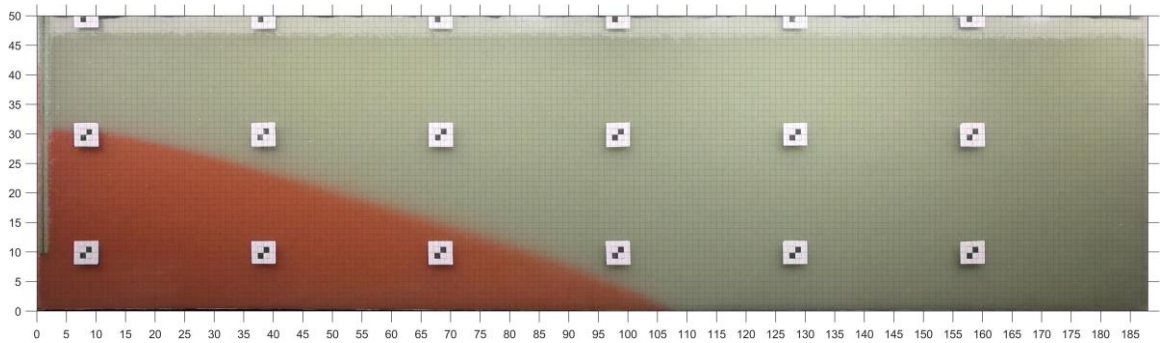

Figure 81 Sea water cline at t= 50 min for the active intrusion hSEA = 40 cm;hINLAND=39 cm and impermeable barrier depth d = 30 cm

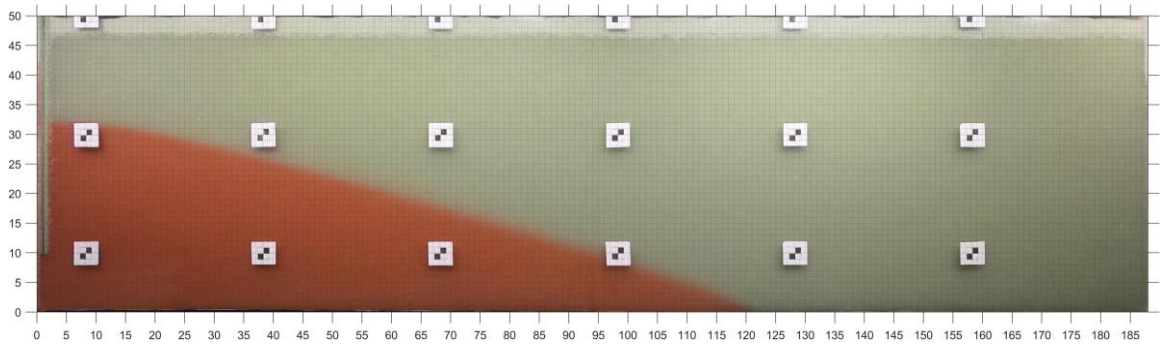

Figure 82 Sea water cline at t= 60 min for the active intrusion hSEA = 40 cm;hINLAND=39 cm and impermeable barrier depth d = 30 cm

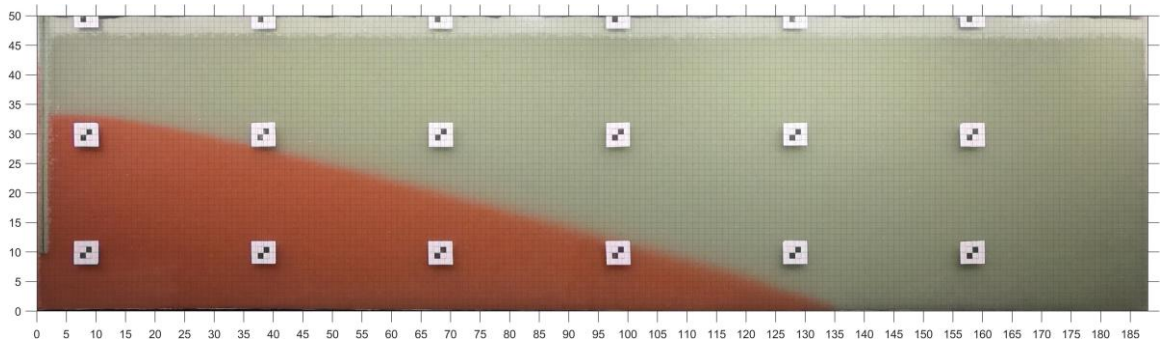

Figure 83 Sea water cline at t= 70 min for the active intrusion hSEA = 40 cm;hINLAND=39 cm and impermeable barrier depth d = 30 cm

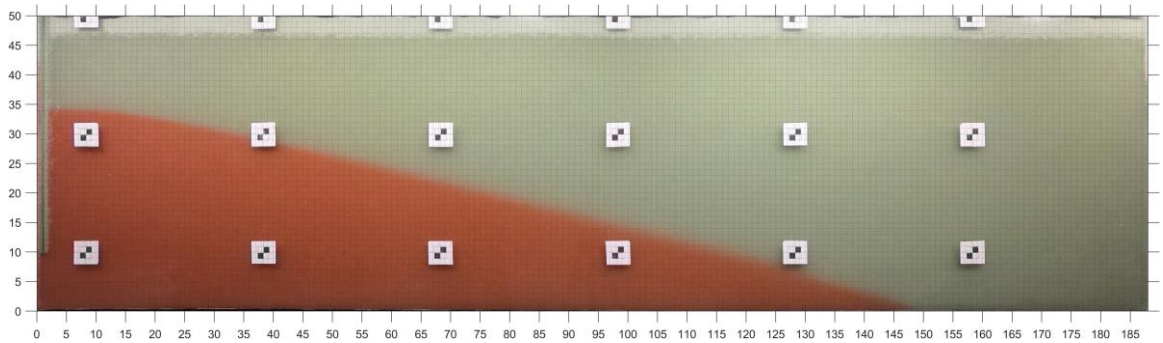

Figure 84 Sea water cline at t= 80 min for the active intrusion hSEA = 40 cm;hINLAND=39 cm and impermeable barrier depth d = 30 cm

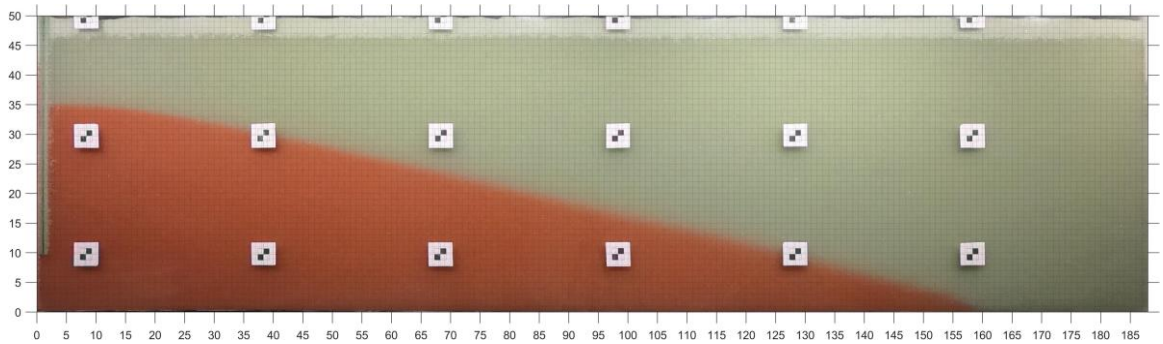

Figure 85 Sea water cline at t= 90 min for the active intrusion hSEA = 40 cm;hINLAND=39 cm and impermeable barrier depth d = 30 cm

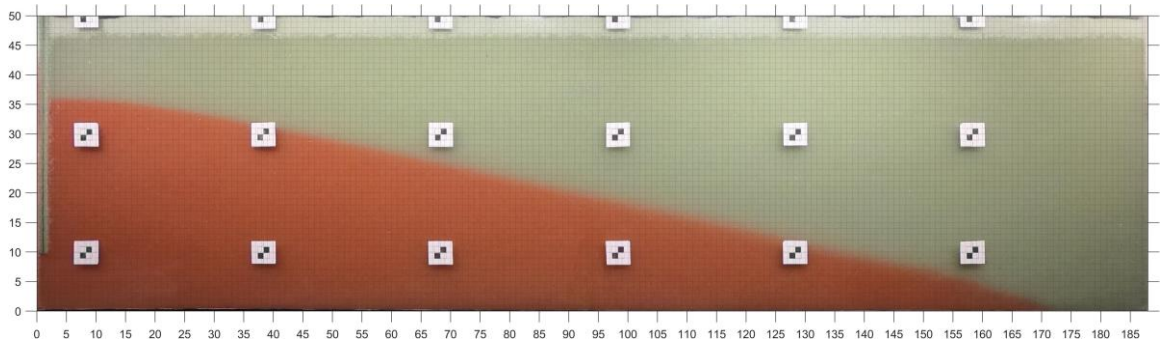

Figure 86 Sea water cline at t= 100 min for the active intrusion hSEA = 40 cm;hINLAND=39 cm and impermeable barrier depth d = 30 cm

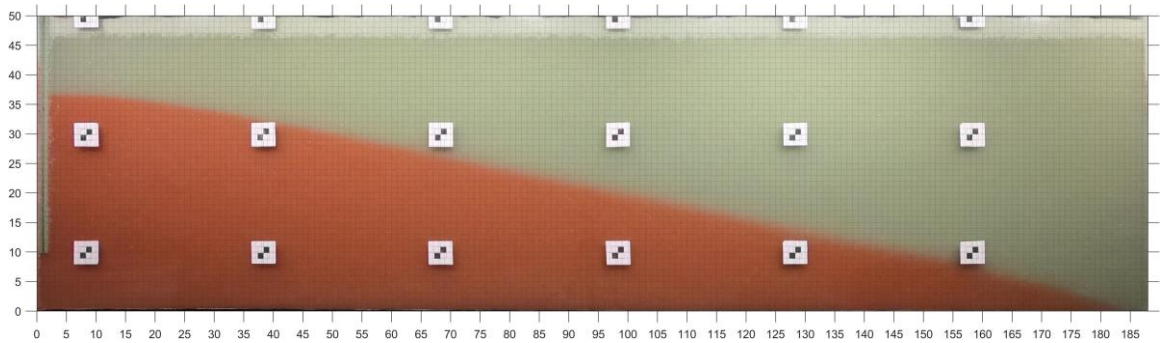

Figure 87 Sea water cline at t= 110 min for the active intrusion hSEA = 40 cm;hINLAND=39 cm and impermeable barrier depth d = 30 cm

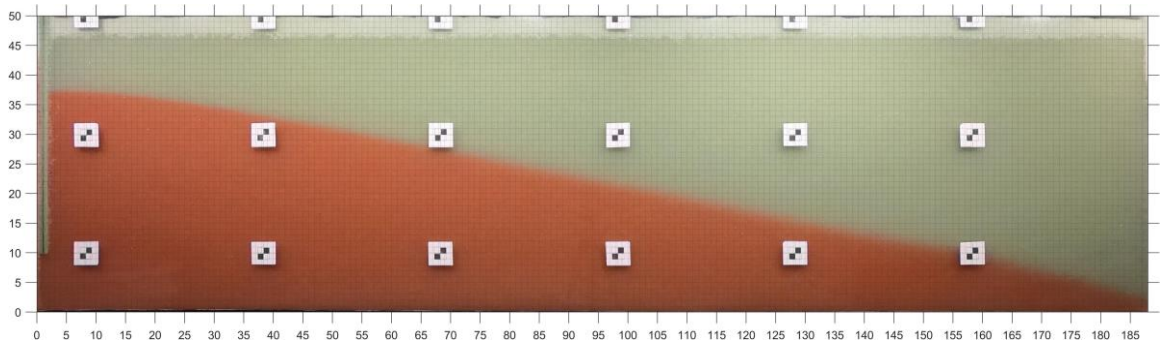

Figure 88 Sea water cline at t= 120 min for the active intrusion hSEA = 40 cm;hINLAND=39 cm and impermeable barrier depth d = 30 cm

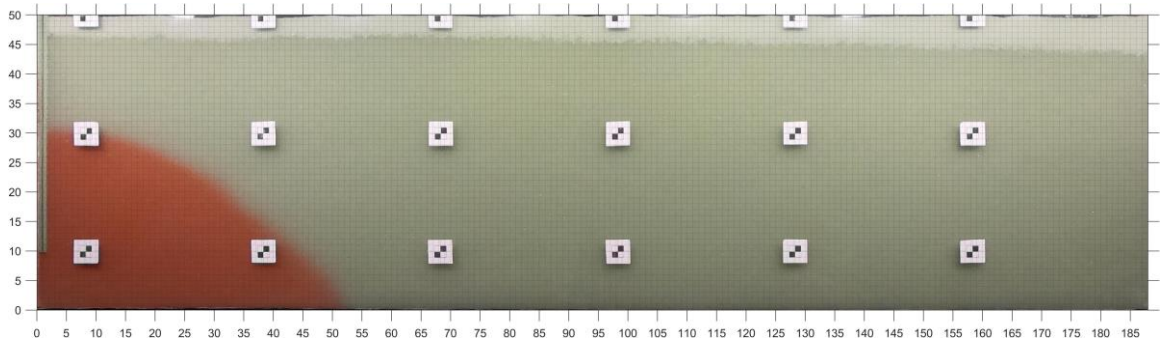

Figure 89 Sea water cline at t= 10 min for the active intrusion hSEA = 40 cm;hINLAND=36 cm and impermeable barrier depth d = 30 cm

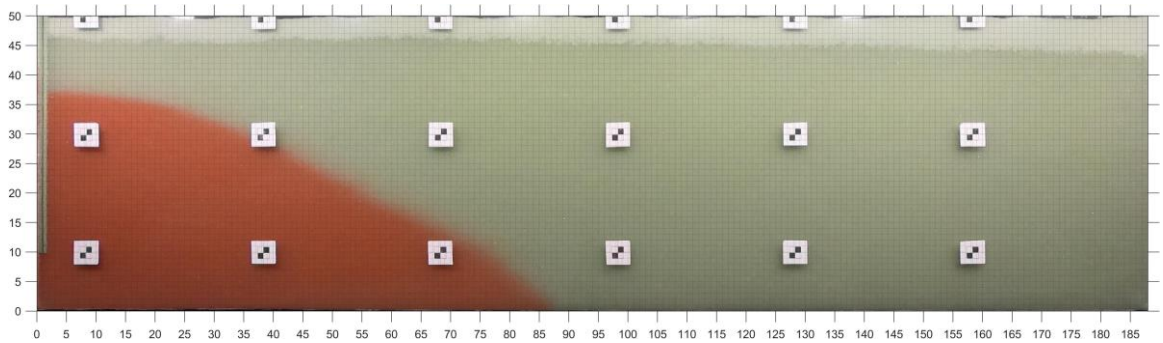

Figure 90 Sea water cline at t= 20 min for the active intrusion hSEA = 40 cm;hINLAND=36 cm and impermeable barrier depth d = 30 cm

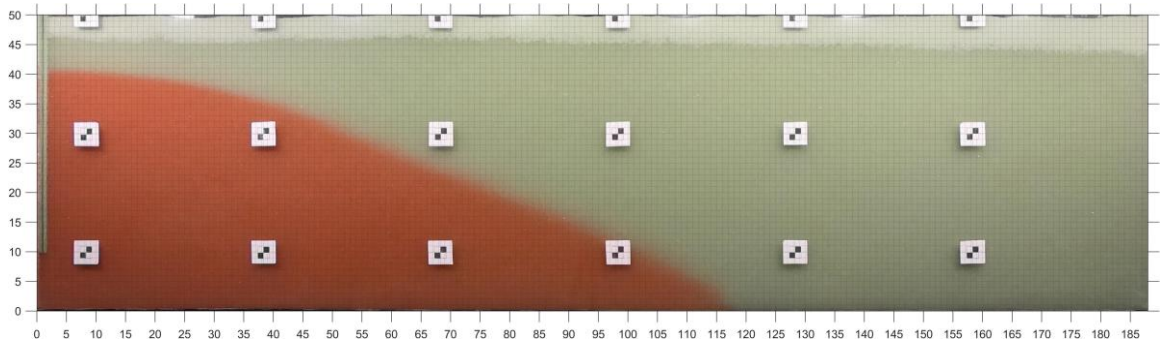

Figure 91 Sea water cline at t= 30 min for the active intrusion hSEA = 40 cm;hINLAND=36 cm and impermeable barrier depth d = 30 cm

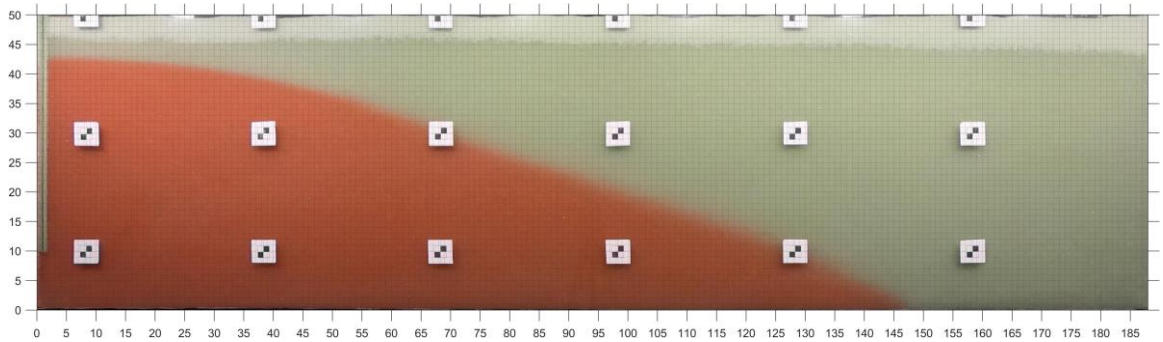

Figure 92 Sea water cline at t= 40 min for the active intrusion hSEA = 40 cm;hINLAND=36 cm and impermeable barrier depth d = 30 cm

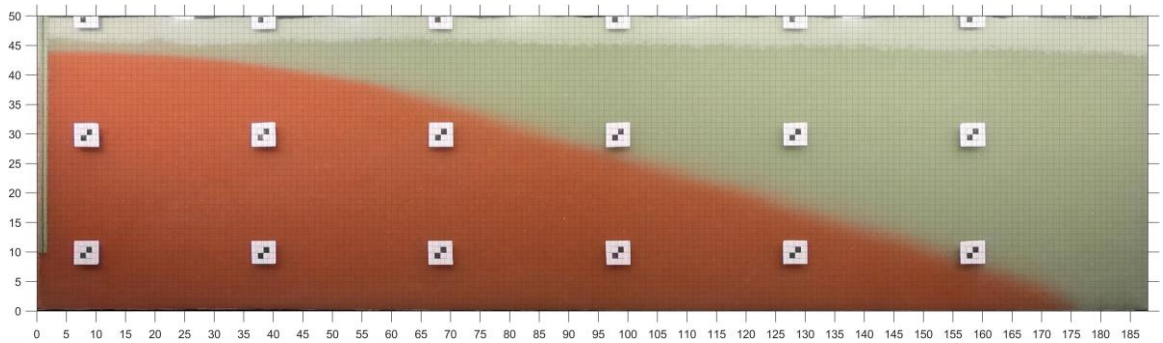

Figure 93 Sea water cline at t= 50 min for the active intrusion h_{SEA} = 40 cm;h_{INLAND}=36 cm and impermeable barrier depth d = 30 cm

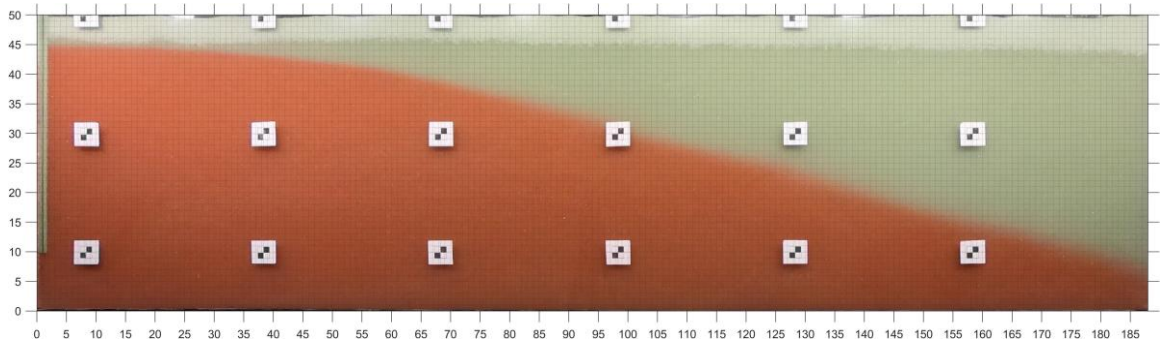

Figure 94 Sea water cline at t= 60 min for the active intrusion hSEA = 40 cm;hINLAND=36 cm and impermeable barrier depth d = 30 cm

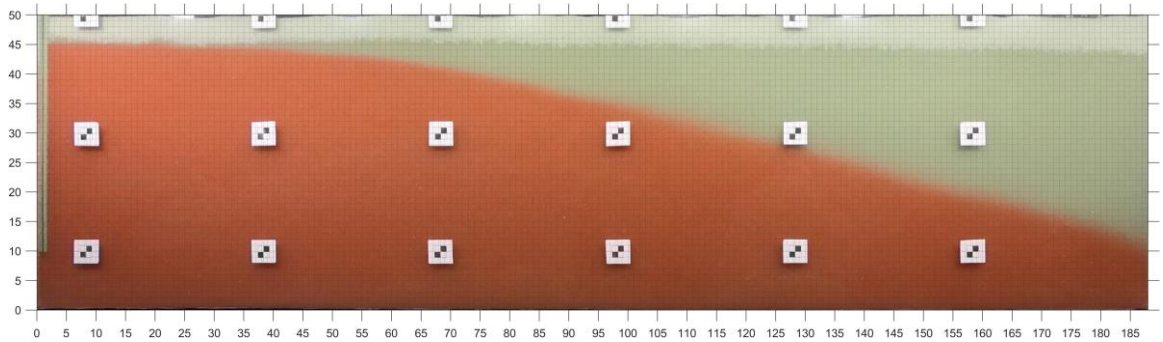

Figure 95 Sea water cline at t= 70 min for the active intrusion hSEA = 40 cm;hINLAND=36 cm and impermeable barrier depth d = 30 cm

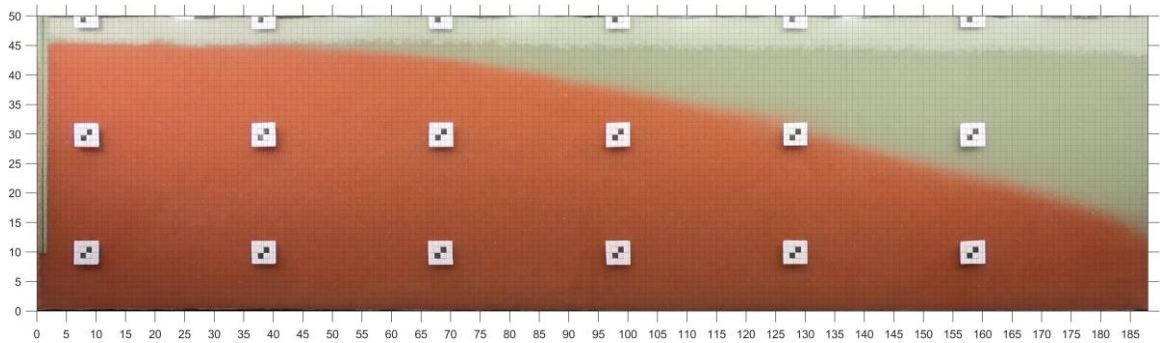

Figure 96 Sea water cline at t= 80 min for the active intrusion hSEA = 40 cm;hINLAND=36 cm and impermeable barrier depth d = 30 cm

Laboratory modelling of mitigation measures- recharge channel

Influence of the recharge channel to seawater cline features for different conditions has been analyzed and presented below. For this purpose, mitigated conditions of the active seawater cline has been demonstrated for different gradients in Figure 97 to Figure 104 and Figure 105 to Figure 111.

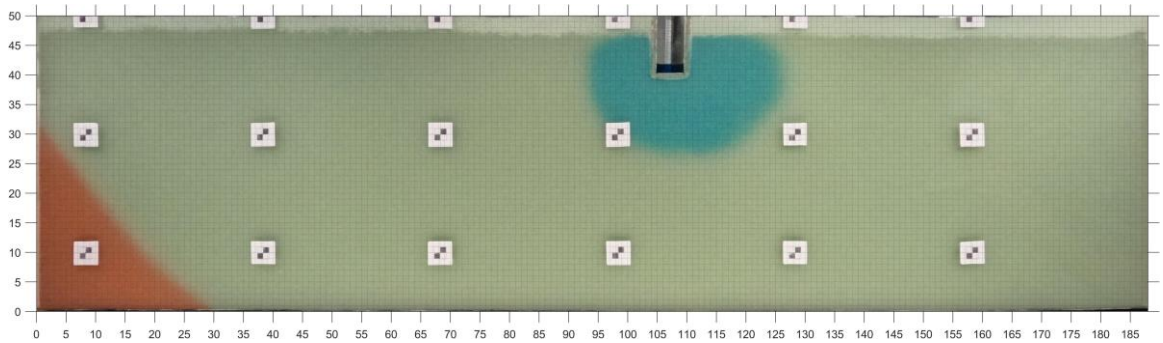

Figure 97 Sea water cline at t= 10 min for the active intrusion hSEA = 40 cm;hINLAND=39 cm and recharge channel with fresh water depth d = 1.75 cm

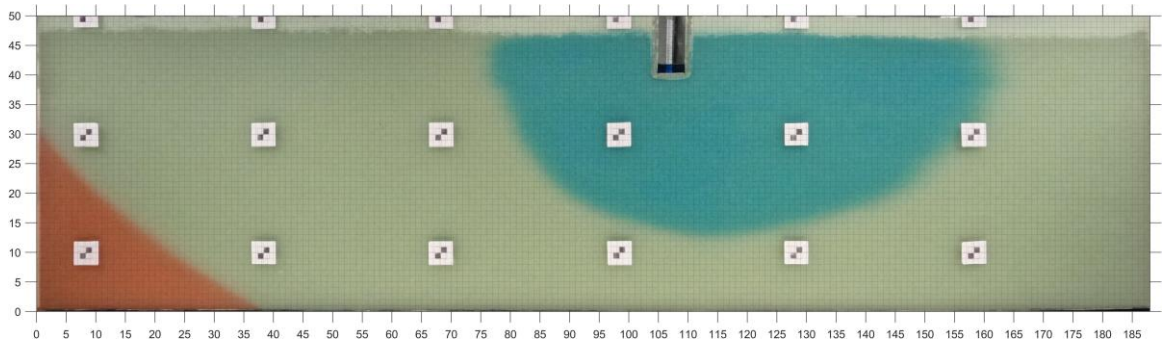

Figure 98 Sea water cline at t= 20 min for the active intrusion hSEA = 40 cm;hINLAND=39 cm and recharge channel with fresh water depth d = 1.75 cm

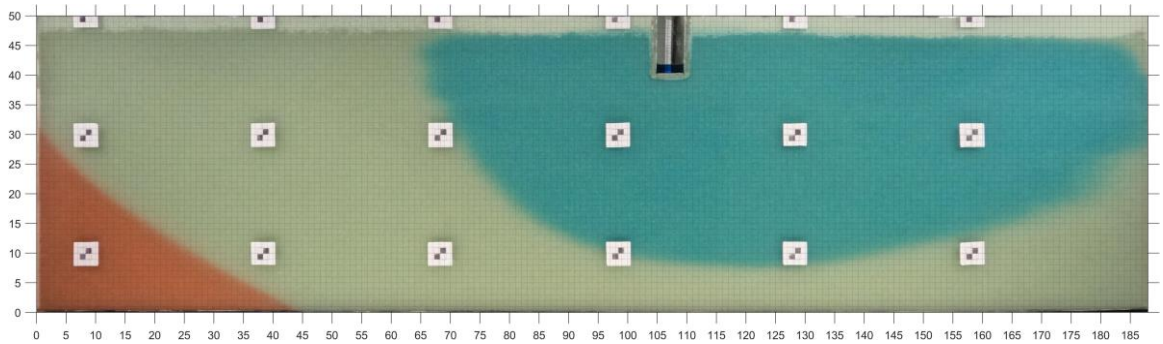

Figure 99 Sea water cline at t= 30 min for the active intrusion hSEA = 40 cm;hINLAND=39 cm and recharge channel with fresh water depth d = 1.75 cm

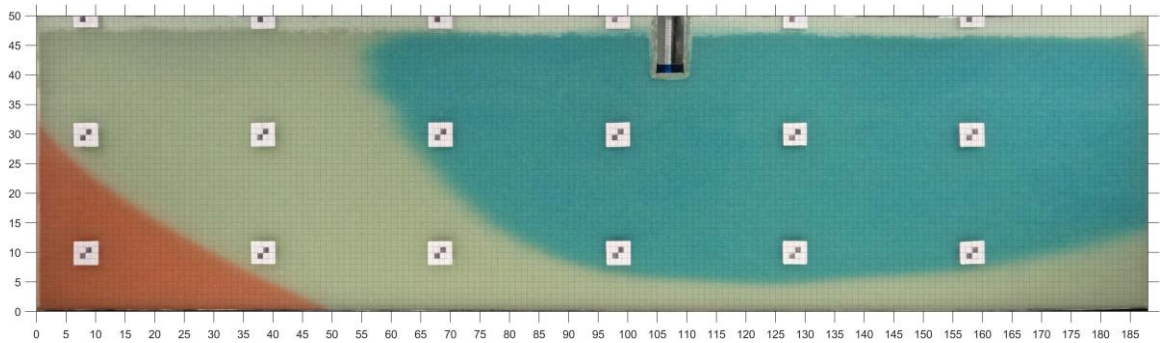

Figure 100 Sea water cline at t= 40 min for the active intrusion hSEA = 40 cm;hINLAND=39 cm and recharge channel with fresh water depth d = 1.75 cm

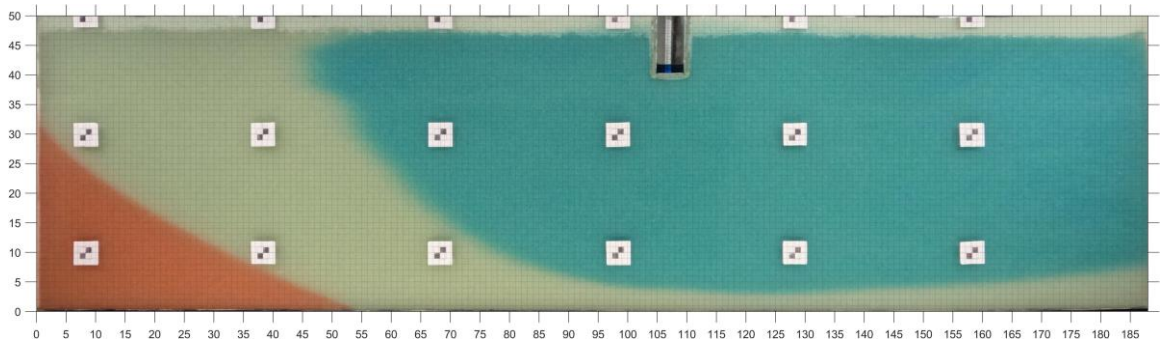

Figure 101 Sea water cline at t= 50 min for the active intrusion hSEA = 40 cm;hINLAND=39 cm and recharge channel with fresh water depth d = 1.75 cm

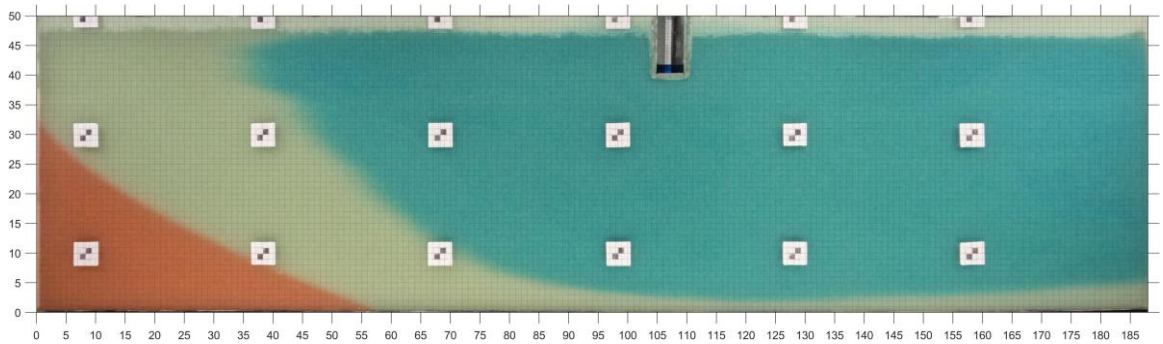

Figure 102 Sea water cline at t= 60 min for the active intrusion hSEA = 40 cm;hINLAND=39 cm and recharge channel with fresh water depth d = 1.75 cm

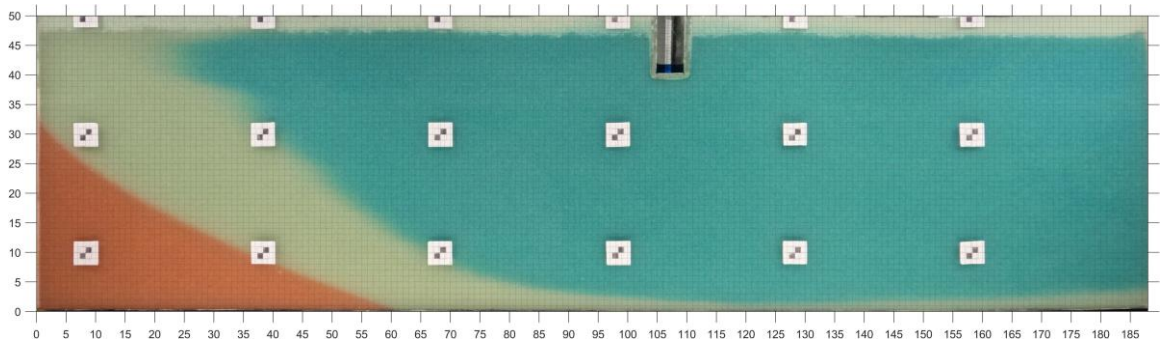

Figure 103 Sea water cline at t= 70 min for the active intrusion hSEA = 40 cm;hINLAND=39 cm and recharge channel with fresh water depth d = 1.75 cm

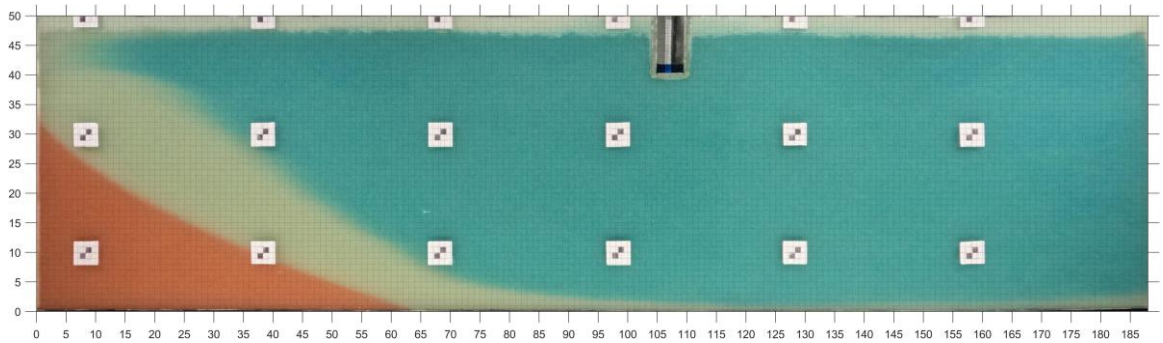

Figure 104 Sea water cline at t= 80 min for the active intrusion hSEA = 40 cm;hINLAND=39 cm and recharge channel with fresh water depth d = 1.75 cm

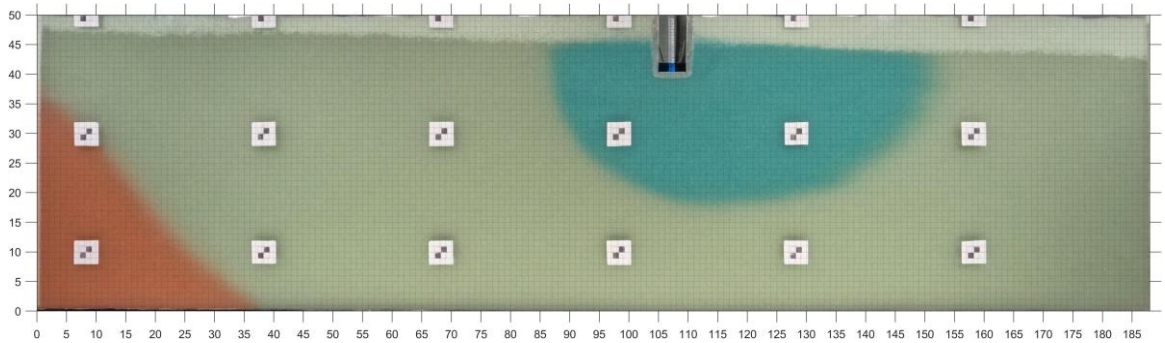

Figure 105 Sea water cline at t= 10 min for the active intrusion hSEA = 40 cm;hINLAND=36 cm and recharge channel with fresh water depth d = 1.75 cm

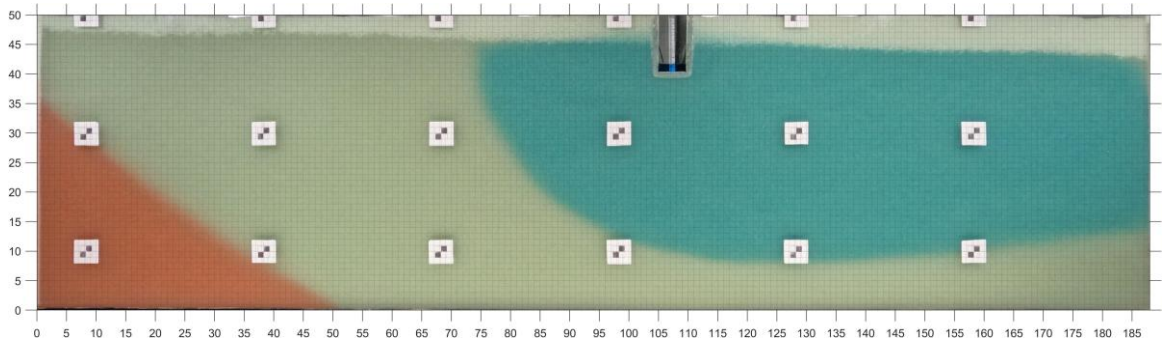

Figure 106 Sea water cline at t= 20 min for the active intrusion hSEA = 40 cm;hINLAND=36 cm and recharge channel with fresh water depth d = 1.75 cm

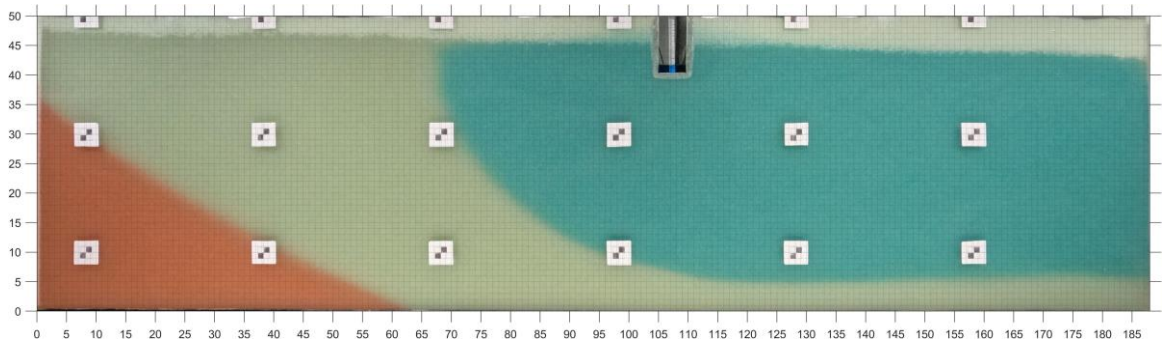

Figure 107 Sea water cline at t= 30 min for the active intrusion hSEA = 40 cm;hINLAND=36 cm and recharge channel with fresh water depth d = 1.75 cm

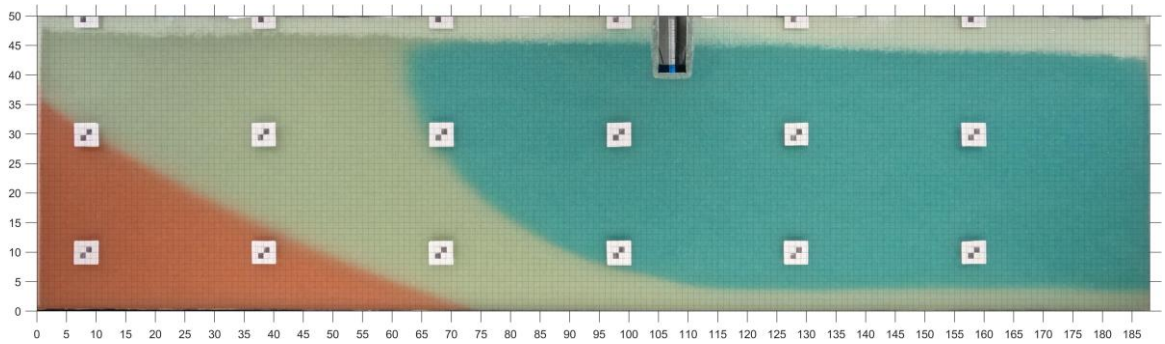

Figure 108 Sea water cline at t= 40 min for the active intrusion hSEA = 40 cm;hINLAND=36 cm and recharge channel with fresh water depth d = 1.75 cm

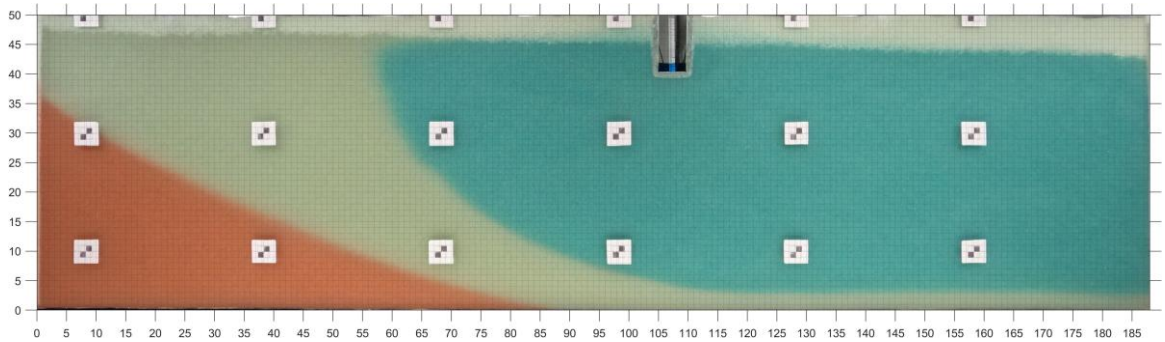

Figure 109 Sea water cline at t= 50 min for the active intrusion hSEA = 40 cm;hINLAND=36 cm and recharge channel with fresh water depth d = 1.75 cm

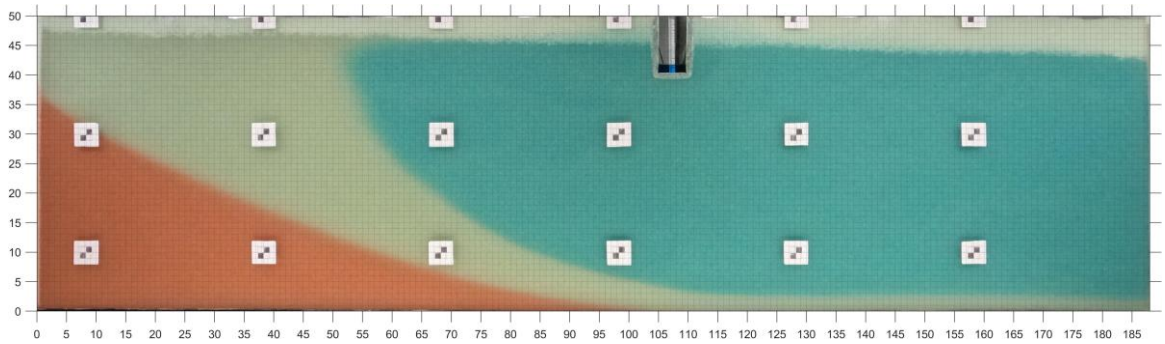

Figure 110 Sea water cline at t= 60 min for the active intrusion hSEA = 40 cm;hINLAND=36 cm and recharge channel with fresh water depth d = 1.75 cm

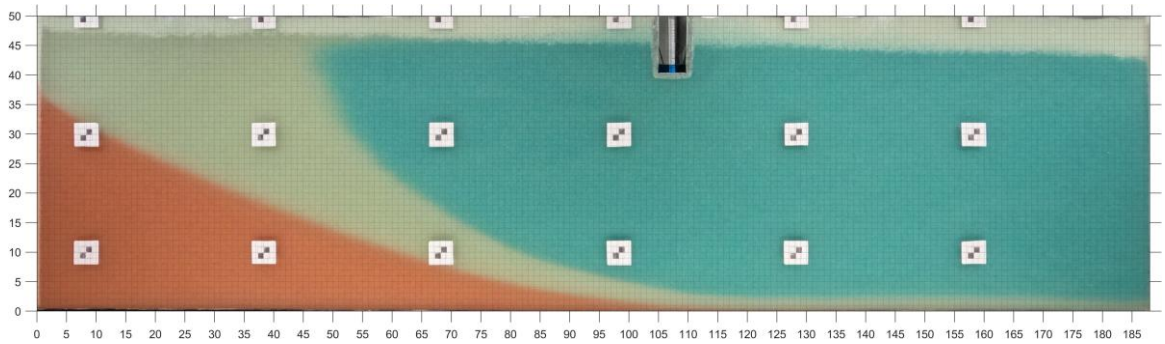

Figure 111 Sea water cline at t= 70 min for the active intrusion hSEA = 40 cm;hINLAND=36 cm and recharge channel with fresh water depth d = 1.75 cm

Mitigation measures testing in laboratory conditions- summary and conclusions

Both aforementioned mitigation measures have been tested and presented below with variable sets of parameters. **Error! Reference source not found.** Figure 112 and Figure 113 demonstrate the sensitivity of the seawater cline shape and size to gradients between the seawater source and inland water table. Implementation and effectiveness of the impermeable barrier to mitigate seawater intrusion have been demonstrated in Figure 114 and Figure 115 while the prevention of the seawater intrusion caused by the recharge channel is demonstrated in Figure 116 and Figure 117.

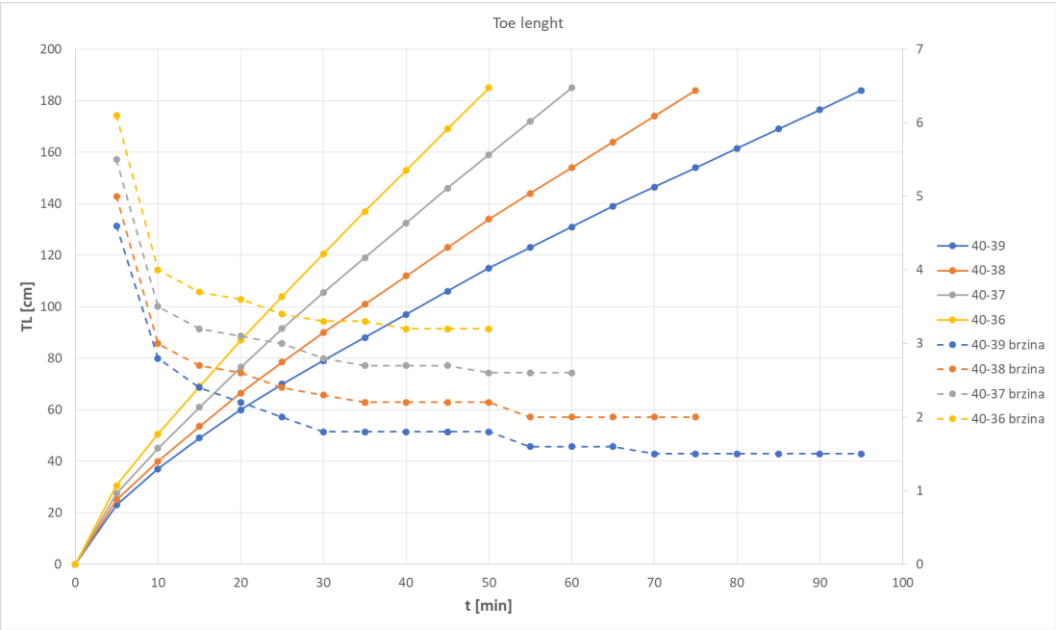

Figure 112 Sea water cline toe length and intrusion velocity for the active intrusion and variable gradients

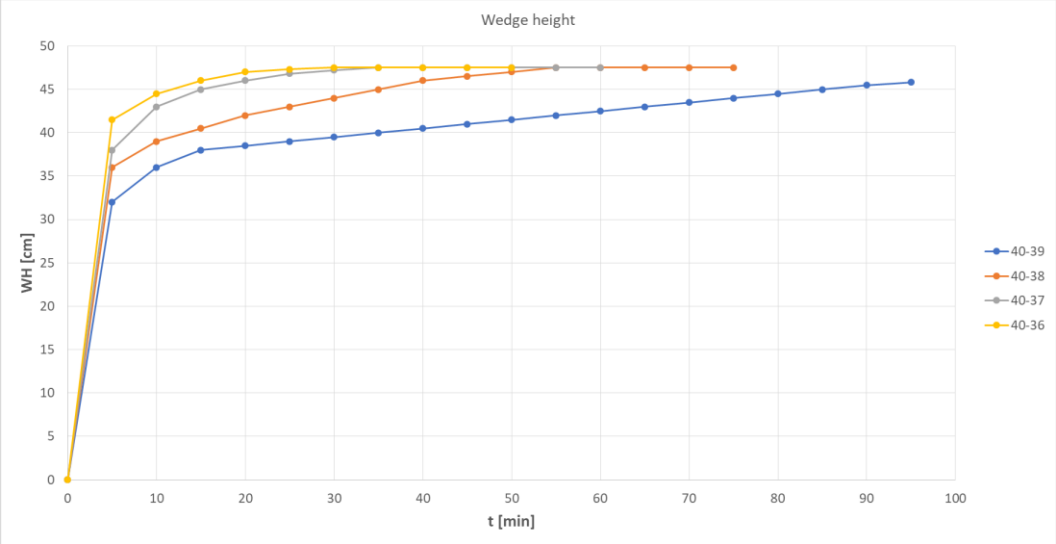

Figure 113 Sea water cline wedge height for the active intrusion and variable gradients

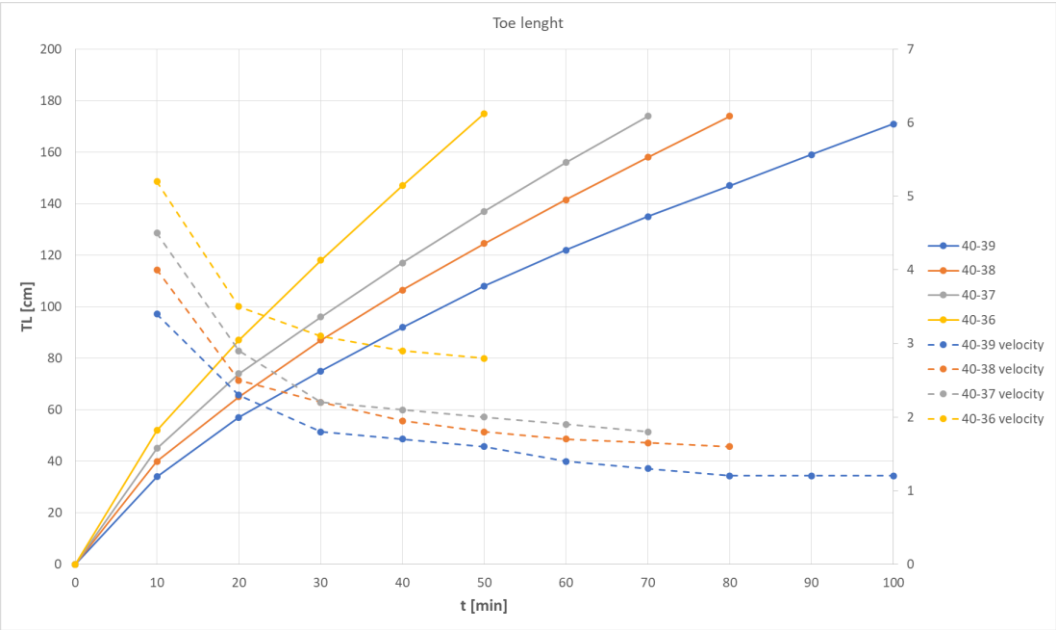

Figure 114 Sea water cline toe length and intrusion velocity for the active intrusion variable gradients and impermeable barrier depth d = 30 cm

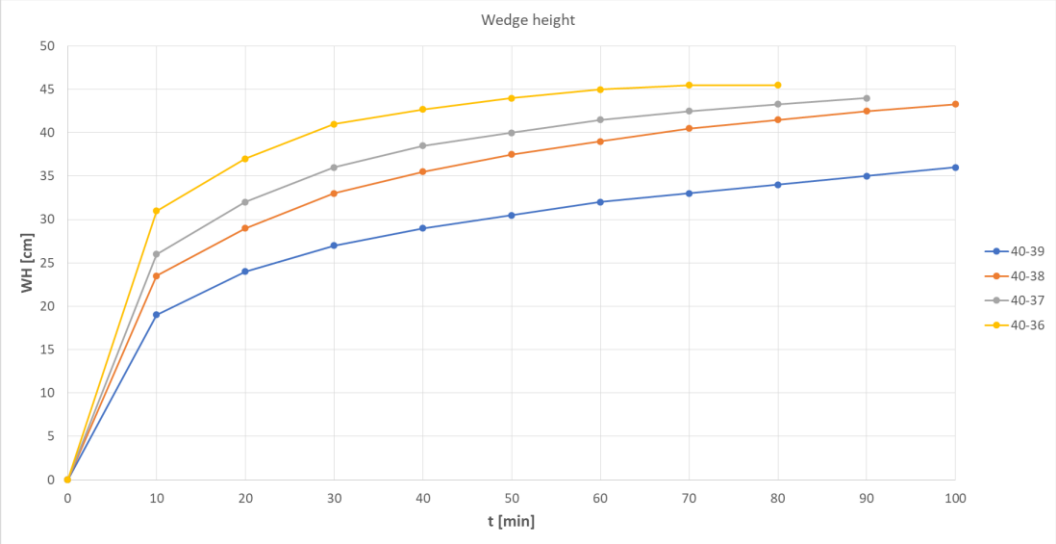

Figure 115 Sea water cline wedge height for the active intrusion variable gradients and impermeable barrier depth d = 30 cm

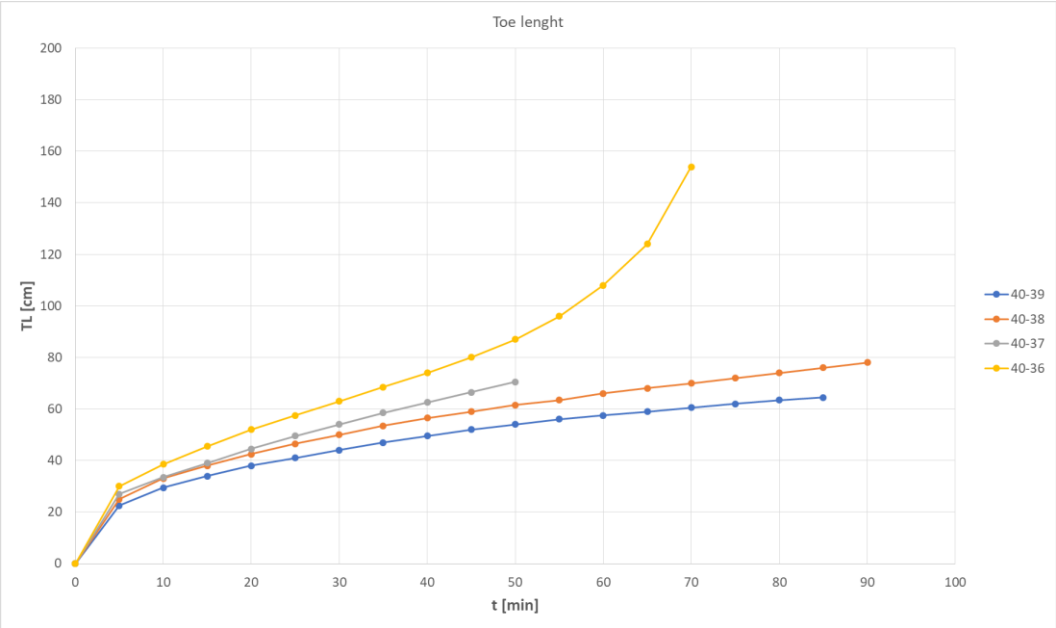

Figure 116 Sea water cline toe length for the active intrusion variable gradients and recharge channel water depth d = 1.75 cm

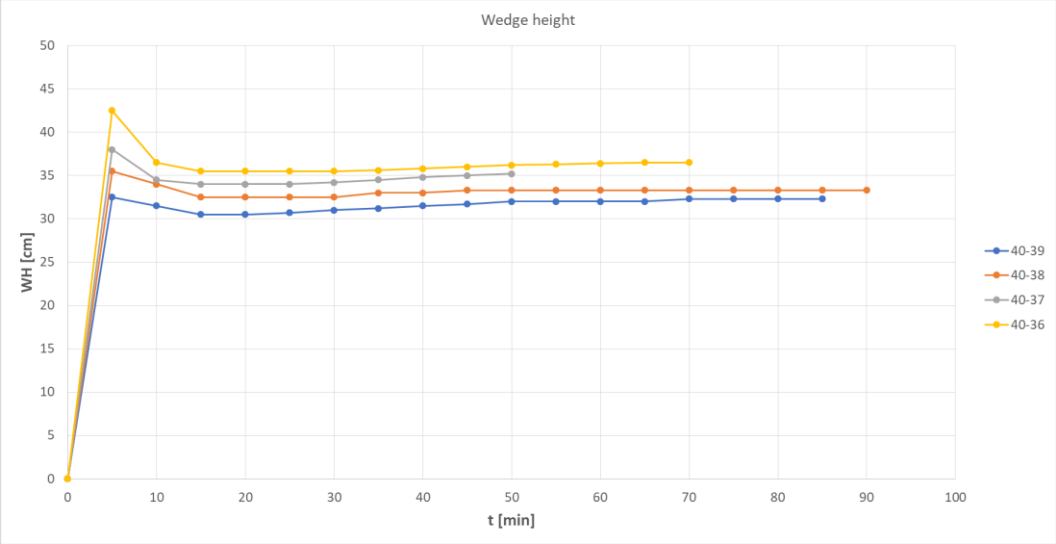

Figure 117 Sea water cline wedge height for the active intrusion variable gradients and recharge channel water depth d = 1.75 cm

Bibliography

https://meteo.hr/klima.php?section=klima_modeli&param=klima_promjene. (n.d.).

https://www.eea.europa.eu/data-and-maps/figures/projected-changes-in-annual-and-5. (n.d.).

https://www.eea.europa.eu/ims/global-and-european-sea-level-rise. (n.d.).

https://www.ipcc.ch/srocc/chapter/chapter-4-sea-level-rise-and-implications-for-low-lying-islands-coasts-and-communities/. (n.d.).

List of figures

List of tables